Interference cancellation and Resource Allocation approaches for Device-to-Device Communications

Chithra R

Department of Electronics and Communication Engineering
National Institute of Technology Rourkela
Rourkela, Odisha, India - 769 008

July 2016

Interference cancellation and Resource Allocation approaches for Device-to-Device Communications

Thesis submitted in partial fulfillment

of the Requirements for the degree of

Doctor of Philosophy

in

Electronics and Communication Engineering

by

Chithra R

Roll no: 512EC109

Under the guidance of

Prof. Sarat Kumar Patra

&

Ing. Robert Bestak, Ph.D.

(Czech Technical University in Prague, Czech Republic)

Department of Electronics and Communication Engineering
National Institute of Technology Rourkela
Rourkela, Odisha, India - 769 008

Dept. of Electronics & Communication Engineering
National Institute of Technology, Rourkela
Odisha-769 008, India.

July 5, 2016

Certificate

This is to certify that the work in the thesis entitled **Interference cancellation and Resource Allocation approaches for Device-to-Device Communications** by **Chithra R** is a record of an original research work carried out under our supervision and guidance in partial fulfillment of the requirements for the award of the degree of **Doctor of Philosophy** in Electronics and Communication Engineering, National Institute of Technology, Rourkela. Neither this thesis nor any part of it has been submitted for any degree or academic award elsewhere.

Ing. Robert Bestak, Ph.D.
(Co-Supervisor)
Faculty of Electrical Engineering
Czech Technical University in Prague

Dr. Sarat Kumar Patra
(Supervisor)
Professor, Dept. of ECE
NIT Rourkela, Odisha

Declaration

I certify that

(a) The work contained in this thesis is original and has been done by me under the guidance of my supervisors.

(b) The work has not been submitted to any other Institute for any degree or diploma.

(c) I have followed the guidelines provided by the Institute in preparing the thesis.

(d) I have conformed to the norms and guidelines given in the Ethical Code of Conduct of the Institute.

(e) Whenever I have used materials (data, theoretical analysis, figures, and text) from other sources, I have given due credit to them by citing them in the text of the thesis and giving their details in the references.

CHITHRA R

Acknowledgments

I avail this opportunity to express my deep sense of gratitude to my supervisors Prof. Sarat Kumar Patra, Department of Electronics and Communication Engineering, NIT Rourkela and Ing. Robert Bestak, Ph.D., Faculty of Electrical Engineering, CTU in Prague for their guidance, advice, and continued support throughout the far-reaching vision of the work. Their key technical insights and tireless editorial efforts vastly improved the quality of this dissertation.

I would like to thank the European Commission for partially funding my studies through the Erasmus Mundus HERITAGE scholarship programme. A very special thanks goes to Dr. Lukas Kencl, Faculty of Electrical Engineering, CTU in Prague for recommending me and introducing at the CTU in Prague. Sincere thanks to my DSC members: Prof. K K Mahapatra, Prof. D P Acharya, Prof. Susmita Das and Prof. S Gopalakrishna for their effort, discussions and constructive comments during the entire duration of the project.

The author would also like to thank all my colleagues in the Advanced Communication Lab, especially, Prasanth, Bhaskar, Pallab, Mangal, Manas, Satyendra and Varun for their accompaniment and enduring support. I would like to

express my sincere thanks to my friends especially Shaibu V B, Shince Joseph and Smitha Chandran who made my stay at Rourkela an unforgettable and rewarding experience. I also convey my deepest gratitude to my parents and family for whose faith, patience and teaching had always inspired me to walk upright in my life. Last but not least, thanks to my dear husband, Mr. Arjun Vijayan, for his continued and unfailing love, support and understanding that makes the completion of this thesis possible.

CHITHRA R

chithrar14@gmail.com

Abstract

Network assisted Device-to-Device (D2D) communication as an underlay to cellular spectrum has attracted much attention in mobile network standards for local area connectivity as a means to improve the cellular spectrum utilization and to reduce the energy consumption of User Equipments (UEs). The D2D communication uses resources of the underlying mobile network which results in different interference scenarios. These include interference from cellular to D2D link, D2D to cellular link and interference among D2D links when multiple D2D links share common resources. In this thesis, an orthogonal precoding interference cancellation method is initially presented to reduce the cellular to D2D and D2D to cellular interferences when the cellular channel resources are being shared by a single D2D link. Three different scenarios have been considered when establishing a D2D communication along with a Base Station-to-UE communication. The proposed method is analytically evaluated in comparison with the conventional precoding matrix allocation method in terms of ergodic capacity. This method is then extended for a cluster based multi-link D2D scenario where interference between D2D pairs also exists in addition to the other two interference scenarios. In this work, cluster denotes a group of devices locally communicating through multi-link D2D communications sharing the same radio resources of the Cluster Head. Performance of the proposed method is evaluated and compared for different resource sharing modes. The analyses illustrate

the importance of cluster head in each cluster to save the battery life of devices in that cluster. The outage probability is considered as a performance evaluation matrix for guaranteeing QoS constrain of communication links. Hence, the mathematical expressions for outage probability of the proposed method for single-link and multi-link D2D communications are presented and compared with an existing interference cancellation technique.

To execute the cluster based interference cancellation approach, a three-step resource allocation scheme is then proposed. It first performs a mode selection procedure to choose the transmission mode of each UEs. Then a clustering scheme is developed to group the links that can share a common resource to improve the spectral efficiency. For the selection of suitable cellular UEs for each cluster whose resource can be shared, a cluster head selection algorithm is also developed. Maximal residual energy and minimal transmit power have been considered as parameters for the cluster head selection scheme. Finally, the expression for maximum number of links that the radio resource of shared UE can support is analytically derived. The performance of the proposed scheme is evaluated using a WINNER II A1 indoor office model.

The performance of D2D communication practically gets limited due to large distance and/or poor channel conditions between the D2D transmitter and receiver. To overcome these issues, a relay-assisted D2D communication is introduced in this thesis where a device relaying is an additional transmission mode along with the existing cellular and D2D transmission modes. A transmission mode assignment algorithm based on the Hungarian algorithm is then proposed to improve the overall system throughput. The proposed algorithm tries to solve two problems: a suitable transmission mode selection for each scheduled transmissions and a device selection for relaying communication between user equipments in the relay transmission mode. Simulation results showed that our proposed algorithm improves the system performance in terms of the overall system throughput and D2D data rate in comparison with traditional D2D communication schemes.

Contents

List of Figures

List of Tables

List of Abbreviations

1/2/3/4/5 G	First/Secong/Third/Fourth/Fifth Generation
3GPP	Third Generation Partnership Project
3GPP2	Third Generation Partnership Project-2
AMPS	Advance Mobile Phone Service
AWGN	Additive White Gaussian Noise
BS	Base Station
BS2UE	Base Station-to-User Equipment
CDF	Cumulative Distribution Function
CDMA	Code Division Multiple Access
CH	Cluster Head
CMP	Conventional MIMO Precoding
CQI	Channel Quality Indicator
CSI	Channel State Information
CH2BS	Cluster Head to Base Station
D2D	Device to Device
DL	Downlink
DSS	Direct Sequence Spreading
FDMA	Frequency Division Multiple Access
FFS	Finite Feedback Scheme

GSM	Global System for Mobile
HSPA	High Speed Packet Access
IC	Interference Cancellation
ISC	Interference Signal Cancellation
ISNR	Interference-to-Signal Noise Ratio
LOS	Line-of-Sight
LTE	Long Term Evolution
LTE-A	Long Term Evaluation Advance
M2M	Machine to Machine
METIS	Mobile and Wireless Communication Enablers for the Twenty-Twenty Information Society
MIMO	Multi-Input Multi-Output
MRC	Maximal Ratio Combining
MRE	Maximum Residual Energy
MSK	Minimum Shift Keying
MTP	Minimum Transmit Power
MU-MIMO	Multi-User Multi-Input Multi-Output
NLOS	Non Line-of-Sight
NOS	Non Orthogonal Sharing
OPS	Orthogonal Precoding Selection
OMP	Orthogonal MIMO Precoding
OS	Orthogonal Sharing
OFDM	Orthogonal Frequency Division Multiplexing
OFDMA	Orthogonal Frequency Division Multiple Access
P2P	Peer-to-Peer
PDF	Probability Density Function
PMI	Precoding Matrix Index
QAM	Quadrature Amplitude Modulation
QoS	Quality of Service
QPSK	Quadrature Phase Shift Keying

RA	Random Allocation
SINR	Signal-to-Interference Noise Ratio
SNR	Signal to Noise Ratio
SMS	Short Message Service
TDD	Time Division Duplexing
TDMA	Time Division Multiple Access
TFFS	Throughput maximization FFS
TMA	Transmission Mode Allocation
UE	User Equipment
UL	Uplink
UE2UE	User Equipment-to-User Equipment
WCDMA	Wideband Code-Division Multiple Access
WiMAX	Worldwide Interoperability Microwave Access
WLAN	Wireless Local Area Network

List of Symbols

Symbol	Description
$\mathbf{E}_i$	Exponential Integral Function.
${}_2F_1\left(a,b;c;d\right)$	Hyperbolic Function.
$\Gamma\left(\cdot\right)$	Gamma Function.
$U\left(\cdot\right)$	Unit Step Function.
$\left\|\mathbf{V}\right\|$	Cardinality of set $\mathbf{V}$.
$f_\gamma(\gamma)$	PDF of γ.
$F_\gamma(\gamma)$	CDF of γ.
CH2BS^{DL}	The cellular downlink communication from BS to CH.
CH2BS^{UL}	The cellular uplink communication from CH to BS.
UE2UE_i^{ab}	The D2D communication from UE_a to UE_b of i^{th} link.
B	Channel Bandwidth.
$\mathbb{C}_k$	Denotes the index set of UEs in k^{th} cluster.
C_n	Maximum data rate at n^{th} UE.
$\mathbf{H}_i$	The i^{th} link channel matrix.
$\left\|h_{ij}\right\|$	Channel gain of $i-j$ link.
$I_r^{j/i}$	The power ratio of i^{th}/j^{th} interference link to the desired j^{th}/i^{th} link.

L	Number of links in a cluster.
$\mathbb{L}$	Denotes the index set of all links established in the cell.
$\mathbb{M}$	Denotes the set of transmitting UEs in the cell.
$\mathbb{N}$	Denotes the set of receiving UEs in the cell.
N	Number of codewords in the codebook.
N_d	Number of elements in $\mathbb{U}_d$.
N_t	Number of Transmit Antennas.
N_r	Number of Receive Antennas.
N_0	Power spectral density of AWGN.
P_i	The transmission power of i^{th} link.
P_{ij}	Transmit power of $i-j$ link.
P_{out}	Outage probability.
$\boldsymbol{\psi}_i$	The precoding vector for i^{th} link.
$\boldsymbol{\Psi}$	Cluster Matrix.
s_i	The transmitted signal through i^{th} link.
$\mathbb{R}$	Denotes the set of idle UEs in the cell.
$\hat{s}_i$	The demodulated signal of i^{th} link.
$\mathbb{U}$	Denotes the index set of active UEs, $\mathbb{U} = \{1, 2, ..., N_u\}$.
$\mathbb{U}_c$	Denotes the index set of UEs in cellular mode.
N_c	Number of elements in $\mathbb{U}_c$.
$\mathbb{U}_d$	Denotes the index set of UEs in D2D mode.
$\mathbb{W}$	Denotes the Codebook.
$\mathbf{W}_i$	Denotes the i^{th} codeword from Codebook, $\mathbb{W}$.
$\mathbf{y}_i$	The received signal vector from the i^{th} link.
α_{mn}	Cellular transmission mode indicator for transmission from UE_m UE_n.
β_{mn}	Relay transmission mode indicator for transmission from UE_m UE_n.
$\boldsymbol{\eta}$, $\bar{\boldsymbol{\eta}}$	Additive White Gaussian Noise (AWGN).
ξ	Signal-to-Noise Ratio (SNR).

γ_i	SINR of i^{th} link.
γ_{ij}	SINR of $i-j$ link where $i, j \in \mathbb{U}$ and $i = 0$ or $j = 0$ denotes the link from BS to UE_j or from UE_i to BS.
$\gamma_{ij}^{c/d}$	SINR of cellular link/D2D link from UE_i to UE_j.
γ_{th}	SINR threshold.
ϱ_c	Maximum transmission power of UEs in cellular mode.
ϱ_d	Maximum transmission power of UEs in D2D mode.
ξ_{mn}	D2D transmission mode indicator for transmission from UE_m UE_n.

CHAPTER 1

Introduction

Contents

The concept of Device-to-Device (D2D) communications have been proposed as a candidate for the future cellular network to satisfy the increasing demand for local traffic and to admit more users in the system. This chapter briefly discussed the history of mobile cellular standards and provided the requisite of D2D communication underlaying cellular networks for future cellular standards. However, many challenges need to be addressed in designing the concept of device-to-device communication. The significance and objectives for carrying out this research work for addressing some of the major design challenges for device-to-device are also outlined in this chapter.

1.1 Historical Background

Among the myriad technologies that revolutionized life throughout the history of humanity, mobile communication stands out as a giant triumph in terms of its speed of adoption and extend of global transformation [1]. The era of electrical telecommunication came with the invention of practical telegraph in the late 1830s and telephone in 1876 [2]. Following this, the telex services evolved into the most popular forms such as Short Message Service (SMS) and email, meanwhile telephony remains the most widely used means of communication in the world today [2]. The technological directions and speed at which the wireless technology reached billions of people have shifted the wired electronic communication to a "wireless world" [3].

Mobile wireless technology evolution is specified by "generations" with major shift in technologies including advancement from analog to digital communication and many other technical enhancements [1, 4]. When the earliest analog cellular system, the Advanced Mobile Phone Service (AMPS), were deployed, the primary industry challenge had been to maximize the use of spectrum [1]. However, with the advent of data services, increasing the capacity to deliver more bits

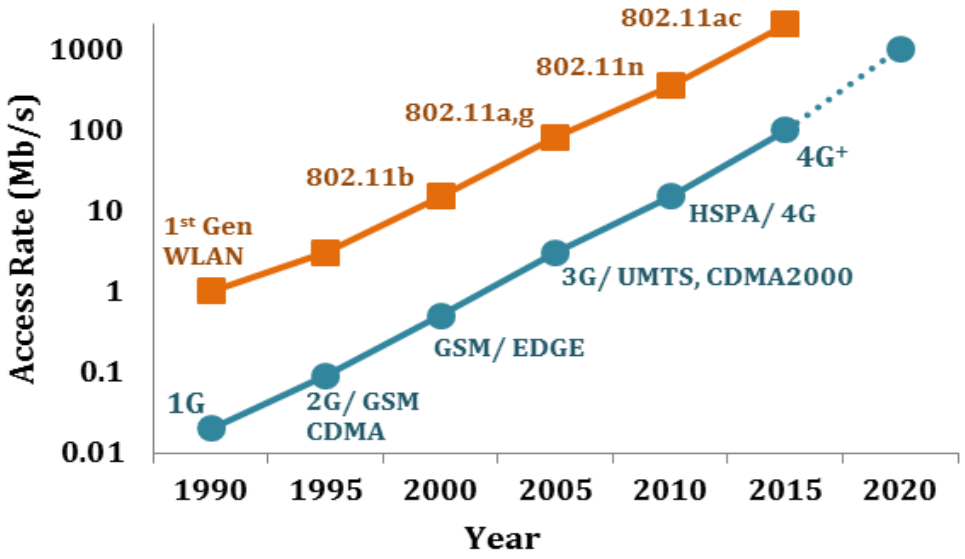

Figure 1.1: The Moore's Law for wireless communication [5]

per second per Hertz (bits/s/Hz) by allowing better Signal-to-Interference Noise Ratio (SINR) became the most important goal [5]. Figure 1.1 shows the Moore's Law advances in achievable data rate for wireless communication [5]. The graph illustrates that there is an approximately exponential increase in the demand for achievable data rate over the past 20 years.

The First-Generation (1G) analog cellular standard was replaced by digital cellular systems based on the Global System for Mobile Communications (GSM) standard which uses generalized Minimum Shift Keying (MSK) modulation, block coding, and Time-Division Multiple Access (TDMA) to achieve circuit switched bit rates 16 kb/s, and packet data rates 100 kb/s [6]. The corresponding Second-Generation (2G) digital cellular standard based on Code-Division Multiple Access (CDMA), IS-95, was also developed parallel to TDMA systems [4]. The advantages of CDMA systems provided with reduction in interferences between UEs made the Third-Generation (3G) cellular systems to adopt CDMA technology. For standardization of 3G technologies, 2 bodies were created: (i) Third Generation Partnership Project (3GPP) which includes Wideband Code-Division Multiple Access (WCDMA) and (ii) Third Generation Part-

nership Project 2 (3GPP2) which includes CDMA 2000 [1]. These 3G standards use wideband spread spectrum, adaptive modulation, convolutional coding, and CDMA to achieve bit rates of up to 144 Kb/s for mobile, 384 Kb/s for pedestrian and 2 Mb/s for indoor cases [7]. The 3G cellular system were extended to High Speed Packet Access (HSPA) to deploy high speed internet services. However, Andy Fuertes and Visant Strategies analysed that 3G has disappointed many in the industry because of its high implementation cost and slow adoption [4]. In parallel to these cellular standards, the widely adopted 802.11 specification for Wireless Local Area Network (WLAN) started out with direct sequence spreading (DSS), quadrature phase shift keying (QPSK) modulation at 1 Mb/s, later adding the option of higher order adaptive quadrature amplitude modulation (QAM) without spreading to achieve up to 11 Mb/s [5].

Subsequently high-speed cellular and WLAN standards (i.e., Fourth-generation (4G) cellular including Worldwide Interoperability for Microwave Access (WiMAX) and Long Term Evolution (LTE), and 802.11 (a, g, n, ac)) have migrated to a single modulation technology called Orthogonal Frequency Division Multiplexing (OFDM) [8]. Both LTE and WiMAX use Orthogonal Frequency Division Multiple Access (OFDMA) with Frequency Division Multiple Access (FDMA)/TDMA to achieve basic service bit rates in the range of 10-20 Mb/s [5]. With the addition of Multiple Input Multiple Output (MIMO) signal processing and wider band channels of 10 MHz or 20 MHz, it has become possible to increase peak data rates to the range of 100 Mb/s in both LTE and WiMax systems [5]. LTE is now evolving to LTE-Advanced (LTE-A) by inclusion of further enhancements.

The need for high-speed data networks is increasing exponentially with an unprecedented revolution of cellphones; from a device primarily used to make phone calls to smart-phones with internet applications accessible to anybody in almost any time, anywhere. Today, smartphones are used like personal assistants to search and locate places on maps, watch videos, and buy products on

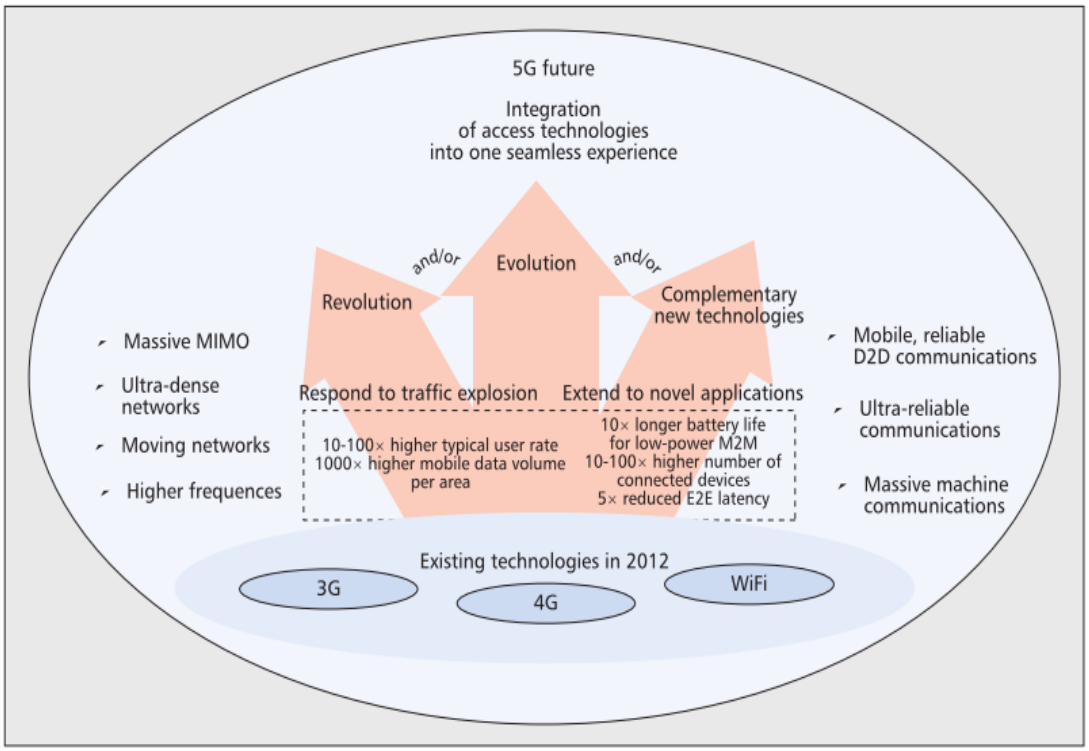

Figure 1.2: The 5G roadmap by METIS [13]

the Internet [9]. The current trends demand the future 5G mobile networks to address the following challenges: higher capacity, higher data-rate, lower end-to-end latency, massive device connectivity, reduced capital and operation cost and longer battery life [10–12]. Based on these demands, the 5G project proposal by Mobile and Wireless Communications Enablers for the Twenty-Twenty Information Society (METIS) is shown in Figure 1.2 [13]. The 5G roadmap presented in Figure 1.2 is constructed in response to the traffic volume explosion with 1000 times higher mobile data volume per area, 10 to 100 times higher number of connected devices, 10 to 100 times higher user data rate, 10 times longer battery life for low-power massive machine communication and 5 times reduced end-to-end latency [13, 14]. These diverse requirements can be met through combination of evolved existing technologies and new radio concepts including massive MIMO, ultra-dense networks, moving networks, direct Device-to-Device (D2D) communication, ultra-reliable and massive machine communication [13, 14].

Several content aware applications are emerging in smart phones to provide plurality of services according to the location information, for example, to search for and locate nearby restaurant and reserve a seat by sending a short message [15]. Since most of these content aware applications involve nearby devices, direct D2D communication can facilitate this service with reduced communication cost. Peer-to-peer (P2P) service or user-to-user service also reflects the trend of streaming media [2]. Hence D2D communication has become a promising technology to meet the 5G requirements. The aim of this thesis work is to analyse the concept of D2D communication, its merits and challenges.

1.2 D2D Communication

Device-to-Device (D2D) communication is currently being specified by 3GPP in LTE Release 12 [16, 17]. The D2D communication is recognized as one of the technology components of the evolving 5G architecture by the European Union project METIS [13, 14] and it refers to the technology that enable User Equipments (UEs) to facilitate high data rate local communication without an infrastructure of Base Station (BS) [18], i.e., the UEs can communicate with other UEs in proximity over direct wireless links using cellular network channel resources without relaying the information through the Base Station (BS) [19]. Here, proximity devices are determined not only based on the physical distance but also based on channel conditions, SINR, throughput, delay, density and load [20]. The concept of D2D communication is illustrated in Figure 1.3. Here the UEs communicating through direct links operate in the D2D mode, while UEs communicating via the BS in the cellular mode.

The traditional direct device communications, for example Bluetooth and WiFi direct, use unlicensed spectrum for communication and result in poor Quality-of-Service (QoS) because of uncontrolled interference [21]. In addition,

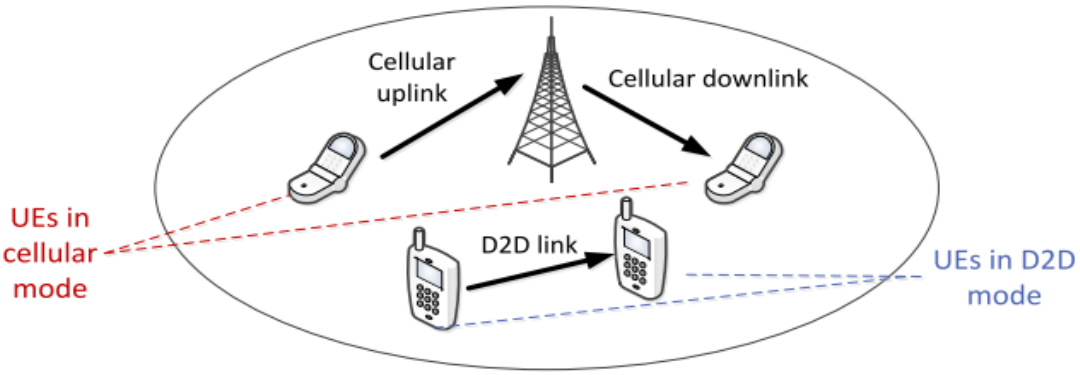

Figure 1.3: D2D and cellular mode of communication

the discovery and setup process fpr establishing connection in traditional direct device communications are quite complicated since it needs user intervention [21, 22]. In contrast to these traditional technologies, the D2D communication uses licensed bands where the above mentioned problems can be solved in a more efficient way and provides better transmission coverage [23, 24]. The D2D communication underlaying cellular network operates in a licensed spectrum allocated to the cellular users where, the D2D users can access the licensed spectrum either in a dedicated mode (also described in the literature as Orthogonal mode) or in a shared mode (also known as non-orthogonal mode) [25, 26]. In comparison to the traditional technologies, the advantages of D2D Communication in Cellular Network can be summarized below:

- Increased spectral efficiency
- Reduced device transmission power
- Decreased traffic load
- Increased overall system throughput
- Reduce the use of resource between the Base Station and the devices
- Extended cell coverage

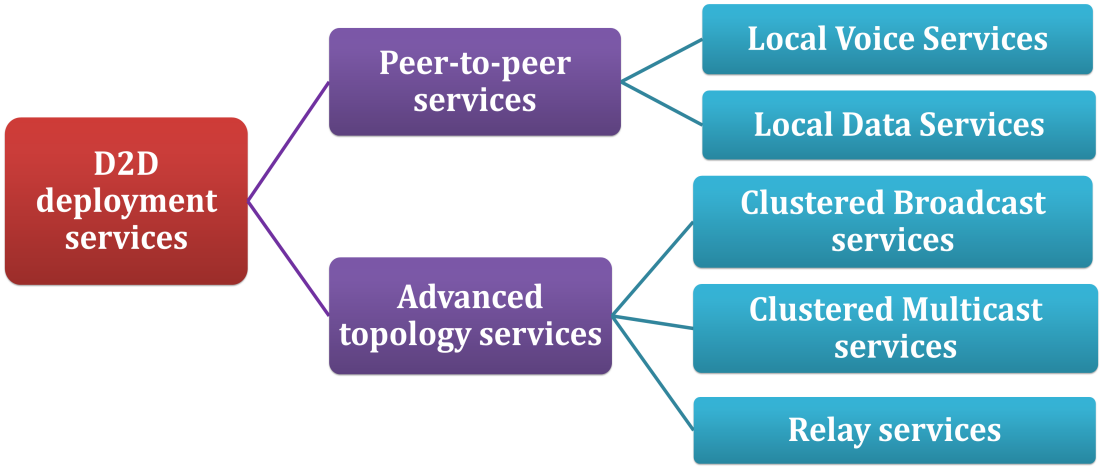

Figure 1.4: D2D Usage Services

- Reduced Communication Delay

1.2.1 D2D Deployment Services

The D2D communication can be used for various deployment services. Figure 1.4 shows various D2D usage services. Direct D2D communication can be used for peer-to-peer and advanced topology services [15]. Here, peer-to-peer services refer to the case where D2D capable UEs form the source and destination for exchange of data, whereas for latter services the D2D capable UEs act as transmission relays for each other to forward the data to the destination [15, 27].

The peer-to-peer usage cases of D2D communication underlaying cellular network include local voice and data services. The local voice traffic can be offloaded via D2D communication when two geographically proximate users like to talk on the phone, for example, people in a large meeting room or stadium wishing to discuss privately, or companions get lost in supermarket, railway station, airport etc. [15]. D2D communication can be used to provide local data services, for example, friends exchange photos or videos or do multi-player gaming through

their smart-phones, or people attending a conference downloading materials from the local server etc. [15]. The peer-to-peer services enhance the capacity of underlaying cellular network by harnessing the full capabilities of mobile devices.

D2D communication can also be exploited for multicast, broadcast and relay purpose communications [20, 28, 29]. The multicast and broadcast D2D communication are executed with the clustering concept and cluster head acting as the master [30]. The multicast services can save the radio resources required to share files among multiple UEs in proximity since there is no need to send shared files to the BS and then retransmit to individual UEs [31]. In D2D broadcast concept, the UEs within the cluster are able to retransmit the data received from the BS to the UEs who fails to decode the received information correctly [32]. A multi-hop relaying decode-and-forward strategy to effectively establishing D2D links as an underlay to cellular network is presented in [33]. The D2D UEs can be utilized for relay purposes without the need to install new BS or relay stations [27, 34, 35]. The relay concept can be used to extend coverage and/or to enhance capacity and/or to improve battery life.

1.2.2 Challenges

Moving towards a wireless world involves more than technology. It is driven by a confluence of forces and affected by a myriad of issues [3]. There are many challenges to be addressed in designing the concept of D2D communication as an underlay to a cellular network. An overview of the technical challenges in D2D communications underlying a cellular network is shown in Figure 1.5.

Peer discovery is the first step of D2D link establishment, in which the UEs and/or the BS discover the presence of peer D2D candidates and identify whether the candidate D2D pairs need to communicate with each other [36]. A D2D candidate is a pair of UEs, a potential D2D transmitter and receiver, which are

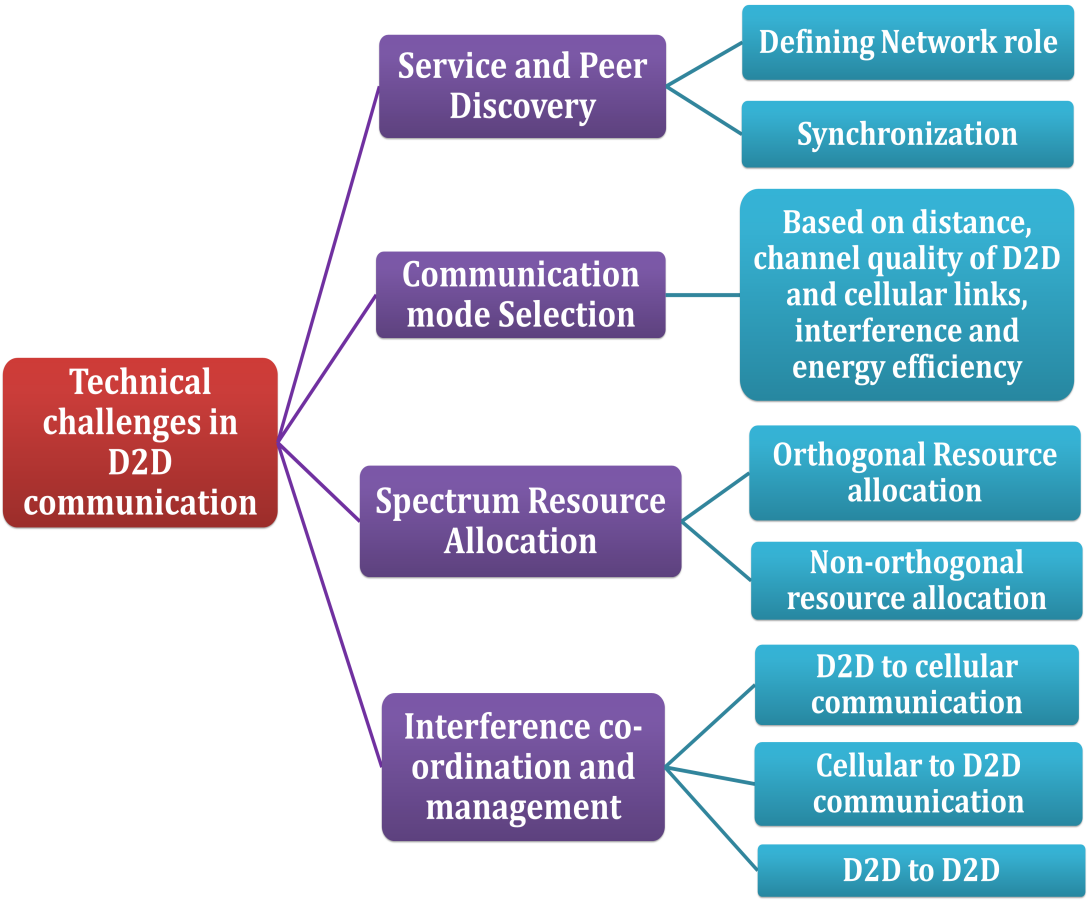

Figure 1.5: Technical design challenges in D2D communication

in the proximity of each other. To identify the D2D candidates and required services, network-controlled and ad hoc network approaches can be employed [37–39]. In network-controlled approach, the network discovers potential D2D candidates whereas in the ad hoc network approach, the discovery is made by the devices themselves [37]. The fundamental problem here is that efficient discovery requires that the two peer devices be synchronized and also network role should also need to be defined in the service and peer discovery process [40]. Peer and service discovery techniques have not been considered in the focus of this thesis work.

In D2D communication underlaying cellular network, a UE can operate either in the cellular or D2D mode [38, 41]. The mode selection is a process of determining the communication mode of potential D2D candidates. The process

of mode selection should be done using various matrices such as distance, channel quality of D2D and cellular links, interference, load of the BS and energy efficiency. Proper mode selection plays a crucial role in D2D communication to increase the spectral efficiency of the system [21].

When a D2D pair needs to communicate underlaying a cellular network, allocation of cellular resources to the D2D transmission is a critical issue [19]. Generally, there are two resource sharing modes in the network: (i) Non-orthogonal sharing (NOS) mode where, D2D links and cellular links reuse the same resource, and (ii) Orthogonal sharing (OS) mode where, D2D links use part of the resources while the other resources are allocated for cellular communication [7,42]. However, to utilize network resources more efficiently, NOS mode of resource allocation is preferred for D2D communications. Given the above resource sharing relations, the resource allocation decides how to share the spectrum between D2D communications and cellular communications in order to attain the maximum system throughput [38].

With the NOS resource sharing mode, the interference level in a D2D communication enabled system is more severe compared to conventional cellular systems [38,41,43]. The interference coordination methods for D2D communication as an underlay to cellular networks are required to handle: (i) D2D to cellular interference, (ii) cellular to D2D interference and (iii) D2D to D2D interference [29]. The D2D to D2D interference co-ordination is required for the case when multiple D2D pairs share common resources. Effective interference coordination and management for D2D communications is vital to better realize the advantages of D2D communication [43].

1.3 Motivation

The greatest changes in consumer experience did not occur until mobile phones and the internet came and become common elements of life, and which continue

to generate great demands in terms of improved data rate. The 2G to 4G systems are based on network centric approach, but 5G is expected to drop towards device centric systems. Hence, D2D communication will become a promising technique to provide wireless peer-to-peer services and spectrum utilization in the future wireless communication networks. For better utilization of the concept of D2D communication, advanced D2D concepts using D2D communication need to be further investigated. For cluster based topology networks like multicast and broadcast networks, a D2D capable UE can simultaneously get connected to multiple similar UEs that are relatively close to each other via multiple UE-to-UE (UE2UE) links and at the same time, it can be connected to the Base Station (BS) via BS2UE link, i.e. a connection between UE and BS. In order to maximize the spectral efficiency the cellular channel resource can be shared by more than one UE2UE link. This improves spectral efficiency but on the other hand results in various interference scenarios. The advantages of D2D communication could be better realized with minimal interference between UE2UE and BS2UE links. Hence interference co-ordination and management plays a vital role in designing D2D communication underlaying cellular network.

1.4 Literature Survey

A survey on various interference cancellation approaches in literature is presented in this section. The coverage of D2D communication gets limited with poor radio channel condition between the potential UE transmitter and receiver or when the UEs are at the cell edges. A study on relay-assisted D2D communication to deal with theses constrains is also carried out in this section.

1.4.1 Interference Mitigation

One of the major challenges in D2D communication is to avoid interference between the D2D UEs and cellular UEs [29, 44]. The introduction of D2D communication should not affect or degrade the performance of underlaying cellular network and if D2D communication is strongly interfered by the cellular communication, its applicability and/or efficiency is hindered. The interference generated with D2D communication can be divided into 3 different scenarios:

(i) **Interference from D2D communication to cellular communication:** In the uplink (UL) direction, the BS signal is interfered by the nearby D2D communication signals. For the downlink (DL), a D2D communication can interfere nearby cellular UE receivers when D2D transmitters are located closed to those UEs.

(ii) **Interference from cellular communication to D2D communication:** The transmission power of cellular communication is much higher than D2D communication causing interference at the D2D receivers for both UL and DL communications.

(iii) **Interference between D2D pairs:** If more than one D2D pair reuses the same radio resources, the interference is always caused by the transmitting D2D UEs to the receiving D2D UEs in different D2D pairs.

Interference possesses a significant risk to both cellular and D2D UEs. Hence efficient interference management is essential for the effective realization of D2D communication underlying cellular networks. In the last few years, several research works have been carried out in the field of interference management with D2D communications. We classify the interference management schemes into 3 categories:

(i) **Power Control Schemes:** where the cellular UEs are considered as the primary users and the transmission power of the D2D UEs are controlled to reduce the interference to cellular UEs.

(ii) **Re-transmission Schemes:** where an additional data either message signal or interference information is sent to the UE2UE link receivers.

(iii) **Resource Allocation Schemes:** deals with allocation/selection of UE2UE links in/for cellular channel resources with minimum interference to both cellular and D2D UEs.

Generally system throughput/data rate, spectral efficiency, power efficiency and outage probability are considered as the performance evaluation matrices in all interference management schemes for D2D communication.

Table 1.1 summarizes some of the relevant power control schemes to reduce the interference generated with D2D communication. In the table, D⇒C denotes that the technique addressed the problem of interference from D2D to cellular communication scenario. The performance indices used for the evaluation of each scheme is also listed in the table. The data listed in the table illustrates that power control is the most straightforward approach used to mitigate the interference from D2D to cellular communication. Various power control schemes have been proposed for downlink [45–49] and for uplink [51,52] to reduce the D2D interference to cellular UEs. These schemes do not consider the interference from BS2UE links to UE2UE links, i.e., the power control schemes try to improve the quality of only BS2UE link not UE2UE link. In addition, the main disadvantage of the power control schemes is the probability of D2D communication between UEs may become very low due to low transmission power [29].

Another area of research for the interference management in D2D communication is the re-transmission scheme. Various retransmission schemes for Interference Cancellation (IC) with their performance indices is presented in Table

Table 1.1: Summary of relevant Power Control Schemes for D2D communication underlying cellular network in literature

Author, Year	**Scenario**	**Contributions**	**Performance Evaluation Matrices**
Pekka Janis et al., 2009 [45–47]	D⇒C	Proposed a mechanism to limit the maximum D2D transmit power by utilizing cellular power control information.	SINR
Klaus Doppler et al., 2009 [48]	D⇒C	Uplink: The serving BS limit the maximum transmit power of the D2D transmitters. Downlink: The BS set the maximum D2D transmit power to a predetermined value.	Throughput
Chia-Hao Yu et al., 2009 [49]	D⇒C	Power control using greedy sum-rate maximization is proposed by guaranteeing a minimum data rate to cellular users.	Data Rate, Outage Probability
Hongnian Xing et al., 2010 [50]	D⇒C	Investigated fixed transmission power, fixed SINR target, open-loop and closed-loop power control schemes for D2D communications.	Transmission Power
Yongsheng Cheng et al., 2013 [51]	D⇒C	An uplink power control algorithm with temporary removal for D2D-enabled systems is proposed.	Outage Probability
Xiaohui Xu et al., 2015 [52]	D⇒C	An open loop fraction power control scheme to mitigate the D2D interference to the cellular UE is proposed.	Outage Probability

1.2. In the table, C⇒D denotes the technique that addressed the problem of interference from cellular to D2D communication scenario. The retransmission schemes [53, 54] tries to reduce the interference from BS2UE links to UE2UE links. The interference cancellation scheme in [53] generates a practical difficulty that the BS should know the Channel State Information (CSI) of links that are not connected to the BS. Interference cancellation methods in [53,54] concentrate to increase the reliability of UE2UE link only and these schemes are defined only for uplink cellular transmissions but not for downlink. Relay aided retransmission schemes [32, 55] require additional radio resources to relay the information from the D2D transmitter to the D2D receiver and thus operate with reduced

Table 1.2: Summary of Re-transmission Schemes for D2D communication underlying cellular network in literature

Author, Year	**Scenario**	**Contributions**	**Performance Evaluation Matrices**
Hyunkee Min et al., 2011 [53]	C⇒D	An interference cancellation scheme for uplink is developed. The BS resends the interference channel details to a D2D receiver to process interference cancellation.	Outage Probability
James C. F. Li et al., 2012 [54]	C⇒D	An incremental relay transmission scheme is proposed where a D2D transmitter sends data to both D2D receiver and BS. If needed, based on the D2D receiver feedback, the BS relays the data to the D2D receiver.	Spectral Efficiency
Bin Zhou et al., 2013 [32]	C⇒D	A method to improve the performance of wireless multicast services is proposed. The UEs which correctly decode the multicast data in a cluster retransmit the data to those UEs experiencing poor channel conditions via D2D links.	PDF of optimal number of retransmitters.
Monowar Hasan et al., 2014 [55]	C⇒D	A relay aided D2D communication underlying network is proposed where the D2D transmissions are directed through relays to enhance the performance.	Data Rate

spectral efficiency.

In comparison to power control and re-transmission schemes, the resource allocation schemes try to ensure QoS requirements for both cellular and D2D UEs. A summary of the relevant resource allocation schemes in literatures with their performance indices is listed in Table 1.3 and Table 1.4. Assigning separate resources for cellular and D2D communication to reduce the interference limits the spectral efficiency [42]. The resource allocation problem has been analysed based on the locations of cellular and D2D UEs to reduce cellular interference to D2D UEs in [56,57]. But here the scenario considered was with only one D2D pair

Table 1.3: Summary of Resource Allocation Scheme for D2D communication underlying cellular network in literature

Author, Year	**Scenario**	**Contributions**	**Performance Evaluation Matrices**
Chia-Hao Yu et al., 2011 [42]	D⇔C	Presented Orthogonal and Non-Orthogonal resource sharing modes for resource allocation between D2D and cellular communications	Throughput
Hyunkee Min et al., 2011 [56]	C⇒D	An interference limited area control scheme to control the interference from cellular UEs to D2D pair was proposed where the method allows the coexistence of BS2UE and a UE2UE pair if the Interference to Signal Noise Ratio (ISNR) at the UE2UE link receiver was less than a predetermined threshold.	Ergodic Capacity
YanfangXu et al., 2012 [58]	D⇔C	Analysed the resource allocation problem when cellular and D2D UEs are allocated resource separately and then the scenario where cellular UEs and D2D UEs are allocated resource jointly.	The number of permitted D2D pairs
H. Wang et al., 2012 [57]	C⇒D	Investigates which BS2UE and UE2UE pair can share a common radio resource with the distance between the cellular UE and D2D pair as the criteria to reduce the interference.	Outage Probability
Daquan Feng et al., 2013 [59]	D⇔C	A scenario with multiple D2D pair in the system is considered. A bipartite matching based scheme for the selection of suitable cellular partner for each UE2UE link is developed.	Throughput
Jiaheng Wang et al., 2013 [61]	D⇒C	An optimized resource sharing strategy is proposed to better utilize uplink cellular resources for a scenario with one D2D link as an underlay to multiple cellular users.	Average Throughput
P. Phunchongharn et al., 2013 [64]	D⇔C	A resource allocation scheme based on a column generation method is proposed to maximize the spectrum utilization by allowing multiple D2D transmissions in the same Resource Block of a cellular user.	Spectral Utilization Efficiency

Table 1.4: Summary of Resource Allocation Scheme for D2D communication underlying cellular network in literature contd.

Author, Year	**Scenario**	**Contributions**	**Performance Evaluation Matrices**
Guanding Yu et al., 2014 [60]	D⇔C	A joint mode selection and resource allocation scheme for D2D communication is proposed by considering cellular, dedicate and reuse modes for transmission	Throughput
Mahdi Hajiaghayi et al., 2014 [62]	D⇔D	Proposed a graph coloring algorithm to determine the set of interference free D2D groups when plurality of D2D connections share common resources.	Throughput
Lingyang Song et al., 2014 [28]	D⇔C	Presented the game-theoretic resource allocation methods for multi-hop cluster based D2D communication underlying a cellular network.	System Sum-rate
Qiang Wang et al., 2015 [63]	D⇔D	Proposed an interference alignment technique to mitigate in-cluster interferences by using nulling matrices at the BS and D2D receivers.	Average Capacity

sharing the cellular radio resources. Several other resource allocation schemes have been proposed [28, 42, 58–60] to maximize the overall system throughput and for avoiding interference from D2D to cellular communication and cellular to D2D communication. The resource allocation problem was also analysed by considering a single D2D pair in the system in [42,60,61]. The resource allocation problem for scenarios where multiple D2D links exist in the system have been extensively analysed [28,58,59], but majority of the proposed algorithms allocate the resources of each cellular UE to only one D2D pair. The problem of mutual interference among D2D users has only been addressed in [62, 63].

1.4.2 Relay-assisted D2D communication

Long distances and poor radio conditions between D2D UEs limit the benefits of D2D communication practically [65]. Therefore, a relay-assisted D2D transmis-

sion was proposed to deal with these constraints [65]. Here, the work considered LTE-Advanced (LTE-A) Layer-3 (L3) relays [66]. But this approach increases signalling overhead at the relays themselves in case of dense D2D communication scenarios. The concept of UE relaying was introduced in [27, 34, 35] where the D2D UEs act as relays between the Base Station (BS) and the cellular UEs when these UEs are located at the cell edges or in a poor coverage area. This transmission relayed through a UE is referred as relay mode of transmission in this thesis. Unlike the existing works, the relay transmission mode can be considered as an additional mode of transmission along with the existing cellular and D2D transmission modes.

Several research works in the field of D2D communication using Hungarian algorithm for solving linear assignment problems are illustrated in Table 1.5. It can be observed from the table that the Hungarian algorithm has been mainly applied in the area of interference cancellation [58,67] and resource allocation [59,68–71]. In case of interference cancellation approaches [58, 67], the Hungarian algorithm has been employed to allocate a cellular UE to each D2D pair in such way that the interference from D2D UEs to the cellular UEs is minimized. Whereas for resource allocation approaches [59, 68–71], the Hungarian algorithm has been employed to allocate resources to cellular and D2D UEs with an objective to maximize the overall throughput. The Hungarian algorithm based relay selection and sub-channel resource allocation in relay-assisted D2D communication scheme was investigated in [71]. In this work, we utilize the Hungarian algorithm to select a suitable transmission mode and a UE which should behave as the relay UE in the relay transmission mode. The overall system throughput is considered as the maximizing parameter for the Hungarian algorithm.

Table 1.5: Summary of research works based on the Hungarian algorithm in D2D communication

Author, Year	**Purpose**	**Use of the Hungarian algorithm**	**Maximizing/ Minimizing Parameter**
Tao Han et al., 2012 [67]	Interference cancellation	Allocating cellular UE partner to each D2D pair with minimum interference to cellular UEs.	Minimizing interference to cellular users
Yanfang Xu et al., 2012 [58]	Interference cancellation & Resource allocation	Independently allocating resources for cellular and D2D UEs with reduced interference from D2D UEs.	Minimizing interference from D2D UEs
Daquan Feng et al., 2013 [59]	Resource allocation	Determine a specific cellular UE partner for each admissible D2D pair.	Maximizing overall network throughput
Nannan Chen et al., 2014 [68]	Resource allocation	Assigning cellular UE partners for D2D pairs in a cluster for closely located D2D users.	Maximizing overall system capacity
Jiang Han et al., 2014 [69]	Resource allocation	Optimally allocate resources for D2D communication underlaying a cellular network.	Maximizing throughput
Li Wang et al., 2014 [70]	Resource allocation	Find an optimal D2D link matching for the cellular user partner.	Maximizing sum data rate of all users
Taejoon Kim et al., 2014 [71]	Relay Selection & Resource allocation	Proposed iterative Hungarian method for relay selection and sub-channel allocation for relay-assisted D2D communications.	Throughput maximization

1.5 Objectives of the work

Several cluster topologies per cell can be considered where the term topology refers to the arrangement of D2D communication links in the cluster. Each cluster comprises of one or several UEs which share the same resources when communicating among themselves. In the Cluster Head (CH) based control topology, one UE assumes master role and acts as the CH within the cluster. The CH is like a BS and help to achieve local synchronization, manage radio resources, schedule D2D transmissions, and more for slave UE devices in its

cluster. The disadvantage of the CH based topology is that the CH becomes the control bottleneck and its battery is drained.

The coexistence of multiple UE2UE links with a cellular channel resource, especially for the case of D2D cluster-based communications, can be considered to enhance the spectral efficiency. As described in Section 1.4, this scenario results in different type of interferences viz. cellular to D2D, D2D to cellular and D2D to D2D interferences. Most of the interference management approaches were reported for handling interference for either cellular to D2D or D2D to cellular, or both. The interference management approaches for handling D2D to D2D interferences need to be further investigated. The interference management approaches for simultaneously handling these three interference scenarios in a cluster based network have been very limited. In addition, most of the aforementioned works considered that the radio resource of a cellular UE is shared by atmost one UE2UE link and interference suppression approaches are formulated and analysed by considering a single interference link. But did not talk of handling the co-channel interferences generated in multi-link environments for cluster-based D2D communications. Other deployment scenarios need to be investigated and analysed for better utilization of the advantages imparted by D2D communication underlaying cellular network.

Under the framework of the above mentioned prerequisites, the objectives that this thesis has worked towards can be outlined as:

- To propose an interference cancellation method for single link and multi-link D2D cluster based approach to guarantee a reliable communication for every UE in the cluster. The proposed method should simultaneously handle cellular to D2D, D2D to cellular and D2D to D2D interferences.

- Mathematical validation of the proposed method need to be carried out in terms of system throughput and outage probability in comparison with

other existing interference cancellation approaches in the literature.

- To propose an efficient resource allocation procedure for network assisted multi-link D2D communication to realize the proposed interference cancellation method.

- To investigate relay transmission mode as an additional mode of transmission along with the existing cellular and D2D transmission modes. The selection of relay UEs need to be tackled by using matching algorithms.

1.6 Contributions of the Thesis

In comparison with previous research works, the major contributions of this research work is summarized in Figure 1.6. The research work initially focused to handle the interferences generated with single link D2D communication where the cellular UE resources are being shared by a D2D link and our work outlined the following major contributions:

- Proposed an IC method based on orthogonal precoding to handle cellular to D2D and D2D to cellular interferences.

- Presented the implementation procedures of the proposed method for intra-cell, inter-cell and neighbouring intra-cell D2D communication scenarios.

- Closed form expressions for the ergodic capacity and outage probability with the proposed method are analytically derived and compared with a conventional IC method [53] for validation.

The proposed method is then extended for the case of cluster based multi-link D2D communication where interference among D2D UEs also exists since the cellular UE resources are being shared by multiple D2D links. For sharing

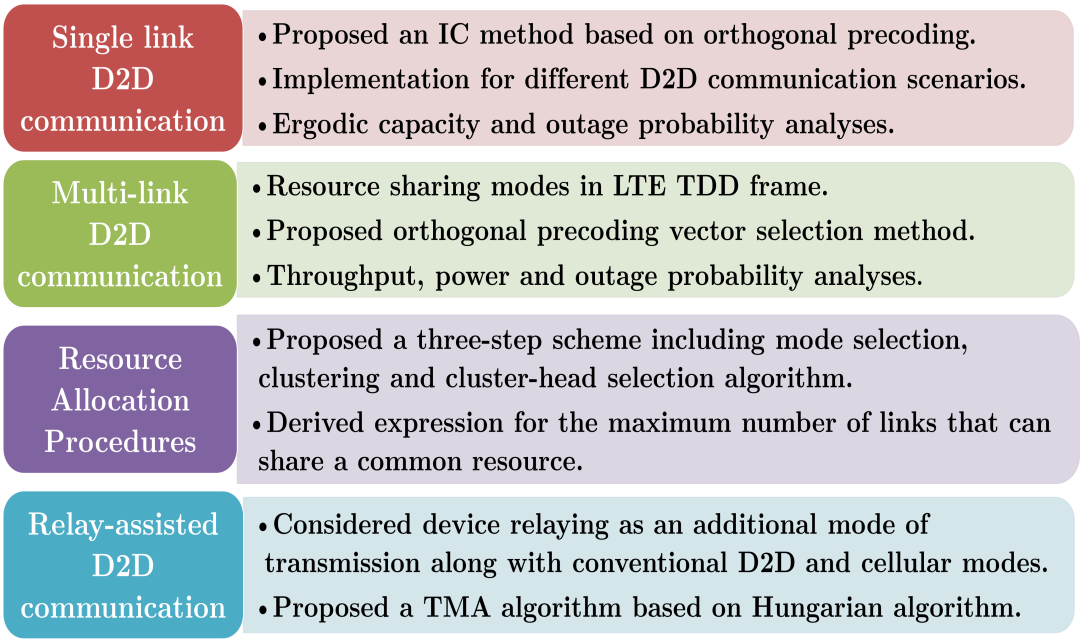

Figure 1.6: Research work outline where IC and TMA denotes Interference Cancellation and Transmission Mode Assignment respectively.

the communication links, two resource sharing modes are addressed by considering the LTE frame structure [72]: (1) Orthogonal Sharing (OS) and (2) Non-Orthogonal Sharing (NOS). An Orthogonal Precoding (OP) vector selection method is then proposed for optimal selection of precoding vectors for both OS and NOS modes. Evaluation of the proposed method is then carried out in terms of throughput and power analysis. Two lemmas are derived to calculate the closed form expressions for the outage probabilities of the proposed method and conventional IC method as in [53].

Subsequently, an efficient resource allocation procedure for network assisted multi-link D2D communication is proposed to better realize the proposed IC method. The resource allocation procedure includes:

- A mode selection algorithm to determine the mode of communication for each UEs in the cell by considering the quality and interference level of D2D and cellular connection.

- A clustering algorithm to determine the UEs that can share a common resource.
- A Cluster Head (CH) selection algorithm based on the maximum residual energy and minimum transmit power criteria to choose the cellular UE whose resources are being shared.

In addition to the resource allocation procedure, the expression for the maximum number of links that the radio resource of CH can support is also analytically derived. A relay-assisted D2D communication is next analysed to extend the D2D coverage when there is large distance between the potential D2D transmitter and receiver. In the relay-assisted communication the relay mode is considered as an additional mode of transmission along with the existing cellular and D2D transmission modes. A transmission mode assignment algorithm based on the Hungarian algorithm is then proposed to solve two main problems: (i) selection of suitable transmission mode for each scheduled transmissions and (ii) selection of relaying UEs for the relay transmission mode. The evaluation of the proposed method along with complexity analysis are carried out in terms of D2D mode access rate and overall system throughput. Comparison of the proposed algorithm is carried out with the traditional D2D communication scheme [59] and a random allocation algorithm as in [69].

1.7 Thesis Organization

This section presents the organization of this thesis work. This thesis is presented in 7 chapters. Following this chapter on introduction, the remaining thesis is organized as follows:

- **Chapter 2:** A novel orthogonal MIMO precoding approach to reduce the mutual interference between BS2UE and UE2UE links is proposed for D2D communication underlaying cellular network. The chapter also discusses

the possibility of implementing the proposed method. The mathematical analysis of the proposed method is carried out in terms of maximum achievable data-rate.

- **Chapter 3:** In this chapter, a novel orthogonal precoding vector selection method is proposed for reducing co-channel interference when multiple D2D links share a common resource as in a cluster and thus maximizing the achievable data rate at each device in the cluster. The evaluation of the proposed method in terms of throughput and power analyses for different resource sharing modes is presented.

- **Chapter 4:** The expression for the outage probability of the proposed orthogonal MIMO precoding method is derived for single and multi-link D2D communication in this chapter.

- **Chapter 5:** In this chapter, a mode selection algorithm is first proposed. Efficient utilization of cellular spectrum can be achieved by sharing cellular links with multiple D2D links which is determined by the process of clustering and a cluster head selection procedure is also proposed based on the maximum residual energy and minimum transmit power criteria. Finally, the expression for maximum number of links that the radio resource of CH can support is analytically derived based on the quality of CH-to-BS (CH2BS) link.

- **Chapter 6:** A transmission mode assignment algorithm based on the Hungarian algorithm is proposed to improve the overall system throughput by considering device relaying as an additional transmission mode along with the existing cellular and D2D transmission modes.

- **Chapter 7:** This chapter provides the concluding remarks along with future research aspects for the thesis work.

1.8 Summary

This chapter begins with a brief history of mobile cellular standard along with the need of D2D communication underlaying cellular network. The survey on different interference cancellation schemes for D2D communication and relay-assisted D2D communication is presented. The chapter outlines the motivation for the research work and provided a concise chapter wise presentation of research work carried out for the thesis.

CHAPTER 2

Interference Cancellation for Single-link D2D communication

Contents

D2D communication underlaying cellular network results in various interference scenarios. This aspect was discussed in Chapter 1. In this chapter, a novel method to reduce the interference at receivers of both the UE2UE and BS2UE links is proposed when the cellular resources are being shared by a single UE2UE link. Additionally, a possible approach to implement the proposed method is also presented. The proposed method is then mathematically analysed in terms of capacity and the performance is compared with conventional MIMO precoding vector allocation method.

2.1 Introduction

In D2D communication, each scheduled transmissions in the cell can be done either through cellular/BS2UE link or D2D/UE2UE link. The UE2UE link can be considered as an underlay to cellular networks and may not necessarily have dedicated channel resources. The UE2UE link communications can use either uplink or downlink cellular channel resources. Such sharing mode bring forth cellular to D2D and D2D to cellular interferences. The cellular to D2D interference refers to interference from BS2UE link at D2D UE and latter refers to interference from UE2UE link at cellular UE. Various interference scenarios generated with D2D communication underlaying cellular network is shown in the Figure 2.1. Figure 2.1(a) and Figure 2.1(b) show the interference scenario with downlink and uplink communications respectively.

When D2D UEs share downlink cellular resources as in Figure 2.1(a), the interference source consist of the BS in the same cell. Since a D2D pair is normally formed between two UEs with physical proximity, the power needed for D2D communications is much lower than that for traditional cellular communications. As a result, the D2D signals are interfered by the high-power BS

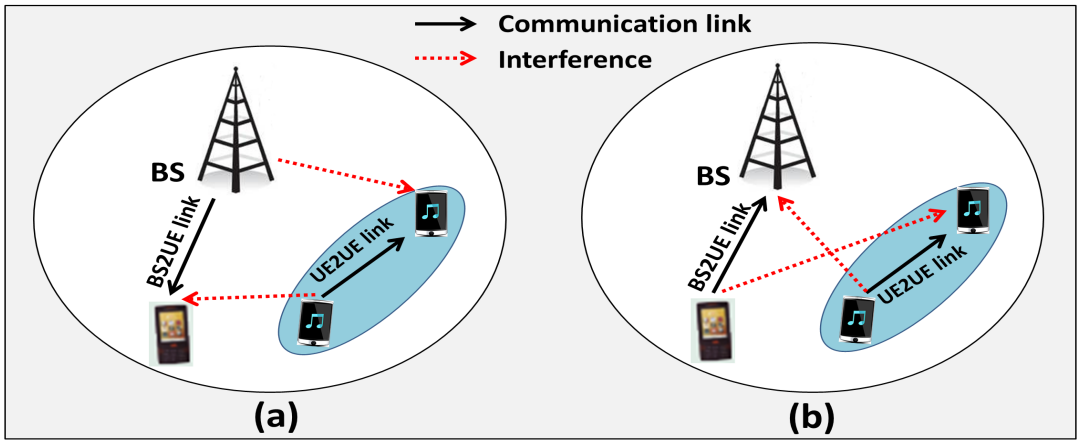

Figure 2.1: Interference in D2D communication: (a) downlink (b) uplink

transmissions. In addition, the D2D communication can interfere with nearby cellular UE receiver(s) when the D2D transmitters are located close to those UEs.

When the D2D UEs share the uplink cellular resources, the interference sources consist of interference from the co-channel cellular UE. Here, the co-channel cellular UE refers to the cellular UE whose resource is being shared by the UE2UE link. For cellular UEs on the uplink, the interference comes from the co-channel D2D UE who shares the cellular channel resource.

Thus, the D2D communication underlaying cellular network bring forth cellular to D2D and D2D to cellular interferences. Hence an interference management technique is required to guarantee reliable communication for both UE2UE and BS2UE links in uplink and downlink.

2.2 Precoding Technique

With the aim of reducing the receiver complexity and due to the lack of cooperation between users, the signal processing complexity is transferred to the BS by means of a processing stage called precoding. There are two main reasons that the precoding techniques are so important in wireless MIMO systems. One is

that if the precoding techniques are applied at the source signals before they are transmitted it reduces the performance loss caused by interference and channel fading. Thus, the advantage of MIMO system will be enhanced. On the other hand, it is well known that the BS has more powerful computing ability and the power supply is normally not an issue at the BS. Therefore, if the detection processing approaches can be removed from the receive side to the transmit side, the structure of UE would be simplified and a significant amount of power can be saved which is very important considering the mobility of the UE.

To know CSI at the transmitter, perfect channel feedback to transmitter is required which is practically not possible. Usually, a limited feedback mechanism is adopted where a receiver informs transmitter about an index of precoding vector from a codebook, $\mathbb{W}$. The index of corresponding precoding matrix is carried by PMI (Precoding Matrix Index) field that is part of CSI [72]. This precoding vector is used at the transmitter and receiver to precode and decode the signal.

2.3 System Model for Single link D2D communication

In our analysis, we consider a model where a bidirectional cellular and D2D communications are established through BS2UE and UE2UE links respectively. It is assumed that all UEs operate in TDD (Time Division Duplex) mode [72] and hence the reciprocity of channels between the uplink and downlink cellular and D2D links apply here.

Lets consider the case shown in Figure. 2.2 when the D2D communication takes place within a cell in which the transmitting device (UE_1) sends data to the receiving device (UE_2) and the UE_0 receives data from the BS. The UE2UE link channel is denoted as $\mathbf{H}_2$ and the BS2UE one as $\mathbf{H}_0$. The interference channel generated by BS at UE_2 is denoted as $\mathbf{H}_3$. Similarly, the interference channel

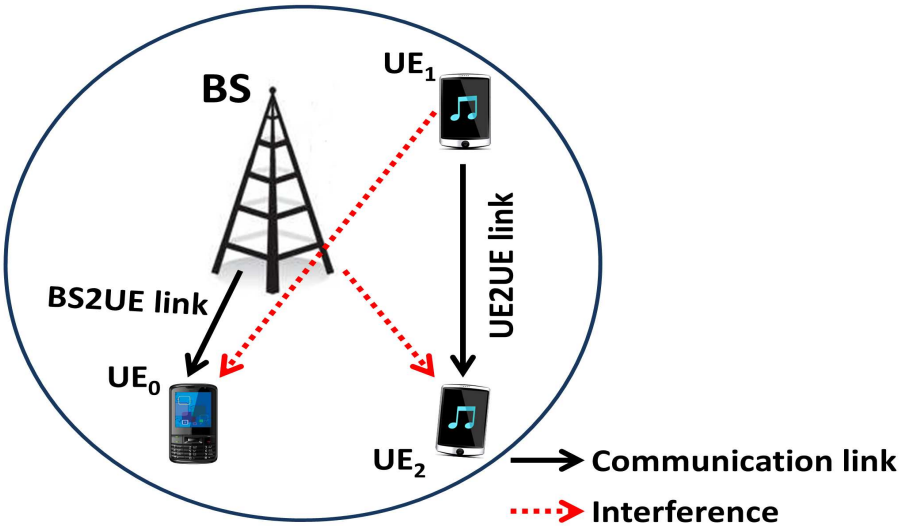

Figure 2.2: The interfering signals in the downlink transmissions of a given cell with Intra-cell D2D communication

generated by UE_1 at UE_0 is denoted as $\mathbf{H}_1$. The received signals $\mathbf{y}_0$ at UE_0 and $\mathbf{y}_2$ at UE_2 can be written based on [75] as:

$$\mathbf{y}_0 = \sqrt{P_0}\mathbf{H}_0\boldsymbol{\psi}_0 s_0 + \sqrt{P_1}\mathbf{H}_1\boldsymbol{\psi}_2 s_2 + \boldsymbol{\eta}_1 \tag{2.1}$$

$$\mathbf{y}_2 = \sqrt{P_2}\mathbf{H}_2\boldsymbol{\psi}_2 s_2 + \sqrt{P_3}\mathbf{H}_3\boldsymbol{\psi}_0 s_0 + \boldsymbol{\eta}_2 \tag{2.2}$$

where P_i is the transmit power for transmission in channel $\mathbf{H}_i$, $\boldsymbol{\psi}_0$ and $\boldsymbol{\psi}_2$ are the transmit precoding vectors of BS2UE and UE2UE links, s_0 and s_2 are the transmitted signals by BS and UE_1 respectively and η_1 and η_2 represent the Additive White Gaussian Noise (AWGN) at receivers UE_0 and UE_2.

We assume a maximal ratio combiner (MRC) with linear combining to be used to decode signals at the receiver [73]. The weights of linear combiner at UE_0 and UE_2 are $\mathbf{w}_0 = \mathbf{H}_0\boldsymbol{\psi}_0$ and $\mathbf{w}_2 = \mathbf{H}_2\boldsymbol{\psi}_2$ respectively [74]. The output of combiner at UE_0, Υ_0, and UE_2, Υ_2, is given by:

$$\Upsilon_0 = \mathbf{y}_0\mathbf{w}_0^H \tag{2.3}$$

$$\Upsilon_2 = \mathbf{y}_2 \mathbf{w}_2^H \tag{2.4}$$

The SINR at UE_0 and UE_2 can be then calculated as:

$$\gamma_0 = \frac{||\mathbf{H}_0 \boldsymbol{\psi}_0 \boldsymbol{\psi}_0^H \mathbf{H}_0^H||^2}{I_r^1 ||\mathbf{H}_1 \boldsymbol{\psi}_2 \boldsymbol{\psi}_0^H \mathbf{H}_0^H||^2 + \frac{1}{\xi_0}\mathbf{I}} \tag{2.5}$$

$$\gamma_2 = \frac{||\mathbf{H}_2 \boldsymbol{\psi}_2 \boldsymbol{\psi}_2^H \mathbf{H}_2^H||^2}{I_r^2 ||\mathbf{H}_3 \boldsymbol{\psi}_0 \boldsymbol{\psi}_2^H \mathbf{H}_2^H||^2 + \frac{1}{\xi_2}\mathbf{I}} \tag{2.6}$$

where I_r^1 and I_r^2 are the power ratio of interference signal to the desired signal at UE_0 and UE_2 respectively and $\xi_0 = \frac{P_0}{N_0}$, $\xi_2 = \frac{P_1}{N_0}$, N_0 is the power spectral density of AWGN. Since the cellular signals have greater power than D2D signals, the value of I_r^2 can be greater than 1 while calculating γ_2. Whereas, the value of I_r^1 will always be less than 1.

2.4 Problem Formulation and Proposed method

To know $\boldsymbol{\psi}_i$ at the transmitter, perfect channel feedback to transmitter is required which is practically not possible. Usually, a limited feedback mechanism is adopted where a receiver informs transmitter about an index of precoding matrix, $\boldsymbol{\psi}_i$, from a codebook, $\mathbb{W}$ [72]. In conventional MIMO precoding (CMP) method, $\boldsymbol{\psi}_i$ is chosen based on the following criteria [75]:

$$arg \max_{\boldsymbol{\psi}_i \in \mathbb{W}} ||\mathbf{H}_i \boldsymbol{\psi}_i||^2 \tag{2.7}$$

The index of corresponding precoding matrix is carried by PMI (Precoding Matrix Index) field that is part of Channel State Information (CSI) [76]. This $\boldsymbol{\psi}_i$ is used at the transmitter and receiver to precode and decode the signal.

With limited feedback mechanism, there is reduction in overall system ca-

pacity. To maximize γ_0 and γ_2, the interference term in the denominator should be minimized. For minimizing the interference term, we propose an orthogonal MIMO precoding (OMP) method. In OMP method, orthogonality between precoding matrices of the BS2UE and UE2UE links is maintained in-order to reduce the interference. For the selection of precoding matrix for UE2UE link using OMP method, a set of matrices which are orthogonal to BS2UE link precoding matrix is initially generated. The CMP method is then used to choose the desired precoding matrix among them.

The interference terms for γ_0 and γ_2 are $I_r^1||\mathbf{H}_1\boldsymbol{\psi}_2\boldsymbol{\psi}_0^H\mathbf{H}_0^H||^2$ and $I_r^2||\mathbf{H}_3\boldsymbol{\psi}_0\boldsymbol{\psi}_2^H\mathbf{H}_2^H||^2$ respectively. If $\boldsymbol{\psi}_0$ and $\boldsymbol{\psi}_2$ are orthogonal to each other, the term $\boldsymbol{\psi}_2\boldsymbol{\psi}_0^H$ in (2.5) and $\boldsymbol{\psi}_0\boldsymbol{\psi}_2^H$ in (2.6) reduce to zero. The cellular to D2D and D2D to cellular interferences are thus minimized.

2.5 Method of Implementation

The MIMO precoding with feedback from the UE is currently used in LTE for the purposes of enhancing the link quality and for the multi-user MIMO scheme (MU MIMO). The UE measures the received channel quality (SINR) and reports it back to the BS via Channel Quality Indicator (CQI) field that is part of Channel State Information (CSI) which provides the time and frequency variant channel quality information for subsequent MIMO transmissions [76].

In our proposition, the measured SINR designates an index based on which the BS allocates precoding vectors for the UE2UE and BS2UE links. More specifically, the BS obtains the SINR from the cellular UE and D2D UE receiver. Then the UE2UE link is assigned a precoding vector orthogonal to the one for the BS2UE link. From the point of view of BS2UE and UE2UE links, we can consider the following three scenarios: A) D2D communication within a serving cell (Intra-cell D2D communication), B) D2D communication across two cells (Inter-cell

D2D communication), and C) D2D communication within a neighbouring cell (Neighbouring Intra-cell D2D communication).

2.5.1 Scenario A: Intra-cell D2D communication

The Scenario A is shown in Figure 2.2. The scenario includes a downlink BS2UE link (i.e., the UE receives signal from the BS) with one UE2UE link where the communication between the UE_1 and UE_2 takes place inside one cell, i.e. serving cell.

Figure 2.3 shows the procedure for allocating precoding matrix with the proposed method. UE_0 may communicate with the BS via the downlink or uplink channel. For downlink transmission, the BS requests feedback from the UE_0. The UE_0 estimates the channel and selects a precoding matrix from the codebook based on the CMP method and transmits the PMI feedback information to the BS. The corresponding precoding matrix is used to precode the signal for downlink transmission. In network assisted D2D communication, the BS assigns resources for direct UE2UE communication between UE_1 and UE_2. At the time of allotting resources, the BS sends the PMI of BS2UE link to UE2UE link receiver, UE_2. UE_2 selects the precoding matrix based on OMP method and the PMI is fed back to UE_1. UE_1 uses the corresponding precoding matrix to precode the signal. Since channel reciprocity occurs between uplink and downlink channel in TDD systems, the chosen precoding matrices can be used for both uplink and downlink channel of cellular and D2D communication. Thus the orthogonality between the precoding matrices of CH2BS and UE2UE links are maintained in both uplink/downlink cellular and D2D transmissions.

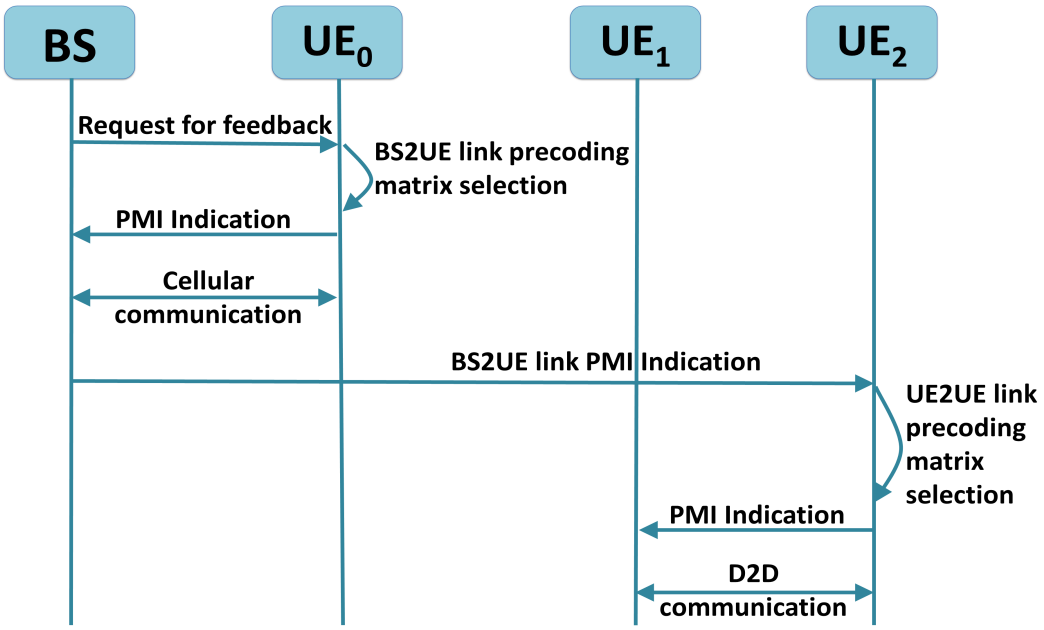

Figure 2.3: Precoding matrix allocation procedure for D2D communication with OMP method

2.5.2 Scenario B: Inter-cell D2D communication

Comparing to scenario A, the inter-cell D2D communication scenario assumes that UE_1 and UE_2 are located in neighbouring cells. The Scenario B is presented in Figure 2.4 where the UE_1 is placed in the serving cell and communicates with UE_2 placed in the neighbouring cell. This scenario results in interference at the UE_0 and UE_2. The selection process of precoding matrix for Scenario B is similar to Scenario A and is illustrated in Figure 2.5. The serving cell base station, BS_1, obtains the CSI from the UE_0 and selects the appropriate precoding matrix for BS2UE link. The PMI of BS2UE link is then sent to UE_2 via neighbouring cell base station, BS_2. Accordingly, UE_2 selects the precoding matrix based on OMP method and the PMI is fed back to UE_1.

In case, if we interchange the position of UE_1 and UE_2 (i.e. the UE_1 is placed in the neighbouring cell and UE_2 in the serving cell), the UE_2 will receive the PMI of BS2UE link directly from BS_1 for precoding matrix selection.

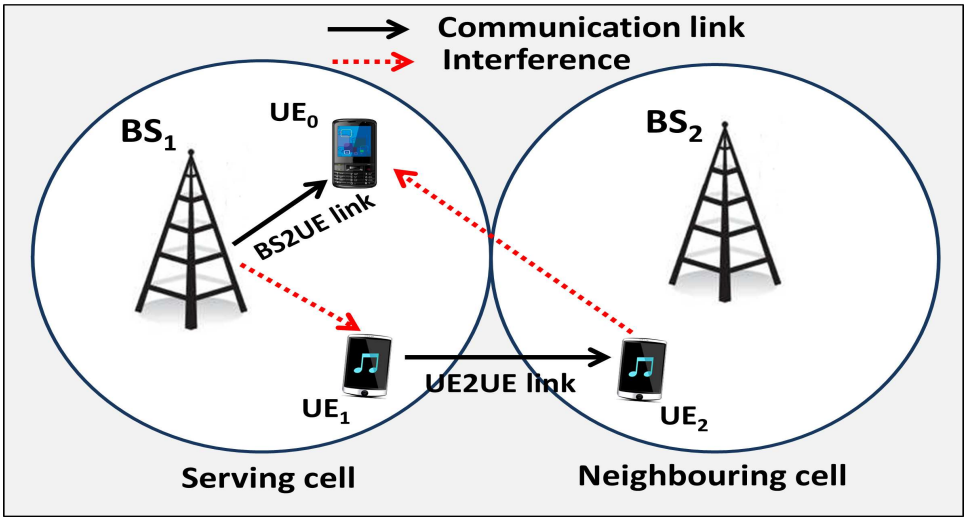

Figure 2.4: D2D communication across two cells (Inter-cell D2D communication)

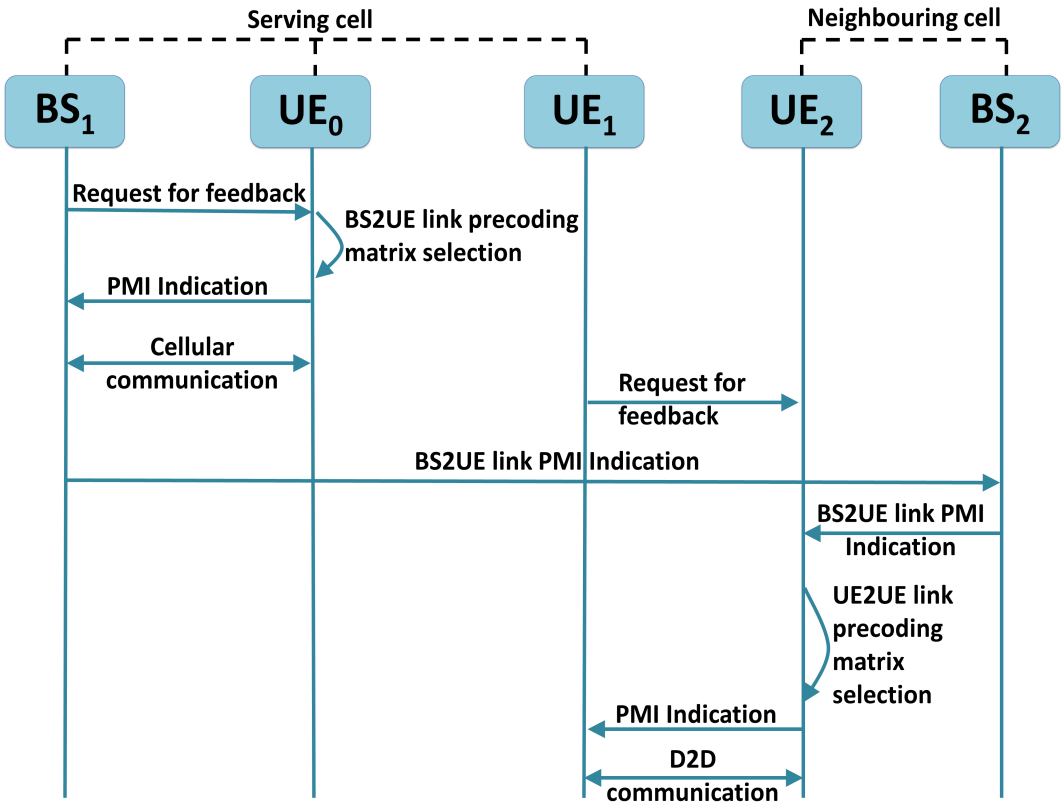

Figure 2.5: Precoding matrix selection process flow of Inter-cell D2D communication

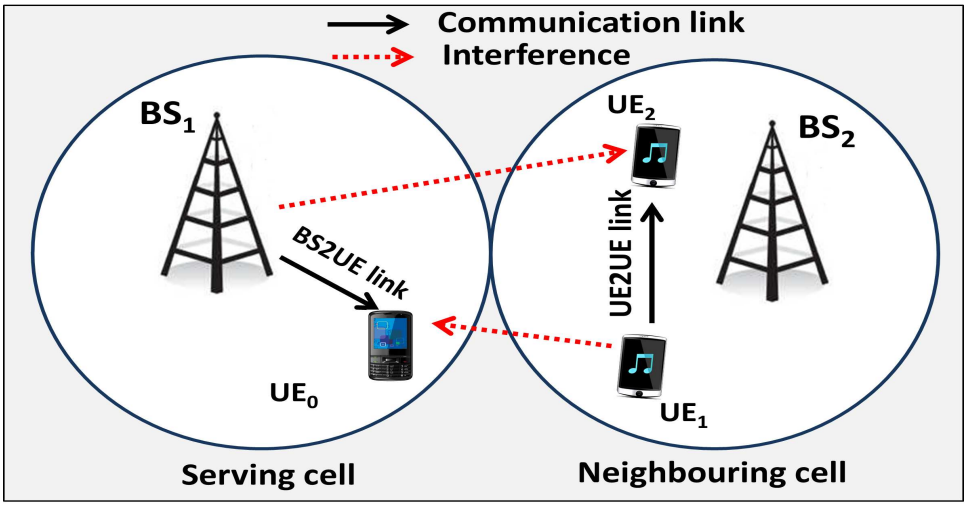

Figure 2.6: D2D communication within a neighbouring cell (Neighbouring Intra-cell D2D communication)

2.5.3 Scenario C: Neighbouring Intra-cell D2D communication

Finally, Figure 2.6 illustrates the third scenario where both UE_1 and UE_2 are located in the neighbouring cell but the UE2UE link still shares the resources with the serving cell. The selection process of precoding matrix with OMP method for Scenario C can be executed similar to Scenario B.

2.6 Ergodic capacity of D2D system with OMP and CMP methods

In this section, we theoretically evaluate the performance of the proposed OMP method and compared with the conventional CMP method of precoding matrix allocation. The performance is evaluated in terms of the ergodic capacity. The system model described in Section 2.3, where the same resource is being shared for a BS2UE and UE2UE transmissions is considered.

For deriving the ergodic capacity, we consider a general scenario with i^{th} and j^{th} links as the desired and interference links respectively. Then, the relationship for SINR can be written as:

$$\gamma_i = \frac{||\mathbf{H}_i \boldsymbol{\psi}_i \boldsymbol{\psi}_i^H \mathbf{H}_i^H||^2}{I_r ||\mathbf{H}_j \boldsymbol{\psi}_j \boldsymbol{\psi}_i^H \mathbf{H}_i^H||^2 + \frac{1}{\xi}\mathbf{I}} \tag{2.8}$$

where I_r is the power ratio of j^{th} link to i^{th} link and ξ is the SNR. In 2005, Maaref et al. derived the expression for the ergodic capacity of MIMO MRC systems and the ergodic capacity in b/s/Hz can be written as [77]:

$$C = \int_0^\infty \log_2(1+\gamma) f_\gamma(\gamma) \mathrm{d}\gamma \tag{2.9}$$

where $f_\gamma(\gamma)$ is the Probability Density Function (PDF) of γ in equation (2.8).

2.6.1 Ergodic capacity with the proposed OMP method

With the proposed OMP method, the precoding vectors of i^{th} and j^{th} links are orthogonal to each other and hence the term $I_r ||\mathbf{H}_j \boldsymbol{\psi}_j \boldsymbol{\psi}_i^H \mathbf{H}_i^H||^2 = 0$ in (2.8). Hence PDF of γ with the proposed OMP method can be written as [53]:

$$f_\gamma(\gamma) = \frac{1}{\xi} \exp(-\frac{\gamma}{\xi}) \mathbf{U}(\gamma) \tag{2.10}$$

where $\mathbf{U}(.)$ is the unit step function [53]. Thus substituting (2.10) into (2.9), the ergodic capacity can be calculated as:

$$C = \int_0^\infty \log_2(1+\gamma) \frac{1}{\xi} \exp(-\frac{\gamma}{\xi}), \mathrm{d}\gamma \tag{2.11}$$

Using integration by parts theorem [78], the expression in (2.11) is reduced to:

$$C = \int_0^\infty \frac{1}{1+\gamma} \exp(-\frac{\gamma}{\xi}), \mathrm{d}\gamma \tag{2.12}$$

The final expression for the ergodic capacity of D2D systems with the proposed OMP method can be derived based on [78] as:

$$C = -\exp\left(\frac{1}{\xi}\right)\mathbf{Ei}(-\frac{1}{\xi}) \tag{2.13}$$

where **Ei** is the exponential integral function which is defined as [78]:

$$\mathbf{Ei}(x) = -\int_{-x}^{\infty} \frac{\exp(-t)}{t}, \mathrm{d}t \tag{2.14}$$

2.6.2 Ergodic capacity with the conventional CMP method

To calculate the ergodic capacity of the conventional CMP method, consider $x = ||\mathbf{H}_i\psi_i\psi_i^H\mathbf{H}_i^H||^2$ and $y = I_r||\mathbf{H}_j\psi_j\psi_i^H\mathbf{H}_i^H||^2 + \frac{1}{\xi}I$. Then, the PDF of x and y based on [53] can be written as:

$$f_X(x) = \exp(-x)\mathbf{U}(x) \tag{2.15}$$

$$f_Y(y) = \frac{1}{I_r}\exp\left(-\frac{y-\frac{1}{\xi}}{I_r}\right)\mathbf{U}\left(y-\frac{1}{\xi}\right) \tag{2.16}$$

Using [[56], eq. (11)], the PDF of $\gamma = x/y$ can be calculated as:

$$\begin{aligned} f_\gamma(\gamma) &= \int_0^\infty y f_{xy}(y\gamma, y)\mathrm{d}y \\ &= \left[\frac{1}{(1+I_r\gamma)\,\xi} + \frac{I_r}{(1+I_r\gamma)^2}\right]\exp\left(-\frac{\gamma}{\xi}\right) \end{aligned} \tag{2.17}$$

In order to reduce the complexity in calculation of ergodic capacity, we use a high SNR approximation of (2.17), i.e., substituting $\frac{1}{\xi} \approx 0$ into (2.17). Then the PDF of γ is obtained as:

$$f_\gamma(\gamma) = \frac{I_r}{(I_r\gamma - 1)^2} \tag{2.18}$$

Thus the ergodic capacity is obtained by substituting (2.18) into (2.9) and can be written as:

$$C = \int_0^\infty \log_2(1+\gamma)\frac{I_r}{(I_r\gamma - 1)^2}, \mathrm{d}\gamma \tag{2.19}$$

The final equation for ergodic capacity in (2.19) is evaluated based on [78] and is expressed as:

$$C = \frac{1}{I_r \ln 2} \times_2 F_1\left(1, 1; 2; 1 + \frac{1}{I_r}\right) \tag{2.20}$$

where ${}_2F_1\left(1, 1; 2; 1 + \frac{1}{I_r}\right)$ is the hyperbolic function [78].

2.7 Results and Discussion

In our simulation, we use the model described in Section 2.3; a single BS2UE and UE2UE links. The transmitter and receiver of UE2UE and BS2UE links are considered to have two antennas, i.e. 2x2 antenna configuration. The precoding matrices for BS2UE and UE2UE links are chosen from the codebook $\mathbb{W}_{2\times2}$ based on the 3GPP specifications (Appendix A). Throughput at a UE receiver (either BS2UE or UE2UE receiver) are evaluated with the proposed OMP method and presented in this section. The simulation tool used for the analysis is developed by using MATLAB software. The simulation parameters and other considered parameters are summarized in Table 2.1.

System performance with the proposed OMP method of precoding matrix allocation in terms of capacity is presented and compared with the conventional CMP method of precoding matrix allocation. With the proposed OMP method, the precoding matrices chosen for BS2UE and UE2UE links are $\mathbf{W}_{(0)}$ and $\mathbf{W}_{(1)}$ respectively from the codebook, $\mathbb{W}_{2\times2}$ [72]. Whereas, the corresponding precoding matrices are $\mathbf{W}_{(0)}$ and $\mathbf{W}_{(3)}$ with conventional CMP method.

Table 2.1: Simulation Parameters for Single link D2D communication analysis

Parameter	**Value**
Channel Bandwidth, B	10 MHz
Power ratio of Interference signal to the Desired signal, I_r	0.5
SNR, ξ	20 dB
MIMO Configuration	2×2

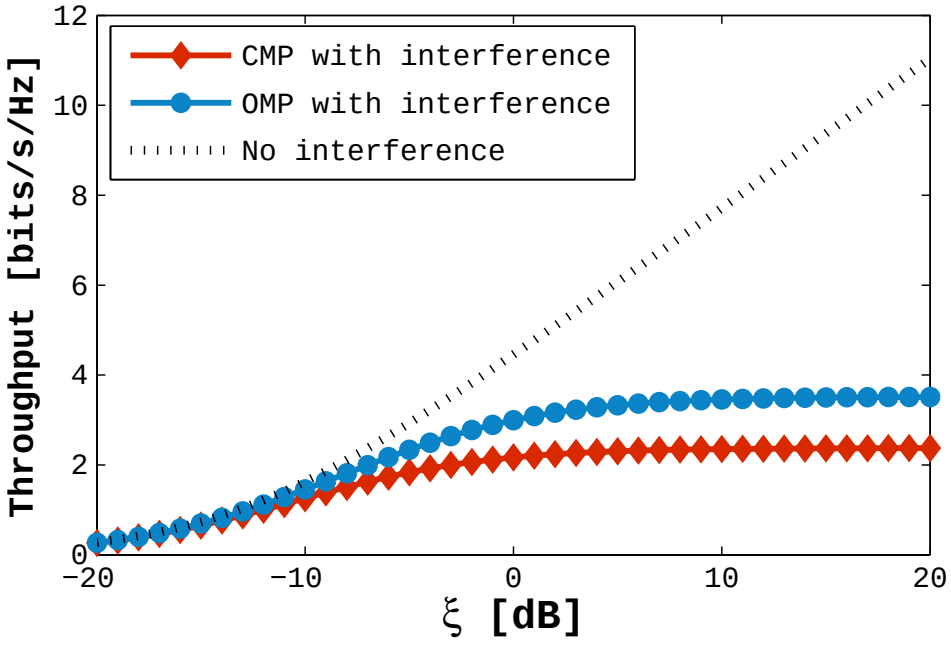

Figure 2.7: Throughput vs SNR, ξ, plot of OMP method, CMP method and the case without interference

Figure 2.7 compares the performance of proposed OMP method and conventional CMP method in terms of throughput. The maximum capacity that can be achieved without any interference is also shown in the figure. Result shows that the proposed method does not bring significant improvement if the noise highly dominates i.e SNR ≤ -10 dB. However, with SNR > -10 dB, our proposition leads in larger capacity enhancement. It can be observed from the figure that

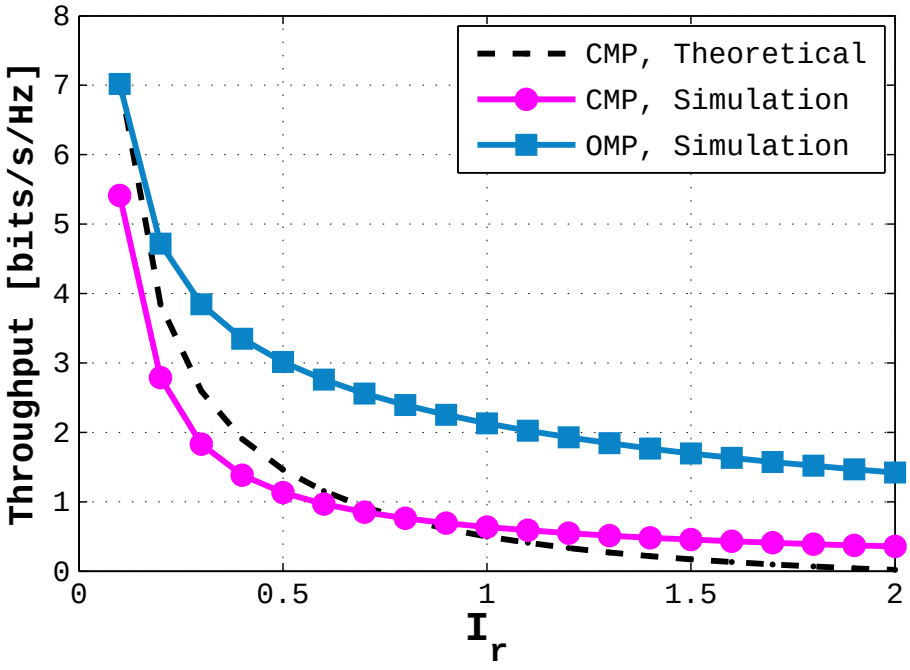

Figure 2.8: Throughput vs Power ratio of interference signal to the desired signal, I_r, plot for OMP and CMP methods

there is about 35% to 40% capacity improvement with the proposed method.

Figure 2.8 presents the throughput vs I_r plot for D2D communication underlaying cellular network. The obtained simulation results for OMP based method is compared with the theoretical analysis of CMP method [56]. The simulation analysis is carried out using the proposed OMP and the conventional CMP method for the precoding vector selection. Since a high SNR approximation is assumed for theoretical analysis, a high value of ξ, say $\xi = 25$ dB, is considered for simulation. The simulation result using the conventional CMP criteria is validated with the theoretical analysis. The theoretical throughput analysis of the D2D communication system for the proposed method is carried out by considering perfect interference cancellation with the proposed method. Hence, the throughput expression for the proposed method is independent of the term I_r. The result shows that the throughput reduces with increase in I_r. Throughput maximization with reduced interference using the proposed method in compari-

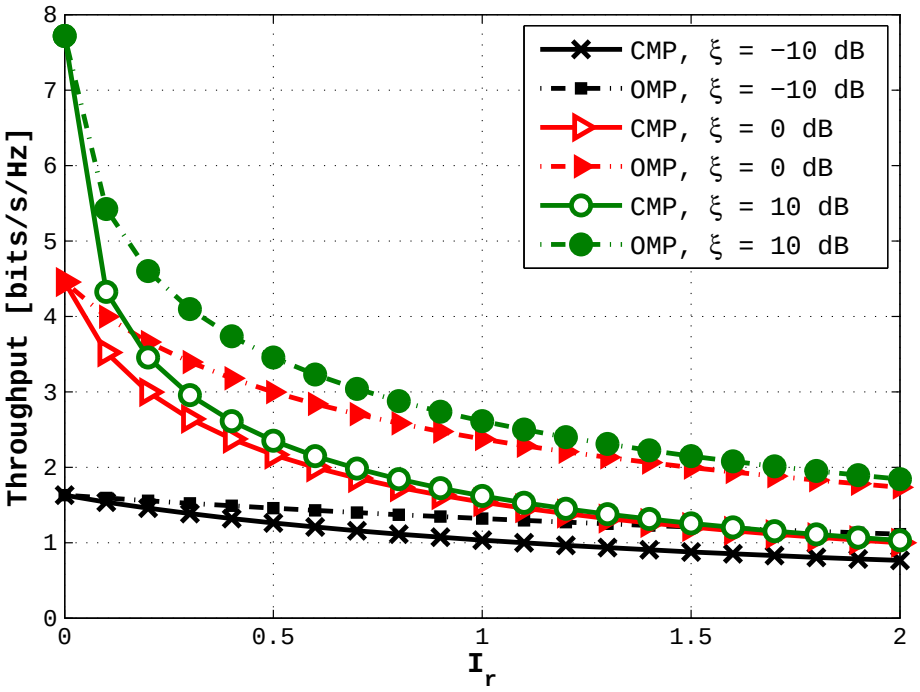

Figure 2.9: Throughput vs Power ratio of interference signal to the desired signal, I_r, plot for OMP and CMP methods, ξ =-10 dB, 0 dB, 10 dB

son with CMP method is also illustrated in the figure.

As explained before, I_r can take values greater than 1 also. Hence, it is mandatory to analyse the performance of the proposed method in strong interference environments. Figure 2.9 shows the capacity variation with respect to I_r for OMP method and CMP method. The analysis is carried for various values of ξ. The result shows that both OMP and CMP methods provides similar capacity at $I_r = 0$. The performance gradually decreases as I_r increases for both OMP and CMP method. However, the transmit precoding with the matrices chosen based on the proposed method shows superior performance in terms of capacity for both weak and strong interference environments.

Next a cell with one BS, 30 cellular UEs, 10 D2D pairs and 30 available resources in the system is considered. Each of the 30 cellular UEs are assigned separate resources and the D2D pairs share the resources with cellular UEs such

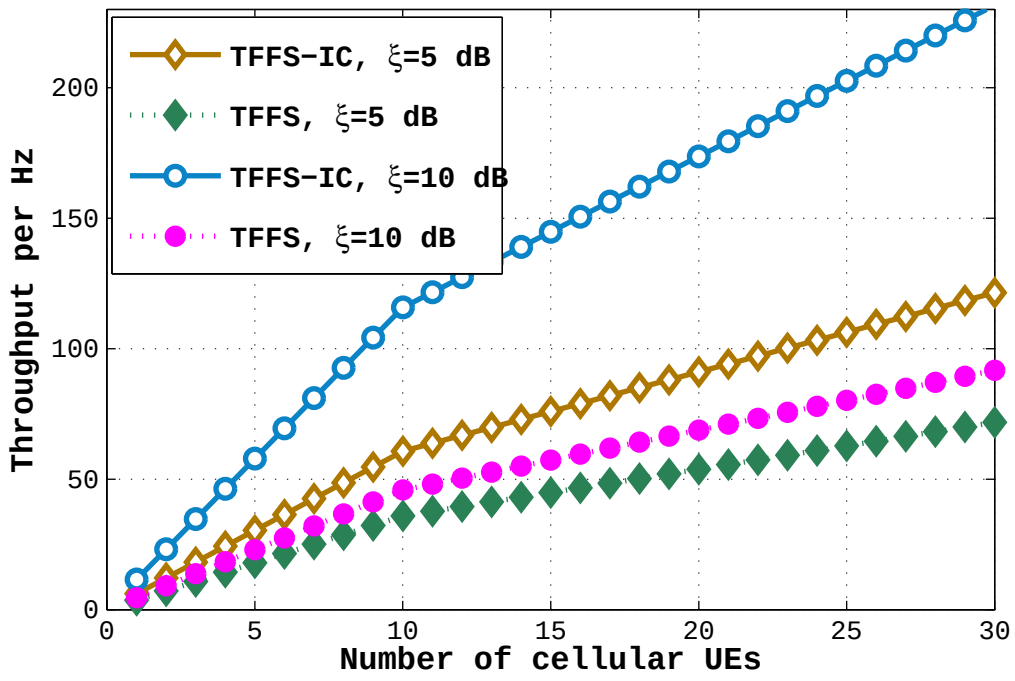

Figure 2.10: Throughput vs Number of cellular UE plot for OMP and CMP methods

that the same resource was being shared by at-most 2 links, one CH2BS link and one D2D link. Thus there exist 10 UEs in the system whose resources are shared by a single D2D pair. Figure 2.10 shows the throughput variation for the increasing number of cellular UEs in the cell. In the figure, the first 10 UEs are with a D2D pair and the next 20 UEs are without D2D pair. The analysis is carried out by using both the OMP and CMP methods for $\xi = 5$ dB and 10 dB. The result shows that the selection of precoding vectors based on the proposed OMP method provides better interference cancellation capability and thus maximizes the overall system throughput when compared to the conventional CMP method. In addition, the throughput increment with increase in ξ is seem to be higher for the proposed method.

2.8 Summary

In this chapter, a novel orthogonal precoding technique to avoid the interference between a BS2UE and D2D link is proposed. The advantage of the proposed method is reduction of interference generated at both receivers of BS2UE and UE2UE links. The proposed method can be applied to both uplink / downlink cellular and D2D communications. The numerical results show that the proposed method provides better interference cancellation capabilities and offers an improvement in throughput when compared to conventional precoding vector selection approach.

CHAPTER 3

Interference Cancellation for Multi-Link D2D communication

Contents

The advanced topology concepts are beneficial from the D2D paradigm beyond conventional D2D communication between two devices in proximity. Advanced topology services include multicast, broadcast and relay services with the aid of D2D communication. The advanced topology services are executed with the clustering concept and Cluster Head (CH) acting as the master. All the links established in a cluster share a common resource for communication.

For realization of advanced topology services with D2D communication, interference between D2D pairs also need to be handled in addition to cellular to D2D and D2D to cellular interferences. The last chapter, Chapter 2, addressed the problem of D2D to cellular and cellular to D2D interferences when the cellular channel resources are being shared by single D2D link. An interference co-ordination scheme for cluster-based D2D services is proposed in this chapter when multiple D2D links share common cellular channel resources.

3.1 Introduction

D2D communication can be exploited for advanced topology service for multicasting, broadcasting and relaying. In order to maximize the spectral utilization efficiency for such services, the cellular channel resources need to be shared by more than one UE2UE links. This has the potential for improved spectral efficiency but on the other hand results in D2D to D2D interferences in addition to cellular to D2D and D2D to cellular interferences.

Several cluster layouts per cell can be considered where the term layout refers to the arrangement of D2D communication links in the cluster. Each cluster comprises of one or several UEs which share the same resources when communicating among themselves. A Cluster Head (CH) is selected in each cluster that controls the assignment of precoding vectors for different links in the cluster. The main

aim of the chapter is to propose an interference cancellation method to guarantee a reliable communication for every links in the cluster. This chapter includes the following major contributions:

- Resource allocation for different links in a mesh-layout cluster considering the LTE frame structure [72] is discussed. Two resource sharing modes are addressed here to allocate resources: (a) Orthogonal Sharing (OS), and (b) Non-Orthogonal Sharing (NOS).

- For the NOS mode, we propose a novel technique to reduce the interference in the cluster by selecting the precoding vectors for the different links in a cluster in such way that these matrices maintain orthogonality between them. In order to maximize the data rate at every device in a cluster, two criteria are considered when selecting the precoding vectors: (a) a conventional *Throughput maximization Finite Feedback Scheme (TFFS)* criterion and (b) a novel *Interference Cancellation (IC)* criterion.

- Finally, to optimally select precoding vectors for links in the cluster, an Orthogonal Precoding (OP) vector selection method is proposed which is based on *TFFS* criterion for the OS mode and a combination of *TFFS* and *IC* criteria for the NOS mode. The main advantage of OP is its applicability to any cluster layout.

Both the throughput and the power analyses have been carried out for the evaluation of the proposed method. Additionally, the work also highlights the importance of defining a CH inside a cluster from the point of energy efficiency.

3.2 Scenario Description

A macro cell as shown in Figure 3.1 is considered with one BS and several UEs. Figure 3.1 presents an example of four different cluster layouts named 1, 2, 3 and

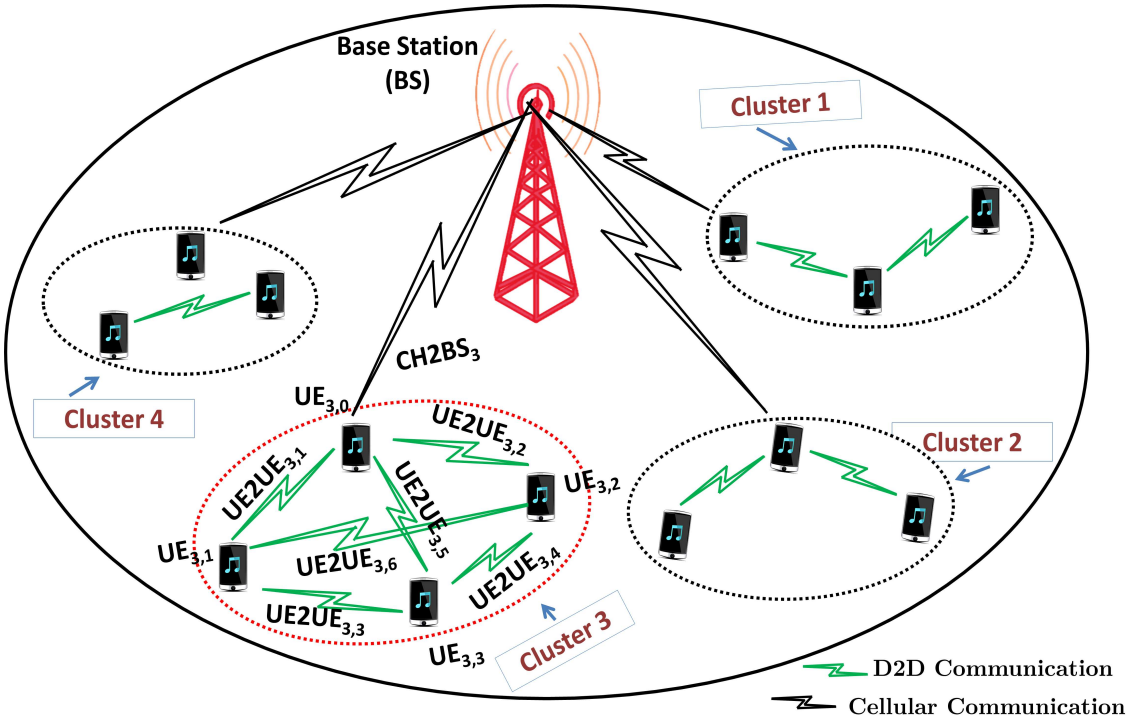

Figure 3.1: A macrocell with different D2D cluster layouts

4. The cluster 1, 2 and 3 depict clusters with multi-link D2D communication whereas cluster 4 illustrates a cluster with single D2D link communication. It is assumed that the BS forms different clusters within its cell based on UE locations and communication requirements. A Cluster Head (CH), i.e., a specific UE, is selected in each cluster by BS.

In this analysis we consider only one cluster, cluster 3, but the analysis can be applied to any cluster layout and to any number of clusters per cell. $UE_{3,0}$ represents the cluster head and $UE_{3,1}$, $UE_{3,2}$, $UE_{3,3}$ are the device members of cluster 3 which are engaged in cellular and D2D communication through the $CH2BS_3$, $UE2UE_{3,1}$, $UE2UE_{3,2}$, $UE2UE_{3,3}$, $UE2UE_{3,4}$, $UE2UE_{3,5}$ and $UE2UE_{3,6}$ links. As the focus is on one cluster, the index denoting the cluster 3 in the symbols are omitted for simplicity.

A bidirectional communication is considered with the assumption that UEs have single transceiver structures operating in the Time Division Duplex (TDD)

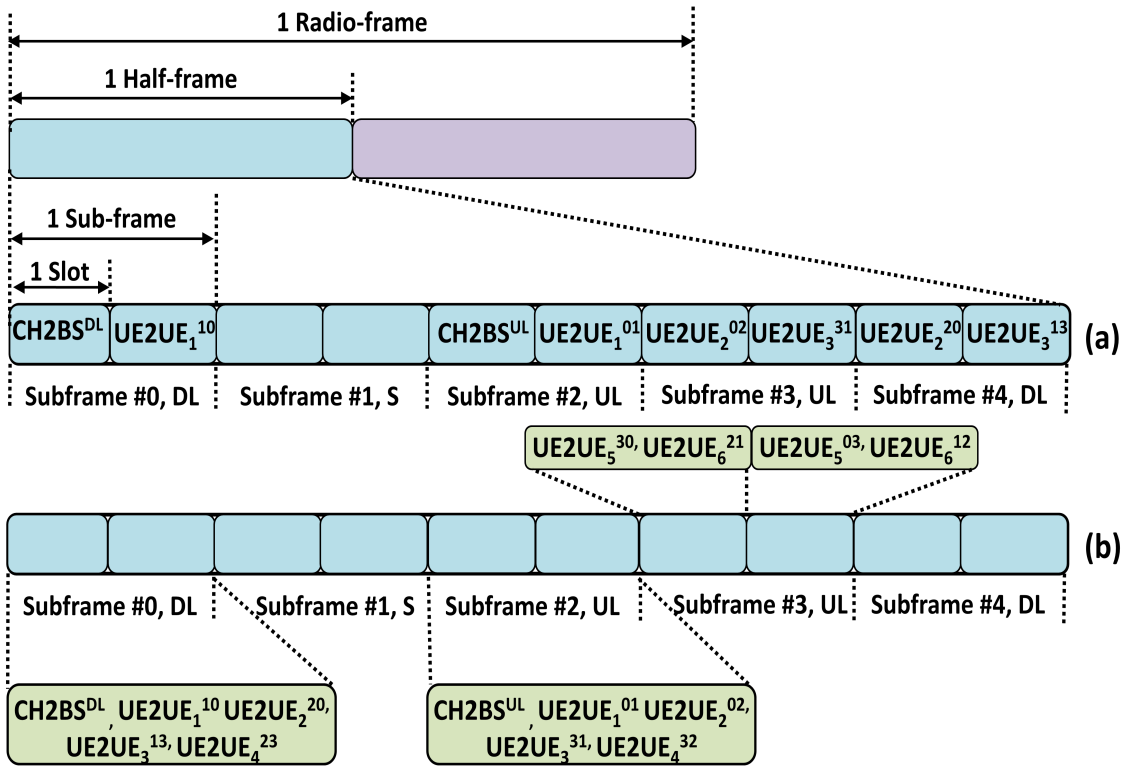

Figure 3.2: Resource allocation in LTE TDD frame (a) Orthogonal Sharing Mode and (b) Non-Orthogonal Sharing Mode

mode [72], i.e., a UE can either receive or transmit data per timeslot. Since the system operates in the TDD mode, reciprocity of channels exists between the uplink and downlink directions for both cellular and D2D links. Each link in the cluster has both downlink and uplink transmissions, i.e., for CH2BS link, CH2BS^{DL} and CH2BS^{UL} denote the cellular downlink and uplink transmissions between the BS and UE_0 respectively. For D2D transmissions, there is no differentiation between uplink and downlink transmissions since the two communicating devices are UEs [15]. Since UE_0 established a cellular communication, the transmissions to and from UE_0 are considered here as downlink and uplink transmissions respectively. Thus, CH2BS^{DL}, UE2UE_1^{10}, UE2UE_2^{20}, UE2UE_3^{13} and UE2UE_4^{23} are considered as downlink transmissions and CH2BS^{UL}, UE2UE_1^{01}, UE2UE_2^{02}, UE2UE_3^{31} and UE2UE_4^{32} are considered as uplink transmissions, where UE2UE_i^{ab} denotes D2D transmissions from UE_a to UE_b through i^{th} link.

Each of the clusters in Figure 3.1 share a common pool of radio resources [29]. The resource allocation for different communication links of cluster 3 in the LTE TDD frame is presented in Figure 3.2. In the LTE TDD frame, the transmissions are organized into radio frames. A radio frame consists of two half-frames each of which is formed by 5 subframes and a subframe comprises of 2 timeslots [72]. The communications in the cluster 3 can be scheduled in such way that the CH2BS^{DL}, UE2UE$_1^{10}$, UE2UE$_2^{20}$, UE2UE$_3^{13}$ and UE2UE$_4^{23}$ transmissions are in the downlink subframe whereas the CH2BS^{UL}, UE2UE$_1^{01}$, UE2UE$_2^{02}$, UE2UE$_3^{31}$ and UE2UE$_4^{32}$ transmissions are in the uplink subframe. The transmissions in the inner links, i.e., UE2UE$_5$ and UE2UE$_6$, are scheduled in separate subframes. Figure 3.2 shows two resource allocation modes for transmissions [42]: (a) Orthogonal Sharing (OS) Mode and (b) Non-Orthogonal Sharing (NOS) Mode.

In the Orthogonal Sharing (OS) mode, each link is reserved a particular timeslot in the subframe. Thus, no interference between links in the cluster is possible. A possible allocation of different communication links for the cluster 3 is shown in Figure 3.2(a). In the figure, DL, S and UL denotes Downlink, Special and Uplink subframe; where the S subframe is dedicated to switch from the downlink to uplink communication. The CH2BS^{DL}, UE2UE$_1^{10}$, UE2UE$_2^{20}$ and UE2UE$_3^{13}$ transmissions are scheduled in the first two downlink subframes whereas the CH2BS^{UL}, UE2UE$_1^{01}$, UE2UE$_2^{02}$ and UE2UE$_3^{31}$ transmissions are scheduled in the first two uplink subframes of the first half-frame. The UE2UE$_4^{32}$, UE2UE$_4^{23}$, UE2UE$_5^{30}$, UE2UE$_5^{03}$, UE2UE$_6^{21}$ and UE2UE$_6^{12}$ transmissions are carried over in the next half-frame. The same configuration can be repeated in the following subframes.

In the Non-Orthogonal Sharing (NOS) mode, the entire timeslot is shared by all allocated links which however leads in interference among these links. A possible allocation of links for the cluster 3 is shown in Figure 3.2(b). As explained before, all links scheduled for the downlink and uplink subframes share

the entire subframes. The inner links can be scheduled in a separate uplink or downlink subframe as there is no differentiation between D2D downlink and uplink communications. In Figure 3.2(b), the inner links share uplink subframe with the UE2UE_5^{30} and UE2UE_6^{21} transmissions in the first timeslot and the UE2UE_5^{03} and UE2UE_6^{12} transmissions in the second timeslot of the 3^{rd} uplink subframe. This order can be repeated in the following subframes.

The link configuration in the TDD frame can vary from frame to frame based on device requirements and network status. The NOS mode provides better resource utilization efficiency. Hence, the NOS mode is preferred to the OS mode even-though the OS mode eases the task of interference management. By sharing of all scheduled resources in the entire subframe for the NOS mode, co-channel interferences occur and hence interference cancellation methods are required to improve the overall system throughput.

3.3 System Model for Multi-link D2D communication

This section describes the system model for multi-link D2D communication. A cluster with N_c links scheduled in a particular timeslot is considered. Each communication pair is assumed to have N_t transmit antennas and N_r receive antennas. Let us consider a user, UE_ξ, in the cluster with i^{th} link as the communication link of interest. If UE_ξ receives data from m_ξ communication links, the interference generated from remaining $(N_c - m_\xi)$ links are considered to be negligible. The $N_r \times 1$ received signal from the i^{th} link with co-channel interferences at UE_ξ can be written as [75]:

$$\mathbf{y}_i = \sqrt{P_i}\mathbf{H}_i\boldsymbol{\psi}_i s_i + \sum_{j=1, j\neq i}^{m_\xi} \sqrt{P_j}\mathbf{H}_j\boldsymbol{\psi}_j s_j + \boldsymbol{\eta} \tag{3.1}$$

where $\boldsymbol{\psi}_i$ is the $N_t \times 1$ precoding vector and $\boldsymbol{\psi}_i^H\boldsymbol{\psi}_i = I$, $\mathbf{H}_i$ is the $N_r \times N_t$

channel matrix and P_i is the transmit power of i^{th} link, s_i is the transmitted signal through i^{th} link and η is the $N_r \times 1$ Gaussian noise. In (3.1), the first and second terms in Right Hand Side (RHS) denote the terms with desired signal and co-channel interferences respectively.

A maximal ratio combiner (MRC) is assumed with linear combining to be used to decode signals at the receiver [73]. The UE_ξ can receive signals from multiple links thus a receiver with several sub-receivers, called fingers, is considered for decoding signals. Each of the fingers decode signal by using linear combining with a $N_r \times 1$ weight vector, $\mathbf{w}_i = \mathbf{H}_i \boldsymbol{\psi}_i$ [74]. The output of combiner at the UE_ξ for decoding the symbol of i^{th} link can be presented as:

$$\Upsilon_i = \mathbf{y}_i \mathbf{w}_i^H \tag{3.2}$$

Substituting (3.1) in the above equation, (3.2) can be rewritten as:

$$\Upsilon_i = \sqrt{P_i}\mathbf{H}_i \boldsymbol{\psi}_i \boldsymbol{\psi}_i^H \mathbf{H}_i^H s_i + \sum_{j=1, j\neq i}^{m_\xi} \sqrt{P_j}\mathbf{H}_j \boldsymbol{\psi}_j \boldsymbol{\psi}_i^H \mathbf{H}_i^H s_j + \bar{\boldsymbol{\eta}} \tag{3.3}$$

For the 0^{th} subframe in Figure 3.2, $m_\xi = 3$ and $m_\xi = 1$ for the NOS and OS modes respectively at UE_0. This sharing of allocated resources by more than one link in NOS mode result in co-channel interferences.

The diversity order refers to the number of independently faded paths that a symbol passes through to supply multiple independent replicas of the same information to the receiver [79]. According to [80], the achievable diversity order of MIMO system simultaneously transmitting S symbols can be analytically derived as $(N_t - S + 1)(N_r - S + 1)$. The employed MRC receiver at UE_ξ receivers m_ξ data simultaneously from $m_\xi N_t$ transmit antennas through N_r receive antennas. Hence, the employed MRC receiver achieves a diversity order of $(m_\xi N_t - m_\xi + 1)(N_r - m_\xi + 1)$ [80].

3.3.1 Problem Formulation

According to the Finite Feedback Scheme (FFS) [81], the i^{th} link receiver uses a feedback function $f : \mathbb{C}^{N_t \times N_r} \rightarrow \{1, ..., N\}$ to select the feedback index $f(\mathbf{H}_i)$ from a codebook. The codebook contains a finite set of precoding vectors/codewords [82] and N denotes the number of codewords in the codebook. The feedback index is carried in Precoding Matrix Index (PMI) field in the channel status report [83] to the transmitter. At the transmitter, $\{\boldsymbol{\psi}_1, ..., \boldsymbol{\psi}_N\}$ are the codewords corresponding to each of the N feedback indices from the codebook.

SINR is considered as the index parameter for the purpose of maximizing the network capacity. If the UE_ξ receives data from m_ξ communication links, the SINR sum for m_ξ links at UE_ξ of MRC output can be written as [84]:

$$\gamma = \frac{||\mathbf{H}_i \boldsymbol{\psi}_i \boldsymbol{\psi}_i^H \mathbf{H}_i^H||^2}{\sum_{j=1, j\neq i}^{m_\xi} I_r^{ji} ||\mathbf{H}_j \boldsymbol{\psi}_j \boldsymbol{\psi}_i^H \mathbf{H}_i^H||^2 + \frac{1}{\xi}\mathbf{I}} \tag{3.4}$$

where I_r^{ji} is the power ratio of interference signal to desired signal and can be written as $I_r^{ji} = \frac{P_j}{P_i}$, ξ is the Signal-to-Noise Ratio (SNR). The expression for the maximum achievable sum data rate in b/s/Hz at UE_ξ for m_ξ receiving links based on [85] can be derived as:

$$C_\xi = \sum_{i=1}^{m_\xi} E\left[\log_2\left(\det\left(I + \frac{||\mathbf{H}_i \boldsymbol{\psi}_i \boldsymbol{\psi}_i^H \mathbf{H}_i^H||^2}{\sum_{j=1, j\neq i}^{m_\xi} I_r^{ji} ||\mathbf{H}_j \boldsymbol{\psi}_j \boldsymbol{\psi}_i^H \mathbf{H}_i^H||^2 + \frac{1}{\xi}\mathbf{I}}\right)\right)\right] \tag{3.5}$$

For the system described in (3.3), there arises a problem of defining a proper feedback function, $f(\mathbf{H}_i)$, for the selection of an optimal precoding vector for the desired i^{th} link that maximizes achievable data rate with reduction of co-channel interferences. Thus the aim is to maximize system data rate subject to the following objectives:

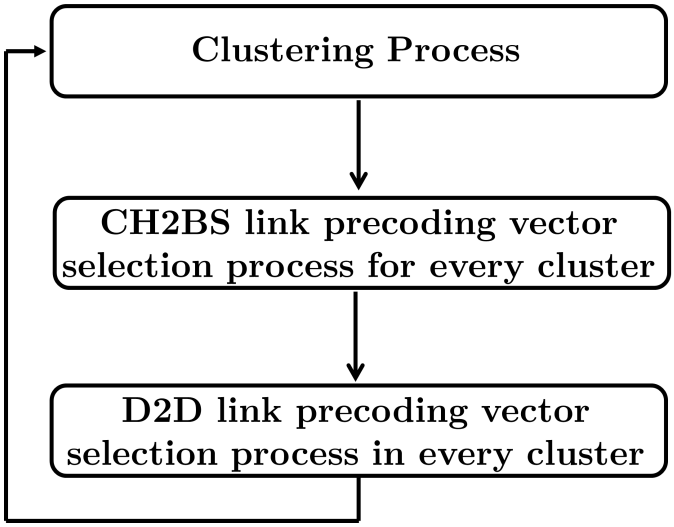

Figure 3.3: Flow chart for the Proposed Orthogonal Precoding vector Selection method

$$AC1 : \max_{\forall\ i} ||\mathbf{H}_i \boldsymbol{\psi}_i \boldsymbol{\psi}_i^H \mathbf{H}_i^H||^2 \tag{3.6}$$

$$AC2 : \min_{\forall\ i \neq j} \sum_{j=1}^{m_\xi} I_r^{ji} ||\mathbf{H}_j \boldsymbol{\psi}_j \boldsymbol{\psi}_i^H \mathbf{H}_i^H||^2 \tag{3.7}$$

$AC1$ defines the condition for the selection of precoding vector for the i^{th} link with throughput maximization [75] and $AC2$ indicates the necessary condition for co-channel interference reduction. The $AC1$ is applicable in both OS and NOS modes whereas the $AC2$ is only applicable in the NOS mode since there is no co-channel interference in the OS mode. To minimize the interference term as explained in the $AC2$, interference cancellation techniques are required.

3.4 Criterion for Optimal Precoding Vector Selection

The solutions to the above formulated objectives, $AC1$ and $AC2$, are discussed in this section. Here, the following two criteria are considered while selecting precoding vectors in a cluster.

1. **Throughput maximization FFS (TFFS)** criterion: The feedback function for the TFFS criterion for the selection of precoding vector, $\boldsymbol{\psi}_i$, of i^{th} communication link is:

$$f(H_i) = arg \max_{n \in \{1,...,N\}} \left\{ ||\mathbf{H}_i \boldsymbol{\psi}_i||^2 \right\} \tag{3.8}$$

The numerator of γ in (3.4) for i^{th} link can be rewritten as:

$$||\mathbf{H}_i \boldsymbol{\psi}_i \boldsymbol{\psi}_i^H \mathbf{H}_i^H||^2 = ||\mathbf{H}_i \boldsymbol{\psi}_i \left(\mathbf{H}_i \boldsymbol{\psi}_i\right)^H||^2 \tag{3.9}$$

From (3.9), it can be observed that maximizing the term $||\mathbf{H}_i \boldsymbol{\psi}_i||^2$ maximizes $||\mathbf{H}_i \boldsymbol{\psi}_i \boldsymbol{\psi}_i^H \mathbf{H}_i^H||^2$ and thus satisfies the design objective explained in *AC1* of (3.6).

2. **Interference Cancellation (IC)** criterion: The co - channel interference from other communication links inside a cluster can be reduced by assigning orthogonal precoding matrices to different links in such way that they satisfy:

$$\boldsymbol{\psi}_i^H \boldsymbol{\psi}_j = \boldsymbol{\psi}_i \boldsymbol{\psi}_j^H = 0, \quad \forall\ i \neq j \tag{3.10}$$

If $\boldsymbol{\psi}_i$ and $\boldsymbol{\psi}_j$ are orthogonal to each other, the term $||\mathbf{H}_j \boldsymbol{\psi}_j \boldsymbol{\psi}_i^H \mathbf{H}_i^H||^2$ in (3.4) approximates to zero which satisfies the objective raised in *AC2*.

Let $\boldsymbol{\Psi}$ be a $N_c \times N_t$ cluster matrix with precoding vectors of all communication links in a cluster, i.e., $\boldsymbol{\Psi} = \left[\boldsymbol{\psi}_1, ..., \boldsymbol{\psi}_{N_c}\right]^T$. Then, the interference from other communication links inside a cluster can be reduced if $\boldsymbol{\Psi}$ forms an orthogonal matrix, i.e., the cluster matrix, $\boldsymbol{\Psi}$, satisfies

$$\boldsymbol{\Psi}^H \boldsymbol{\Psi} = \boldsymbol{\Psi} \boldsymbol{\Psi}^H = \mathbf{I} \tag{3.11}$$

If $\mathbf{\Psi}$ forms an orthogonal matrix with dimension $N_c \times N_t$, then

$$\sum_{i=1}^{N_t} |\mathbf{\Psi}(j,i)|^2 = 1, \qquad \forall\ j = 1, 2, ..., N_c \tag{3.12}$$

$$\sum_{i=1}^{N_t} \mathbf{\Psi}(j,i)\Psi(k,i) = 0, \qquad \forall\ j,k = 1, 2, ..., N_c;\ j \neq k \tag{3.13}$$

Thus, any combination of rows or columns of $\mathbf{\Psi}$ form orthogonal vector sets thus satisfying (3.10).

3.5 Orthogonal Precoding (OP) Vector Selection Method

To optimally select precoding vectors for links in the cluster based on the TFFS and IC criteria, an Orthogonal Precoding (OP) vector selection method is proposed in this section.

Figure 3.3 shows main processes of the proposed OP method which consists of: i) a clustering process implemented at the BS, ii) a CH2BS link precoding vector selection process implemented at CHs, and iii) a D2D link precoding vector selection process implemented at D2D receivers. The clustering and the CH2BS link precoding vector selection processes are common for both the OS and NOS modes. Finally, the D2D link precoding vector selection process is implemented in such way that the OS mode only employs the TFFS criterion whereas the NOS mode uses both the TFFS and IC criteria.

3.5.1 Clustering Process

The clustering process fulfils two main functions: a) creation of clusters and b) selection of cluster heads.

Initially, a UE informs the BS about its D2D capabilities and communication requirements. In this study, it is assumed that the BS knows SINRs and positions of each UE in the cell. Based on this knowledge, the BS forms clusters. A cluster can be composed of a single cellular UE or single/multiple D2D UEs or a combination of both.

A UE having established cellular link and with the highest SINR is selected as the CH. In case of cluster without a cellular link, the UE with the highest value of SINR is chosen as the CH. The BS establishes D2D links in a cluster [15] and informs the CH about the D2D links inside its cluster. The CHs may or may not have direct data communication with other UEs in that cluster. In this study, it is considered that the UEs have direct communication with cluster head in the cluster.

3.5.2 CH2BS link precoding vector selection process

A CH may communicate with the BS via the downlink or uplink channel. In case of downlink channel, additional training symbols may be added before the data transmission to estimate the CH2BS channel. The CH selects a precoding vector from the codebook based on the channel information and transmits the index of the selected precoding vector to the BS. The precoding vector is selected using the TFFS criterion described in Section 3.4. Since, channel reciprocity exists between downlink and uplink in the TDD system, the knowledge of downlink channel at a CH can also be exploited for the uplink transmission also.

Steps involved in the CH2BS link precoding vector selection process for a particular cluster can be summarized as follows:

1. Selecting $\boldsymbol{\psi}_0$ from the codebook for the CH2BS channel based on the TFFS criterion.

2. Forming the first vector of the cluster matrix, $\boldsymbol{\Psi}$, at CH with the selected

$\boldsymbol{\psi}_0$ as the first element.

3. Reporting to the BS, the codebook index of $\boldsymbol{\psi}_0$.

In case of clusters having only D2D UEs, the CH2BS link precoding vector selection process is not necessary.

3.5.3 D2D links precoding vector selection process

In case of the OS mode, the selection of precoding vectors for all links in the cluster is achieved using the TFFS criterion as there is no co-channel interference between links. A combination of TFFS and IC criteria, which is denoted as TFFS-IC criterion, is used for the case of NOS mode. In TFFS-IC, a set of vectors which are orthogonal to the cluster matrix is calculated initially and then the TFFS criterion is used to choose the desired precoding vector among them.

Steps involved in the UE2UE$_i$ link precoding vector selection process for a particular cluster can be summarized as follows:

1. Informing the UE2UE$_i$ receiver about the index of the selected precoding matrix in $\boldsymbol{\Psi}$ by the CH.

2. Selection of $\boldsymbol{\psi}_i$ by UE2UE$_i$ receiver from the codebook based on the TFFS criterion for the OS mode and the TFFS-IC criterion for the NOS mode. To incorporate the IC criterion to select precoding vector for D2D links in the NOS mode, the IC criterion can be rewritten as follows:

   For UE2UE$_i$ link in the cluster, the precoding vectors are chosen in such way that the updated cluster matrix, $\boldsymbol{\Psi}$, formed by combination of cluster matrix after precoding vector selection of UE2UE$_{i-1}$ links and the UE2UE$_i$ link precoding vector is an orthogonal matrix.

3. Reporting the codebook index of the selected percoding vector to the UE2UE$_i$ transmitter and updating of $\mathbf{\Psi}$ at the CH.

Figure 3.4 summarizes the precoding vectors selection procedure for the CH2BS and D2D links within a cluster in the form of a flow chart. The procedure starts with the selection of CH2BS link precoding vector. The CH performs the selection based on CH2BS link precoding vector selection process discussed in Section 3.5.2. If there are no D2D links in the cluster, i.e., for $L = 0$, the procedure terminates. Here L denotes the number of D2D links in the cluster. Otherwise, a cluster matrix, $\mathbf{\Psi}$, is generated at the CH with the CH2BS link precoding vector as the first element of $\mathbf{\Psi}$. The CH informs the UE2UE$_i$ receiver about the index of selected precoding vector in $\mathbf{\Psi}$. An optimal precoding vector for the UE2UE$_i$ link is selected by UE2UE$_i$ receiver using TFFS (for the OS mode)/TFFS-IC (for the NOS mode). The UE2UE$_i$ receiver sends PMI indication to UE2UE$_i$ transmitter. The CH updates the cluster matrix, $\mathbf{\Psi}$. This procedure for the selection of precoding vectors for D2D links is repeated L times.

For clusters having only D2D UEs, the D2D link precoding vector selection procedure starts with an empty $\mathbf{\Psi}$. Since the precoding matrices for the D2D links are based on the initial element in $\mathbf{\Psi}$, it is not possible to determine the exact number of precoding vectors that are orthogonal to each other.

When a UE terminates communication or moves out of a cluster, the UE informs the CH. The CH updates the $\mathbf{\Psi}$ by removing corresponding precoding vectors. If a new UE appears in the cell, the BS informs the corresponding CH about the new cluster member. The CH sends the $\mathbf{\Psi}$ to this UE which decides its own precoding vector to be used for the D2D communication. If a CH itself moves out of cluster, the BS designates a new CH and all cluster details, including $\mathbf{\Psi}$, are transferred to the new CH.

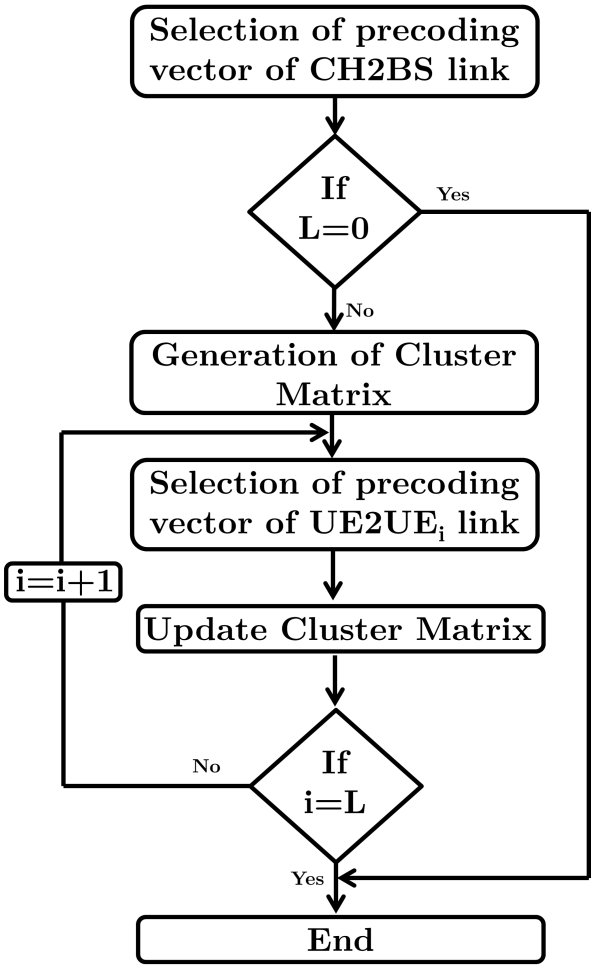

Figure 3.4: Flow chart for the precoding vector selection procedure inside a cluster

3.6 Results and Discussion

For validation of the proposed method, a cluster layout as shown in Figure 3.1 was considered, consisting of 1 cellular and 6 D2D links. The transmissions and receptions of signals are assumed to be through 4 antenna ports [72] and the channel matrices are independent across different transmit-receive pairs. Shadowing and fast fading were not taken into account. The simulation tool for the analysis was developed by using MATLAB software. Parameters and values used in the simulations are summarized in Table 3.1. The system throughput analysis was carried out for both the OS and NOS modes. To evaluate the proposed

Table 3.1: Simulation Parameters for Multi-link D2D communication analysis

Parameter	**Value**
Channel bandwidth, B	10 MHz
Power ratio of interference signal to the desired signal	$I_r^{ji} = I_r = 0.5$
Noise spectral density, N_0	-174 dBm/Hz [51]
SNR threshold for both D2D and cellular communication, γ_{th}	7 dB
Maximum transmit power constraint, ϱ	24 dBm for D2D links [51] 46 dBm for Cellular links [86]
Distance between D2D transmitter and receiver	100 m [51]

orthogonal precoding vector selection method, the following two analyses were done:

1. Throughput analysis: The system throughput analysis was carried out for both the OS and NOS modes. In case of the NOS mode, the OP method with the conventional TFFS along with the proposed TFFS-IC criterion were presented. The utilized precoding vectors were chosen from the codebook $\mathbb{W}_{4\times4}$ based on the 3GPP specifications (Appendix A) [72]. With the proposed TFFS-IC criterion, the precoding vectors chosen for CH2BS, UE2UE$_1$, UE2UE$_2$, UE2UE$_3$ and UE2UE$_3$ links were $\mathbf{W}_4^{\{1\}}$, $\mathbf{W}_5^{\{1\}}$, $\mathbf{W}_7^{\{1\}}$, $\mathbf{W}_6^{\{1\}}$ and $\mathbf{W}_3^{\{1\}}$ respectively. The corresponding precoding matrices with TFFS criterion were $\mathbf{W}_4^{\{1\}}$, $\mathbf{W}_3^{\{1\}}$, $\mathbf{W}_1^{\{1\}}$, $\mathbf{W}_0^{\{1\}}$ and $\mathbf{W}_2^{\{1\}}$. Where $\mathbf{W}_\alpha^{\{\beta\}}$ denotes the matrix formed of the columns given by the set $\{\beta\}$ from the Householder matrix, $\mathbf{W}_\alpha$, from the codebook $\mathbb{W}_{4\times4}$.

2. Power analysis: The proposed OP method can be implemented with or without a CH. In the absence of CH, the precoding matrix allocation is

controlled by the BS where the BS is aware of the matrix Ψ and each receiver UE has to send the PMI information to the BS for updating the matrix Ψ. Th power analyses aim to demonstrate the impact of cluster head existence for the proposed OP method in terms of transmit power. The total power required to allocate precoding matrix with and without the CH was evaluated using the TSPC scheme [46].

3.6.1 Throughput analysis

The normalized throughput, χ, per timeslot with the proposed *TFFS-IC* criterion of precoding vector allocation was evaluated and compared with the conventional *TFFS* criterion of precoding vector allocation. Here, the timeslot refers to the first timeslot of the 0^{th} subframe where we consider 5 links for the NOS mode and 1 link for the OS mode (as shown in Figure. 3.2). The normalized throughput, χ, is the sum of throughput value normalized to the peak data rate, C_{peak}, at each UE and it is calculated as

$$\chi = \sum_{n=1}^{\alpha} \frac{C_n}{C_{peak}} \tag{3.14}$$

where α represents the number of UEs behaving as receivers in the given timeslot and C_n is the maximum data rate at n^{th} UE during that timeslot.

Figure 3.5 shows the normalized throughput, χ, per timeslot as function of SNR for the OS mode and the NOS mode using the *TFFS* and *TFFS-IC* criteria. As can be seen from Figure 3.5, the NOS mode provides better results compared to the OS mode. This is due to the fact that 5 links share one time slot (in NOS mode) compared to 1 link in case of the OS mode, thus the throughput should theoretically be 5 times higher. However, due to the presence of co-channel interference, the throughput reduces. For example, a maximum of 3 times increase can be observed from Figure 3.5 at $\xi = 0$ dB. The figure shows that the proposed

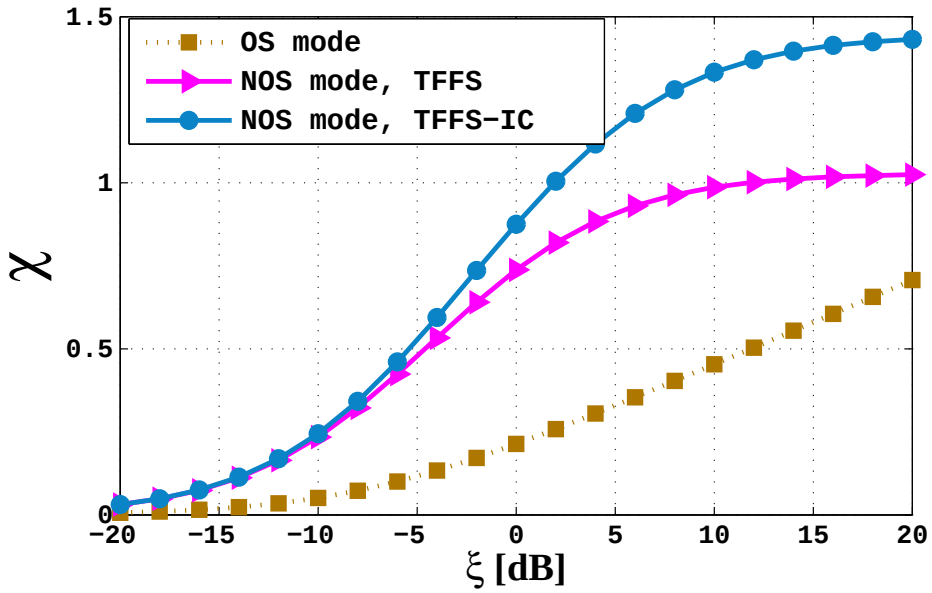

Figure 3.5: Normalized Throughput, χ, vs SNR, ξ, plot for OS mode and NOS mode using transmit precoding of matrices chosen based on *TFFS* and *TFFS-IC* criteria

method with the *TFFS-IC* criterion does not play any significant role in noisy environments ($\xi < -5$ dB). However, in case of better radio conditions ($\xi > -5$ dB), the proposed *TFFS-IC* criterion leads in 10 % to 40 % throughput increase compared to the *TFFS* criterion.

Inside a cluster, a UE receives signals from multiple links including both cellular and D2D links. The interference power at a UE receiver can be similar to the desired signal power for D2D interference links or greater than the desired signal power in case of cellular link due to the higher transmission power of the BS. Figure 3.6 shows the normalized throughput, χ, per timeslot as function of I_r ($I_{r,1} = I_{r,2} = I_r$) for the OS mode and the NOS mode using the *TFFS* and *TFFS-IC* criteria. The analysis is evaluated from weak to strong interference environments for $\xi = 0$ dB and $\xi = 10$ dB. Since there is no co-channel interference in the OS mode, the χ is independent to I_r, (evident straight lines in the figure). In case of NOS mode, the throughput gradually decreases as the interference power increases. It can be noted that χ is almost equal for the OS mode and the

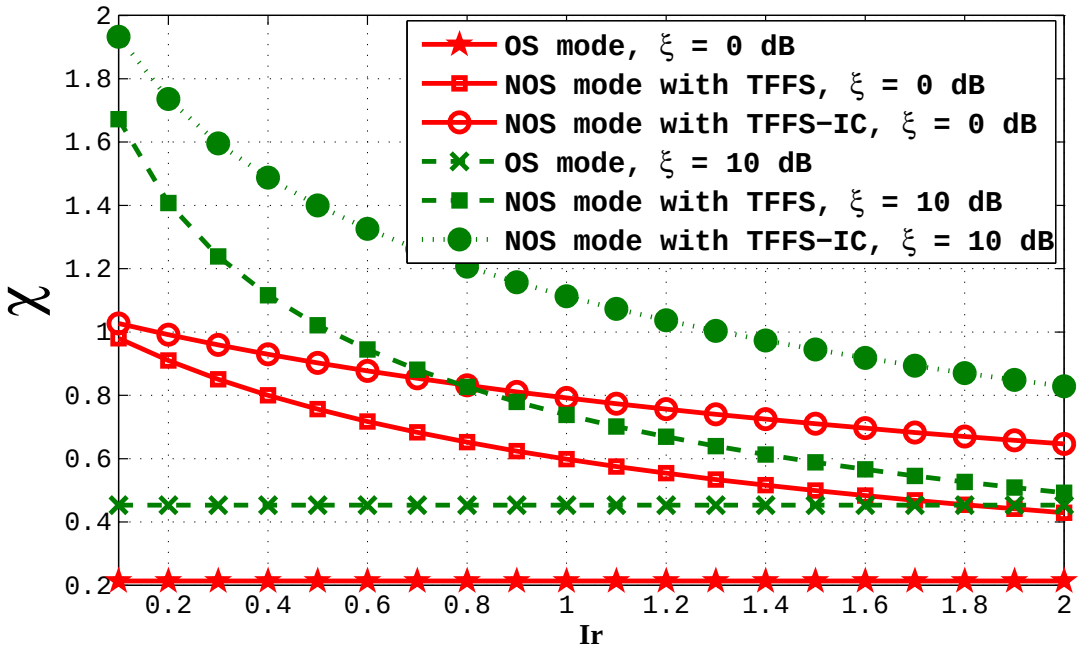

Figure 3.6: Normalized Throughput, χ, vs Power ratio of interference signal to the desired signal, I_r, plot for OS mode and NOS mode using transmit precoding with the matrices chosen based on *TFFS* and *TFFS-IC* criteria

NOS mode with *TFFS* at $\xi = 10$ dB and $I_r = 2$ (i.e., the interference power is 2 times higher than the desired signal power). However the proposed *TFFS-IC* criterion leads in throughput improvement for both weak and strong interference environments in the case of NOS mode.

Figure 3.7 shows the variation of normalized throughput, χ, for the desired link at a UE behaving as receiver (i.e., $\alpha = 1$ in (3.14)) in the NOS mode when considering different number of receiving links. The χ is plotted as a function of SNR, ξ, using the *TFFS* and *TFFS-IC* criteria. The figure shows that the *TFFS* and *TFFS-IC* criteria result in same throughput if a single receiving link per UE (see e.g. the timeslots of 3^{rd} subframe in Figure 3.2b) is assumed. However, for the case of 2 receiving links per UE (e.g. UE_3 during the timeslots of 0^{th} and 2^{nd} subframes in Figure 3.2b) or 3 receiving links per UE (e.g. UE_0 during the timeslots of 0^{th} and 2^{nd} subframes in Figure 3.2b), the proposed *TFFS-IC* criterion outperforms the *TFFS* criterion. The improvement in throughput with

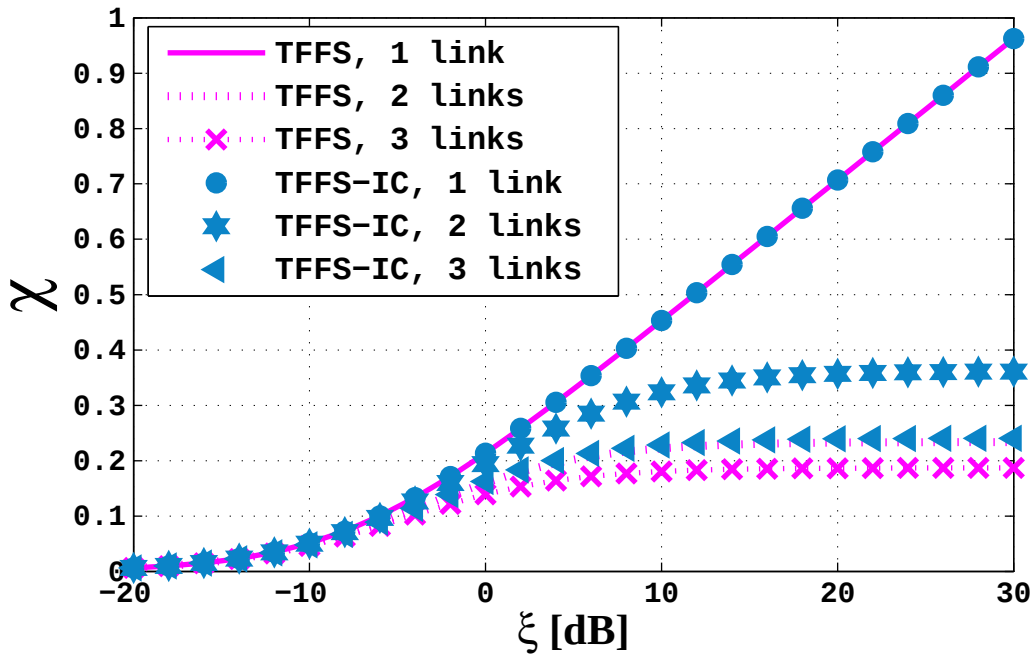

Figure 3.7: Normalized Throughput, χ, vs SNR, ξ, plot for 1 link, 2 links and 3 links with *TFFS* and *TFFS-IC* criteria

the *TFFS-IC* criterion can be attributed to multi-link interference reduction by assigning orthogonal precoding matrices to different links in a cluster.

The CH2BS link channel resources can be shared by more than one D2D link to maximize the spectral efficiency. The number of links, N_c, that the radio resource of the CH can support is determined based on the quality of the CH2BS link. Figure 3.8 shows the variation of N_c with various minimum required SINR threshold, γ_{th}, values for CH2BS link and for various values of ξ. The result shows that the number of links that a cellular resources can share reduces with an increase in the γ_{th} value at the CH2BS receiver. The result illustrates that with the proposed TFFS-IC criterion, a higher number can be accommodated in comparison with TFFS criterion, i.e., with the TFFS-IC criterion the resource can share around 50% additional number of links than that with TFFS criterion at $\gamma_{th} = -5$ dB for all values of ξ.

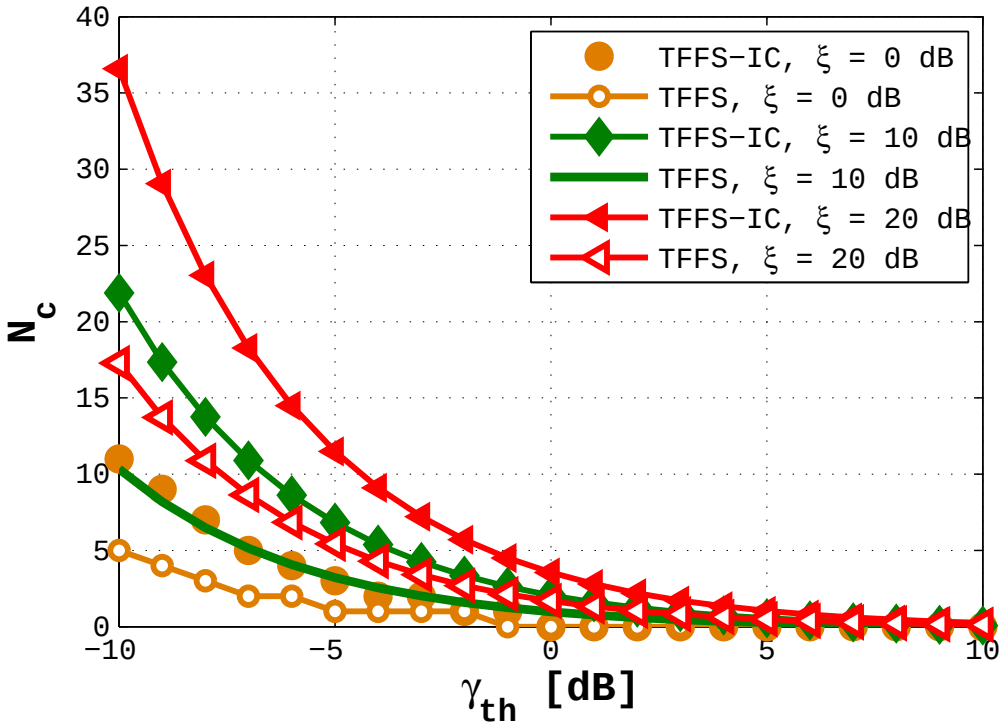

Figure 3.8: Number of links, N_c, vs SINR threshold, γ_{th}, plot with *TFFS* and *TFFS-IC* criteria

3.6.2 Power Analysis

We consider a free space propagation path-loss model, $Pr_i = P_i \left(\frac{d_i}{d_0}\right)^{-\alpha}$ where P_i and Pr_i represent signal power measured at distances d_0 and d_i from the transmitter and α is the pathloss exponent [87]. As in [87], the received power at $d_0 = 1$ equals the transmit power and d_i becomes the distance between the transmitter and receiver of i^{th} link. The transmit power is selected in such way to reach a SNR threshold, γ_t (according to Target SNR Power Control (TSPC) scheme [46]), i.e., $P_i = \gamma_t N_0 (d_i)^{\alpha}$, where N_0 is the noise power spectral density. The TSPC scheme is an example of fixed SNR power control scheme for D2D communication [18].

The total power required to allocate the precoding matrices to all links in the cluster 3 (Figure 3.1) is calculated with and without the presence of CH. The

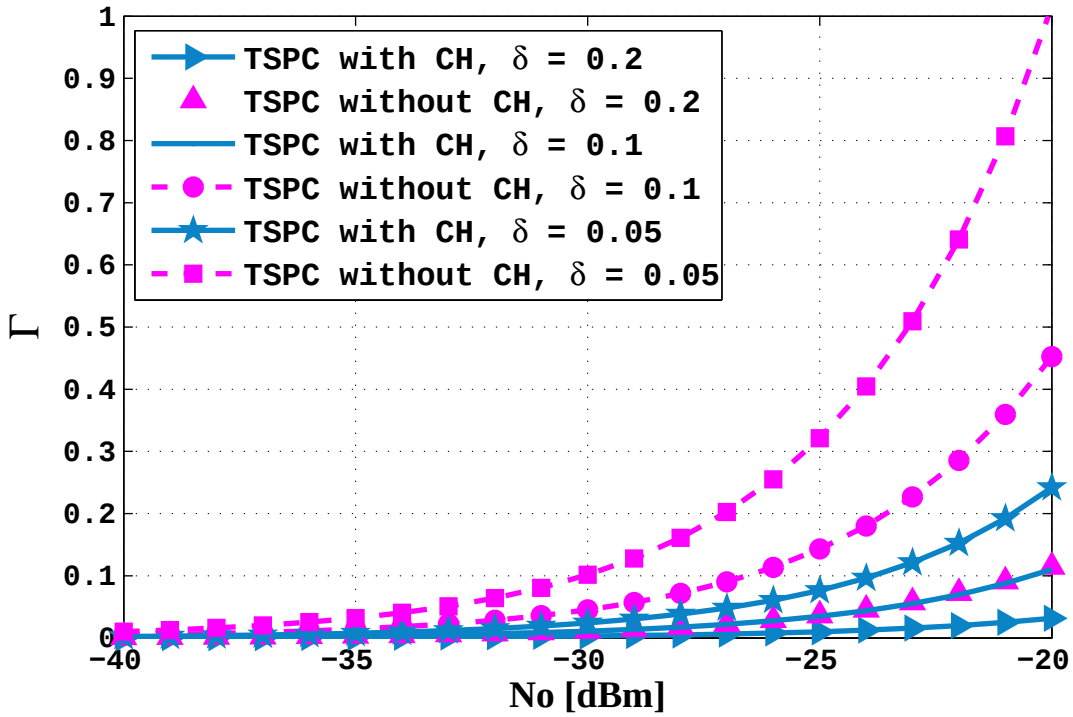

Figure 3.9: Normalized power, Γ, vs Noise Power, N_0, plot with and without CH for various values of δ, $\alpha = 2$

transmit power for each link is calculated based on the TSPC scheme where the maximum transmit power is set to ϱ as indicated in Table 5.2. In our study, the normalized transmit power, Γ, is the sum of required transmit power normalized to the maximum transmit power constrain, ϱ, for each link in the cluster and is calculated as:

$$\Gamma = \sum_{i=1}^{N_c} \frac{\min\left\{\gamma_t N_0 \left(d_i\right)^{\alpha}, \varrho\right\}}{\varrho} \tag{3.15}$$

Figure 3.9 presents the normalized transmit power as function of N_0 with and without the CH for different values of δ where δ is the ratio between the D2D to cellular link lengths. The result shows that high noise power requires higher transmit power. As the distance between transmitter and receiver increases, the required transmit power exponentially increases in the absence of CH. In case of the presence of CH, there is only gradual increase in power and the required

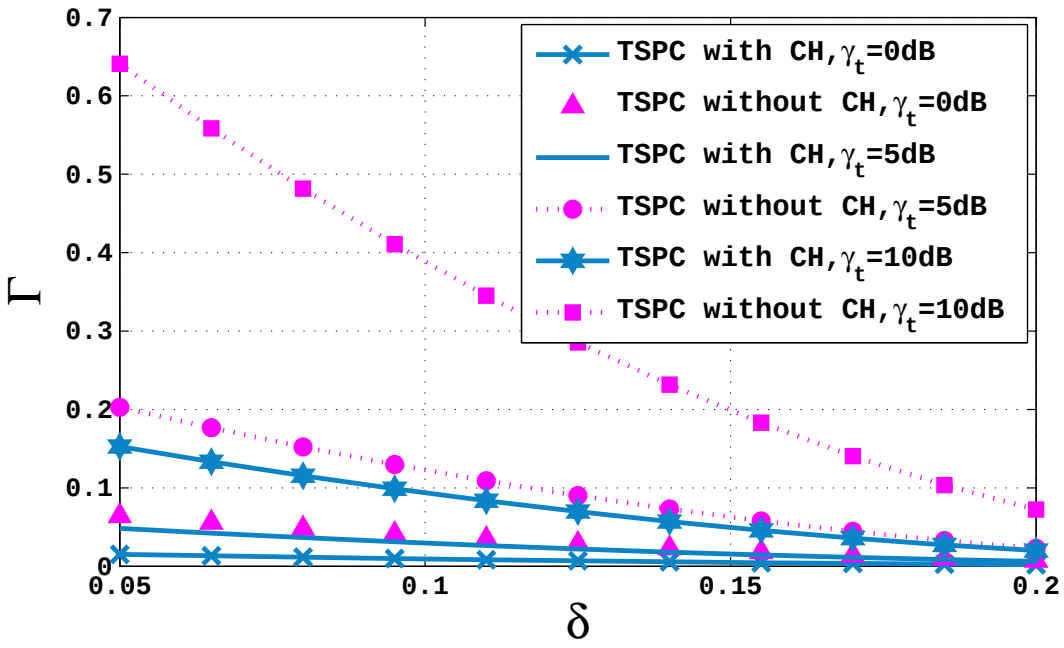

Figure 3.10: Normalized power, Γ, vs Ratio of D2D link length to cellular link length, δ, plot with and without CH, $\alpha = 2$

power is always lower compared to the case without the CH. For example, a power reduction of about 3 times is observed for the case with CH at $\delta = 0.05$ and $N_0 = -25$ dBm compared to case without the CH. Thus, the establishment of CH in a cluster can significantly save the battery life of devices in the cluster.

The normalized transmit power as function of δ with and without the CH for different values of γ_t is shown in Figure 3.10 where δ ranges from 0.05 to 0.2. The result demonstrates that the proposed method with the CH can greatly reduce the required power when increasing γ_t or increasing distance between transmitter and receiver. For example, the required power is almost half at $\gamma_t = 0$ dB and $\gamma_t = 5$ dB when compared to the case without the CH for $\delta = 0.1$.

From Figure 3.9 and Figure 3.10, it is obvious that implementation of OP method with CH is preferred in terms of power efficiency and to avoid signalling overhead at the BS, i.e., informing every cluster member by the BS and updating at the BS regarding the matrix $\mathbf{\Psi}$.

3.7 Limitations of the proposed method

For the proposed OP vector selection method, N_c orthogonal precoding vectors of length, N_t, need to be determined from N codewords in the codebook, where $N_c < N$. As the number of links, N_c, in the cluster increases, the computational complexity to determine orthogonal precoding vectors increases. In addition, the number of bits required to carry the PMI filed increases as the length of the codeword increases. The memory required to store the cluster matrix, Ψ, at the CH increases as N_c and N_t values increases. Moreover, the proposed method is limited to handle co-channel interferences in an intra-cluster communication scenario and do not consider the movement of UEs.

3.8 Summary

In this chapter, a novel orthogonal precoding method to reduce the co-channel interferences in a cluster, called OP method, was proposed. The main advantage of the proposed method is to guarantee quality of service for every device in the cluster by maintaining orthogonality between the precoding vectors of all links in the cluster. Furthermore, the proposed method can be applied to a cluster with devices using a combination of single and multi-layered precoding matrices. The numerical results show that the proposed OP method results in better interference cancellation and offers a capacity improvement compared to the OS mode and the conventional multi-link precoding selection approach. The chapter also highlights the advantage of managing the precoding vector allocation by cluster head rather than by BS in terms of energy efficiency. Additionally, the proposed study can easily be extended to a dense D2D environment with many D2D links per cluster by considering other vector combinations of the Householder matrix, $\mathbf{W}_\alpha$.

CHAPTER 4

Outage Probability analysis with Orthogonal Precoding

Contents

4.1 Introduction

The outage probability is considered as a performance evaluation matrix for guaranteeing QoS constrain to all communication links in a D2D scenario [51–53, 57]. In this chapter, the outage probability of the proposed interference cancellation approach using orthogonal precoding for D2D communication is derived. The mathematical expression for the outage probability of OP method for single-link D2D communication as explained in Chapter 2 and for multi-link D2D communication as explained in Chapter 3 is presented.

Comparison of the proposed OP method with existing interference cancellation technique for D2D communication is also done. The outage probability analysis in [51] and [52] were done by simulation based approach but not based on mathematical approach. The outage probability calculations in [57] were done by considering the distance between the cellular UE and D2D pair as the parameter. The comparison with [51, 52, 57] may not be fair considering their operational principles and hence the Interference Signal Cancellation (ISC) method proposed by Min et al. in [53] is considered for comparison.

4.2 Outage Probability

The outage probability of a particular link is defined as the probability that the SINR, γ, falls below the predefined threshold, γ_{th}. The expression for calculating the outage probability can be written as [88]:

$$P_{out} = Pr\left[\gamma \leq \gamma_{th}\right] = \int_{0}^{\gamma_{th}} f_{\gamma}\left(\gamma\right) d\gamma = F_{\gamma}\left(\gamma_{th}\right) \tag{4.1}$$

where $f_{\gamma}\left(\gamma\right)$ and $F_{\gamma}\left(\gamma\right)$ are the PDF and CDF of γ respectively. By substituting $\gamma = \gamma_{th}$ into the CDF, the outage probability can be obtained. To derive

the outage probabilities, the following Lemmas are used.

Lemma 1 [53]

Let $x = \delta||f||^2$, $y = \lambda||g||^2 + \frac{1}{\xi}$. Consider that $||f||^2$ and $||g||^2$ follow independent exponential distributions, then the CDF of $z = x/y$ is:

$$F_Z(z) = 1 - \frac{\delta}{\delta + \lambda z} \exp\left(-\frac{z}{\xi\delta}\right) \tag{4.2}$$

Proof:

The proof of Lemma 1 is presented in [53]. ■

Lemma 2

Let $x = \delta||f||^2$, $y = \lambda||g_1||^2 + \mu||g_2||^2 + \frac{1}{\xi}$. Consider that $||f||^2$, $||g_1||^2$ and $||g_2||^2$ follow independent exponential distributions, then the CDF of $z = x/y$ is:

$$F_Z(z) = \begin{cases} 1 - \frac{\delta^2}{(z\lambda+\delta)(z\mu+\delta)} \exp\left(-\frac{z}{\xi\delta}\right), & \forall \lambda \neq \mu \\ 1 - \frac{\delta^2}{(z\lambda+\delta)^2} \exp\left(-\frac{z}{\xi\delta}\right), & \forall \lambda = \mu \end{cases} \tag{4.3}$$

Proof:

The PDFs of x is expressed as [53]

$$f_X(x) = \frac{1}{\delta} \exp(-\frac{x}{\delta}) U(x) \quad \forall\ \lambda, \mu \tag{4.4}$$

where $U()$ is the unit step function. Let $p = \lambda||g_1||^2$ and $q = \mu||g_2||^2 + \frac{1}{\xi}$, then $y = p + q$ and the PDF of y can be evaluated as follows [89, 90]:

$$f_Y(y) = \int_{1/\xi}^{y} \frac{1}{\mu} f_p(p) f_q\left(\frac{(y-p)-\frac{1}{\xi}}{\mu}\right) dp \tag{4.5}$$

$$f_Y(y) = \begin{cases} \frac{1}{(\mu-\lambda)}\left[\exp\left(-\frac{y-\frac{1}{\xi}}{\mu}\right) - \exp\left(-\frac{y-\frac{1}{\xi}}{\lambda}\right)\right] U\left(y-\frac{1}{\xi}\right), & \forall \lambda \neq \mu \\ \frac{\left(y-\frac{1}{\xi}\right)}{\lambda^2} \exp\left(-\frac{y-\frac{1}{\xi}}{\lambda}\right) U\left(y-\frac{1}{\xi}\right), & \forall \lambda = \mu \end{cases} \tag{4.6}$$

The PDF of $z = x/y$ can be evaluated as:

$$f_Z(z) = \int_{1/\xi}^{\infty} y f_{xy}(yz, y)\, dy \tag{4.7}$$

The final expression for $f_Z(z)$ can be expressed as:

$$f_Z(z) = \begin{cases} \frac{\mu \exp\left(-\frac{z}{\xi\delta}\right)}{\xi(\mu-\lambda)(z\lambda+\delta)} + \frac{\delta\mu^2 \exp\left(-\frac{z}{\xi\delta}\right)}{(\mu-\lambda)(z\mu+\delta)^2} - \frac{\lambda \exp\left(-\frac{z}{\xi\delta}\right)}{\xi(\mu-\lambda)(z\lambda+\delta)} - \frac{\delta\lambda^2 \exp\left(-\frac{z}{\xi\delta}\right)}{(\mu-\lambda)(z\lambda+\delta)^2} & , \forall \lambda \neq \mu \\ \frac{\delta}{\xi(z\lambda+\delta)^2} \exp\left(-\frac{z}{\xi\delta}\right) + \frac{2\delta^2\lambda}{(z\lambda+\delta)^3} \exp\left(-\frac{z}{\xi\delta}\right) & , \forall \lambda = \mu \end{cases} \tag{4.8}$$

The CDF $F_Z(z)$ in (4.3) can be obtained by integrating $f_Z(z)$ with limits 0 to z.

■

Lemma 3

Let $x = \delta||f_1||^2 + \lambda||f_2||^2$, $y = \mu||g||^2 + \frac{1}{\xi}$. Consider that $||f_1||^2$, $||f_2||^2$ and $||g||^2$ follow independent exponential distributions, then the CDF of $z = x/y$ can be written as:

$$F_Z(z) = \begin{cases} 1 - \frac{1}{\lambda-\delta}\left[\frac{\lambda^2 \exp\left(-\frac{z}{\xi\lambda}\right)}{(z\mu+\lambda)} - \frac{\delta^2 \exp\left(-\frac{z}{\xi\delta}\right)}{(z\mu+\delta)}\right], & \forall \delta \neq \lambda \\ 1 - \left[\frac{(z+\xi\lambda)}{\xi(z\mu+\lambda)} + \frac{z\lambda\mu}{(z\mu+\lambda)^2}\right] \exp\left(-\frac{z}{\xi\lambda}\right), & \forall \delta = \lambda \end{cases} \tag{4.9}$$

Proof:

Let $p = \delta||f_1||^2$ and $q = \lambda||f_2||^2$, then $x = p + q$ and the PDF of x can be evaluated based on [89] as follows::

$$f_X(x) = \int_0^x f_p(p) f_q(x-p) dp \tag{4.10}$$

$$f_X(x) = \begin{cases} \frac{1}{(\lambda-\delta)} \left[\exp\left(-\frac{x}{\lambda}\right) - \exp\left(-\frac{x}{\delta}\right)\right] U(x), & \forall \delta \neq \lambda \\ \frac{x}{\delta^2} \exp\left(-\frac{x}{\delta}\right) U(x), & \forall \delta = \lambda \end{cases} \tag{4.11}$$

The PDFs of y is expressed as [53]

$$f_Y(y) = \frac{1}{\mu} \exp\left(-\frac{y - \frac{1}{\xi}}{\mu}\right) U\left(y - \frac{1}{\xi}\right) \quad \forall\ \delta, \lambda \tag{4.12}$$

Then, the PDF of $z = x/y$ can be evaluated as:

$$f_Z(z) = \int_{1/\xi}^{\infty} y f_{xy}(yz, y)\, dy \tag{4.13}$$

The final expression for $f_Z(z)$ is:

$$f_Z(z) = \begin{cases} \frac{\lambda\ \exp\left(-\frac{z}{\xi\lambda}\right)}{\xi(\lambda-\delta)(z\mu+\lambda)} + \frac{\mu\lambda^2 \exp\left(-\frac{z}{\xi\lambda}\right)}{(\lambda-\delta)(z\mu+\lambda)^2} - \frac{\delta\ \exp\left(-\frac{z}{\xi\delta}\right)}{\xi(\lambda-\delta)(z\mu+\delta)} - \frac{\mu\delta^2 \exp\left(-\frac{z}{\xi\delta}\right)}{(\lambda-\delta)(z\mu+\delta)^2}, & \forall \delta \neq \lambda \\ \frac{z \exp\left(-\frac{z}{\xi\lambda}\right)}{\lambda\xi^2(z\mu+\lambda)} + \frac{2z\mu \exp\left(-\frac{z}{\xi\lambda}\right)}{\xi(z\mu+\lambda)^2} + \frac{2z\mu^2\lambda \exp\left(-\frac{z}{\xi\lambda}\right)}{(z\mu+\lambda)^3}, & \forall \delta = \lambda \end{cases} \tag{4.14}$$

The CDF $F_Z(z)$ in (4.9) can be obtained by integrating $f_Z(z)$ with limits 0 to z.

■

The outage probabilities of the proposed and conventional methods are derived based on the above three *Lemmas*. For the proposed method in [53], the advantage of D2D communication disappears since the BS participates in the process of interference cancellation. Hence, the conventional interference sig-

nal cancellation (ISC) method proposed by Min et al. in [53] is considered for comparison in terms of outage probability. In ISC method, the desired signal is demodulated after cancelling the interference using the estimated interference signal at the receiver. A single-link D2D communication scenario is first considered and then the analysis is extended for a multi-link D2D communication case.

4.3 Single-link D2D communication

A single-link D2D communication scenario is presented in Figure 4.1. In the figure, the i^{th} link is considered as the desired link and j^{th} as the interference link. The term I_r denotes the power ratio of i^{th} link to j^{th} link. From Figure 2.2 of Chapter 2, the receiver can be either UE_1 or UE_0 for single-link D2D communication. For UE_1 as receiver, UE2UE forms the i^{th} link and BS2UE forms the j^{th} link and vice-versa for UE_0. The received SINR of the MRC output for i^{th} link is can be written as [75]:

$$\gamma = \frac{||\mathbf{H}_i \boldsymbol{\psi}_i \boldsymbol{\psi}_i^H \mathbf{H}_i^H||^2}{I_r ||\mathbf{H}_j \boldsymbol{\psi}_j \boldsymbol{\psi}_i^H \mathbf{H}_i^H||^2 + \frac{1}{\xi} I} \tag{4.15}$$

where $I_r = \frac{P_j}{P_i}$ and ξ denotes the SNR. Then, the outage probabilities of the OP and ISC methods for the described scenario are derived according to the power ratio of interference signal to the desired signal, I_r.

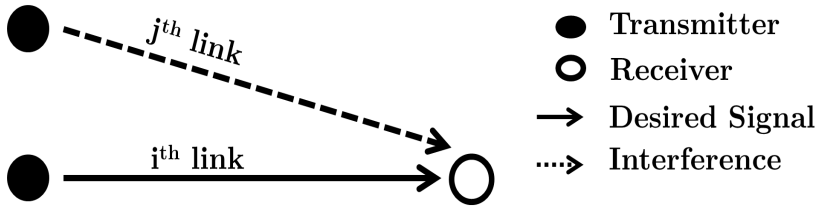

Figure 4.1: A single-link D2D communication scenario

4.3.1 Outage Probability of OP method

The success of OP method in interference cancellation affects the outage performance. Outage of i^{th} link can occur in either of the two cases: (i) Failure of OP method resulting in an outage with probability P_{op}^{21} and (ii) Outage probability of SNR, P_{pic}, occurs when the orthogonality between the precoding vectors of i^{th} and j^{th} links are maintained at the receiver. Failure of OP method occurs with an imperfect CSI, where the transmitter fails to receive the proper feedback index from the receiver. On failure of OP method, the desired signal is demodulated directly by treating interference as noise. The combined outage probability, P_{op}^{2}, of i^{th} link, can be evaluated as:

$$\begin{aligned} P_{op}^{2} &= P_{op}^{21} \cup P_{pic} \\ &= P_{op}^{21} + P_{pic} - P_{op}^{21} P_{pic} \end{aligned} \tag{4.16}$$

P_{op}^{21} is the CDF of γ presented in (4.15) and is evaluated from *Lemma 1* of (4.2). With perfect interference cancellation using OP method, the term $I_r||\mathbf{H}_j\boldsymbol{\psi}_j\boldsymbol{\psi}_i^H\mathbf{H}_i^H||^2 = 0$ in (4.15). Hence, P_{pic} can also be computed using *Lemma 1* with $y = \frac{1}{\xi}$ and can be written as:

$$P_{op}^{21} = 1 - \frac{1}{(\gamma_{th} I_r + 1)} \exp\left(-\frac{\gamma_{th}}{\xi}\right) \tag{4.17}$$

$$P_{pic} = 1 - \exp\left(-\frac{\gamma_{th}}{\xi}\right) \tag{4.18}$$

Finally substituting (4.17) and (4.18) in (4.16), P_{op}^{2} can be calculated as:

$$P_{op} = 1 - \frac{1}{(\gamma_{th} I_r + 1)} \exp\left(-\frac{2\gamma_{th}}{\xi}\right) \tag{4.19}$$

4.3.2 Outage Probability of ISC method

The outage probability of i^{th} link with ISC method can be written as [53]:

$$P_{isc} = 1 - \frac{I_r}{(\gamma_{th} + I_r)} \exp\left(-\frac{\gamma_{th}}{\xi I_r} - \frac{\gamma_{th}}{\xi}\right) \tag{4.20}$$

Relationships (4.19) for OP method and (4.20) for ISC method can be used to calculate outage probabilities of both CH2BS and UE2UE links.

4.4 Multi-link D2D communication

In this section, we analyse the proposed OP method in terms of outage probability for a multi-link D2D communication. In our analysis, it was considered that the mesh-layout cluster as shown in Figure 4.2 with UE_0, UE_1, UE_2, UE_3 are the members in the cluster. However, the analysis can be extended to any cluster layout. A possible allocation of UEs that are enabled to transmit in each timeslot of LTE TDD frame structure is shown in Figure 4.3. In the 0^{th} subframe, 5 links are scheduled in both the timeslots with UE_0 and UE_3 as the receivers. UE_0 receives data simultaneously from 3 links, $BS2UE^{DL}$, $UE2UE_1^{10}$, $UE2UE_2^{20}$, and UE_3 from 2 links, $UE2UE_3^{13}$ and $UE2UE_4^{23}$. Similarly, for the 2^{nd} subframe, the UE_1 and UE_2 are the receivers in the cluster each receiving data from 2 links. In the first timeslot of the 3^{rd} subframe, UE_0 and UE_1 are the receivers each with one receive link and similar is the case for UE_2 and UE_3 in the second timeslot of the 3^{rd} subframe. In short, three different scenarios arises while allocating resources for communication links in Figure 4.2 depending on the number of receiving links per UE. These three scenarios are presented in Figure 4.4 and their description is summarized below:

(i) Scenario I: A UE receiving signals simultaneously from 3 links per timeslot, where i^{th} link is the desired link, j^{th} and k^{th} links are the interferences. For

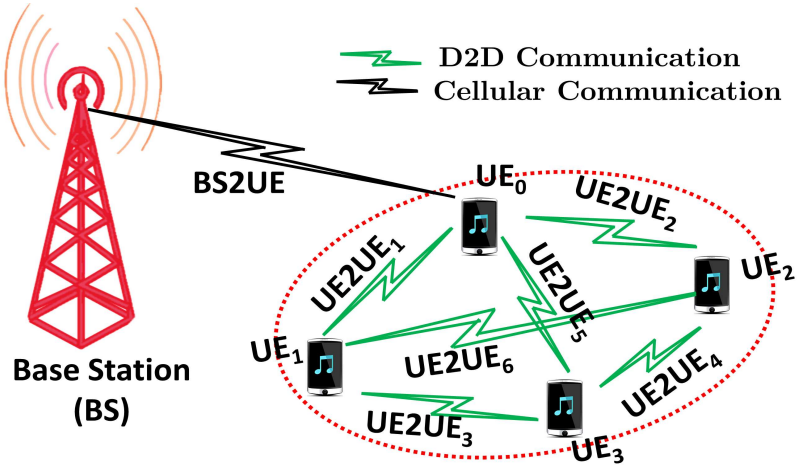

Figure 4.2: A mesh-type layout of cluster with multiple D2D communications

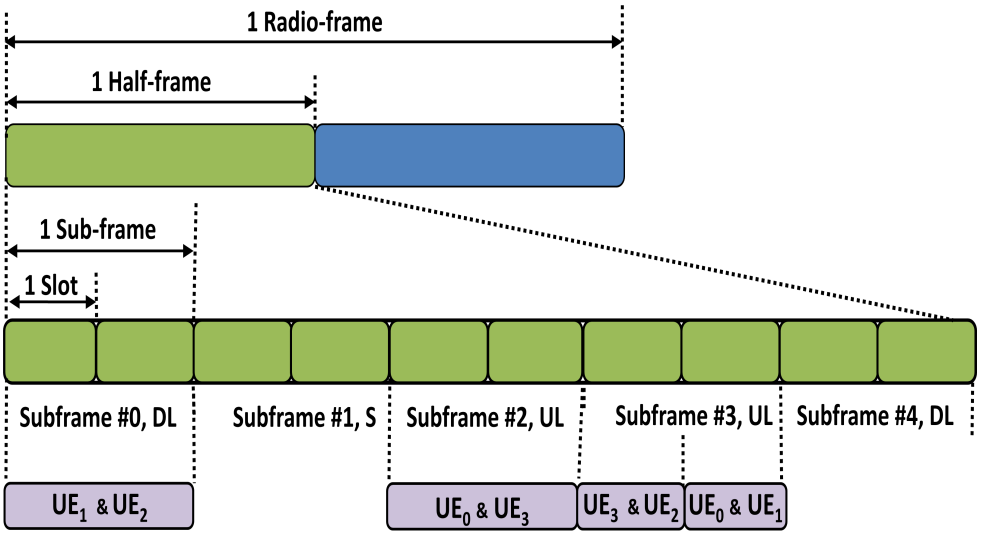

Figure 4.3: UEs in the mesh-type cluster that are enabled to transmit in each timeslot of LTE TDD frame.

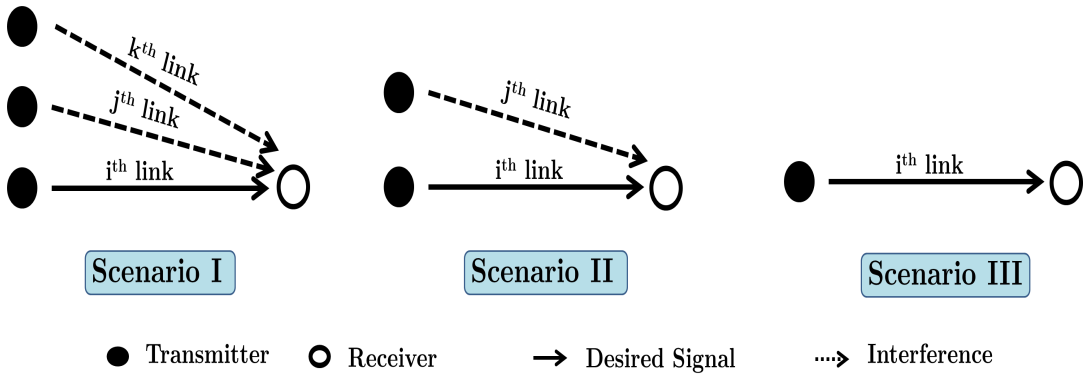

Figure 4.4: Different scenarios considered for deriving the outage probabilities of multi-link D2D communications

example, the case of UE_0 receiving signals from the BS, UE_1 and UE_2 in the first timeslot of the 0^{th} subframe.

(ii) Scenario II: A UE receiving signals from 2 links per timeslot, where i^{th} link is the desired link and j^{th} link is the interference. For example, the case of UE_3 receiving signals from the UE_1 and UE_2 in the first timeslot of the 0^{th} subframe.

(iii) Scenario III: A UE receiving signals from 1 link per timeslot with i^{th} link as the desired link. For example, the case of UE_2 receiving signals from the UE_1 in the second timeslot of the 3^{rd} subframe.

In general, the outage probabilities of the proposed and conventional methods for the above mentioned scenarios are derived here. To calculate the outage probability, a case with i^{th} link as the desired one and j^{th} and k^{th} links as the interfered ones is assumed with I_r^j (resp. I_r^k) as the power ratio of i^{th} link to j^{th} (resp k^{th}) link.

4.4.1 Outage Probability of OP method

Sharing of allocated resources by multiple D2D links result in co-channel interferences. The received SINR of the MRC output for i^{th} link for the worst case

scenario (Scenario I) can be written [75]:

$$\gamma = \frac{||\mathbf{H}_i \boldsymbol{\psi}_i \boldsymbol{\psi}_i^H \mathbf{H}_i^H||^2}{I_r^j ||\mathbf{H}_j \boldsymbol{\psi}_j \boldsymbol{\psi}_i^H \mathbf{H}_i^H||^2 + I_r^k ||\mathbf{H}_k \boldsymbol{\psi}_k \boldsymbol{\psi}_i^H \mathbf{H}_i^H||^2 + \frac{1}{\xi} I} \tag{4.21}$$

where I_r^j (resp. I_r^k) is the power ratio of j^{th} (resp. k^{th}) link to i^{th} link, i.e, $I_r^j = \frac{P_j}{P_i}$, $I_r^k = \frac{P_k}{P_i}$.

Scenario I

The outage probability for Scenario I is influenced by the effectiveness of OP method. Success of co-channel interference cancellation with the OP method occurs when precoding vectors of the desired link is orthogonal to the precoding vectors of the interfering ones at the receiver. Failure of OP method occurs with an imperfect Channel State Information (CSI), where the transmitter fails to receive the proper feedback index from the receiver. In such cases, the interference is processed as noise for calculating the outage probability. Thus, the outage of i^{th} link can occur in any of the following situations:

(i) Failure of orthogonality of precoding vectors of both j^{th} and k^{th} links with i^{th} link that results in an outage probability P_{op}^{31},

(ii) Failure of orthogonality of precoding vector of j^{th} (resp. k^{th}) link with i^{th} link resulting in an outage probability P_{op}^{21} (resp. P_{op}^{22}),

(iii) Outage probability of SNR, P_{pic}, occurring after perfect interference cancellation.

P_{op}^{31} is the CDF of γ in (4.21). According to [75], $\mathbf{H}_i \boldsymbol{\psi}_i \boldsymbol{\psi}_i^H \mathbf{H}_i^H$ and $\mathbf{H}_j \boldsymbol{\psi}_j \boldsymbol{\psi}_i^H \mathbf{H}_i^H$ in (4.21) are independent exponential random variables. Let $x = ||\mathbf{H}_i \boldsymbol{\psi}_i \boldsymbol{\psi}_i^H \mathbf{H}_i^H||^2$ and $y = I_r^j ||\mathbf{H}_j \boldsymbol{\psi}_j \boldsymbol{\psi}_i^H \mathbf{H}_i^H||^2 + I_r^k ||\mathbf{H}_k \boldsymbol{\psi}_k \boldsymbol{\psi}_i^H \mathbf{H}_i^H||^2 + \frac{1}{\xi}$ then CDF of γ can be evaluated from *Lemma 2*. According to *Lemma 2*, P_{op}^{31} can be evaluated as:

$$P_{op}^{31}=\begin{cases} 1-\frac{1}{\left(\gamma_{th}I_r^j+1\right)\left(\gamma_{th}I_r^k+1\right)}\exp(-\frac{\gamma_{th}}{\xi}), & \forall I_r^j \neq I_r^k \\ 1-\frac{1}{\left(\gamma_{th}I_r^j+1\right)^2}\exp(-\frac{\gamma_{th}}{\xi}), & \forall I_r^j = I_r^k \end{cases} \tag{4.22}$$

For the case of evaluating P_{op}^{21}, the precoding vectors of i^{th} and k^{th} links are orthogonal and hence $I_r^k||\mathbf{H}_k\boldsymbol{\psi}_k\boldsymbol{\psi}_i^H\mathbf{H}_i^H||^2 = 0$ according to OP method. P_{op}^{21} can be calculated from the equation (4.3), for $y = I_r^j||\mathbf{H}_j\boldsymbol{\psi}_j\boldsymbol{\psi}_i^H\mathbf{H}_i^H||^2 + \frac{1}{\xi}$, and is given as:

$$P_{op}^{21} = 1 - \frac{1}{\left(\gamma_{th}I_r^j + 1\right)}\exp\left(-\frac{\gamma_{th}}{\xi}\right) \tag{4.23}$$

Similarly, P_{op}^{22} can be evaluated from the *Lemma 2* for $y = I_r^k||\mathbf{H}_k\boldsymbol{\psi}_k\boldsymbol{\psi}_i^H\mathbf{H}_i^H||^2 + \frac{1}{\xi}$, and is given as:

$$P_{op}^{22} = 1 - \frac{1}{\left(\gamma_{th}I_r^k + 1\right)}\exp\left(-\frac{\gamma_{th}}{\xi}\right) \tag{4.24}$$

Perfect interference cancellation occur when the precoding vectors of the interfering links are orthogonal to the precoding vector of the desired link. Hence for the case of P_{pic}, $I_r^j||\mathbf{H}_j\boldsymbol{\psi}_j\boldsymbol{\psi}_i^H\mathbf{H}_i^H||^2 = I_r^k||\mathbf{H}_k\boldsymbol{\psi}_k\boldsymbol{\psi}_i^H\mathbf{H}_i^H||^2 = 0$. P_{pic} is evaluated from the *Lemma 2*, equation (4.3), for $y = \frac{1}{\xi}$ and is given in (4.18). Thus the combined outage probability of *Scenario I*, P_{op}^3 can be written as:

$$\begin{aligned} P_{op}^3 &= P_{op}^{31} \bigcup P_{op}^{21} \bigcup P_{op}^{22} \bigcup P_{pic} \\ &= 1 - \left(1 - P_{op}^{31}\right)\left(1 - P_{op}^{21}\right)\left(1 - P_{op}^{22}\right)\left(1 - P_{pic}\right) \end{aligned} \tag{4.25}$$

Substituting (4.22), (4.23), (4.24) and (4.18) in (4.25), the final expression for P_{op}^3 can be evaluated. Since (4.22) is a conditional relationship, the final expression for P_{op}^3 will also have separate relationships for $I_r^j \neq I_r^k$ and $I_r^j = I_r^k$,

$$P_{op}^{3}=\begin{cases} 1-\frac{1}{\left(\gamma_{th}I_r^j+1\right)^2\left(\gamma_{th}I_r^k+1\right)^2}\exp(-\frac{4\gamma_{th}}{\xi}), & \forall I_r^j \neq I_r^k \\ 1-\frac{1}{\left(\gamma_{th}I_r^j+1\right)^4}\exp(-\frac{4\gamma_{th}}{\xi}), & \forall I_r^j = I_r^k \end{cases} \tag{4.26}$$

Scenario II

In this case, we consider i^{th} link as desired link and j^{th} as the interfering one. The Scenario II is similar to the single link communication model as shown in Figure 4.1. From (4.19), the combined outage probability for Scenario II can be written as:

$$P_{op}^{2} = 1 - \frac{1}{\left(\gamma_{th}I_r^j + 1\right)}\exp\left(-\frac{2\gamma_{th}}{\xi}\right) \tag{4.27}$$

Scenario III

Since there exist no interfering links for Scenario III, the outage probability for this case is same as the outage probability of SNR after perfect interference cancellation, i.e,

$$P_{op}^{1} = P_{pic} \tag{4.28}$$

4.4.2 Outage Probability of ISC method

In the ISC method, the desired signal is demodulated after cancelling the interference by using the estimated interference signal at the receiver. The received signal for the i^{th} link with both j^{th} and k^{th} interfering signals after interference cancellation with ISC method is given as:

$$\hat{y_i} = \sqrt{P_i}\mathbf{H}_i\boldsymbol{\psi}_i s_i + \sqrt{P_j}\mathbf{H}_j\boldsymbol{\psi}_j(s_j - \hat{s_j}) + \sqrt{P_k}\mathbf{H}_k\boldsymbol{\psi}_k(s_k - \hat{s_k}) + \eta \tag{4.29}$$

where $\hat{s_j}$ and $\hat{s_k}$ denote the demodulated interference signal and s_i is the desired signal which is decoded after the MRC linear combining with $\mathbf{H}_i\boldsymbol{\psi}_i$. An improper decoding of the interference signal results in an outage probability of Interference-to-Signal-and-Noise-ratio (ISNR) and perfect interference cancellation occurs if the interference is decoded correctly [53]. The ISNR for the i^{th} received signal can be written as:

$$\chi = \frac{I_r^j||\mathbf{H}_j\boldsymbol{\psi}_j\boldsymbol{\psi}_i^H\mathbf{H}_i^H||^2 + I_r^k||\mathbf{H}_k\boldsymbol{\psi}_k\boldsymbol{\psi}_i^H\mathbf{H}_i^H||^2}{||\mathbf{H}_i\boldsymbol{\psi}_i\boldsymbol{\psi}_i^H\mathbf{H}_i^H||^2 + \frac{1}{\xi}I} \tag{4.30}$$

Scenario I

Similar to OP method, the combined outage probability of ISC method can be evaluated as:

$$P_{isc}^3 = 1 - \left(1 - P_{isc}^{31}\right)\left(1 - P_{isc}^{21}\right)\left(1 - P_{isc}^{22}\right)\left(1 - P_{pic}\right) \tag{4.31}$$

where P_{isc}^{31} is the outage probability due to improper decoding of the interference signal from j^{th} and k^{th} links. The outage occurs with probability P_{isc}^{21} with improper decoding of the interference signal for j^{th} link and proper decoding of the interference signal for k^{th} link. Similarly, P_{isc}^{22} is the outage probability due to improper decoding of the interference signal for k^{th} link and P_{pic} is the outage probability of SNR with perfect interference cancellation for k^{th} and j^{th} links. These outage probabilities can be evaluated from *Lemma 3*.

P_{isc}^{31} is the CDF of χ in (4.30). Let $x = I_r^j||\mathbf{H}_j\boldsymbol{\psi}_j\boldsymbol{\psi}_i^H\mathbf{H}_i^H||^2 + I_r^k||\mathbf{H}_k\boldsymbol{\psi}_k\boldsymbol{\psi}_i^H\mathbf{H}_i^H||^2$ and $y = ||\mathbf{H}_i\boldsymbol{\psi}_i\boldsymbol{\psi}_i^H\mathbf{H}_i^H||^2 + \frac{1}{\xi}$ then CDF of χ can be evaluated from *Lemma 3*, (4.9). According to *Lemma 3*, P_{isc}^{31} can be evaluated as:

$$P_{isc}^{31} = \begin{cases} 1 - \frac{1}{I_r^k - I_r^j}\left[\frac{\left(I_r^k\right)^2 \exp(-\frac{\gamma_{th}}{\xi I_r^k})}{\left(\gamma_{th}+I_r^k\right)} - \frac{\left(I_r^j\right)^2 \exp(-\frac{\gamma_{th}}{\xi I_r^j})}{\left(\gamma_{th}+I_r^j\right)}\right], & \forall I_r^j \neq I_r^k \\ 1 - \left[\frac{\left(\gamma_{th}+\xi I_r^j\right)}{\xi\left(\gamma_{th}+I_r^j\right)} + \frac{\gamma_{th} I_r^j}{\left(\gamma_{th}+I_r^j\right)^2}\right] \exp(-\frac{\gamma_{th}}{\xi I_r^j}), & \forall I_r^j = I_r^k \end{cases} \tag{4.32}$$

With proper decoding of the interference signal for the k^{th} link, the interference term $I_r^k||\mathbf{H}_k\boldsymbol{\psi}_k\boldsymbol{\psi}_i^H\mathbf{H}_i^H||^2 = 0$ for the case of P_{isc}^{21}. Hence P_{isc}^{21} can be calculated from *Lemma 3* with $x = I_r^j||\mathbf{H}_j\boldsymbol{\psi}_j\boldsymbol{\psi}_i^H\mathbf{H}_i^H||^2$ and can be written as:

$$P_{isc}^{21} = 1 - \frac{I_r^j}{I_r^j + \gamma_{th}} \exp\left(-\frac{\gamma_{th}}{I_r^j \xi}\right) \tag{4.33}$$

Similarly P_{isc}^{22} can be evaluated from *Lemma 3* with $x = I_r^k||\mathbf{H}_k\boldsymbol{\psi}_k\boldsymbol{\psi}_i^H\mathbf{H}_i^H||^2$ and can be written as:

$$P_{isc}^{22} = 1 - \frac{I_r^k}{I_r^k + \gamma_{th}} \exp\left(-\frac{\gamma_{th}}{I_r^k \xi}\right) \tag{4.34}$$

The perfect interference cancellation occurs with proper decoding of all interference signals which results in an outage probability, P_{pic}, and was presented in (4.18). By substituting (4.32), (4.33), (4.34) and (4.18) in (4.31), the final expression for P_{isc}^3 will also have separate relationships for $I_r^j \neq I_r^k$ and $I_r^j = I_r^k$. For $I_r^j \neq I_r^k$, the combined outage probability, P_{isc}^3, can be written as:

$$P_{isc}^3 = 1 - \frac{I_r^j I_r^k \exp\left(-\frac{\gamma_{th}}{I_r^j\xi} - \frac{\gamma_{th}}{I_r^k\xi} - \frac{\gamma_{th}}{\xi}\right)}{\left(I_r^k - I_r^j\right)\left(I_r^j + \gamma_{th}\right)\left(I_r^k + \gamma_{th}\right)} \left[\frac{\left(I_r^k\right)^2 \exp\left(-\frac{\gamma_{th}}{\xi I_r^k}\right)}{\left(\gamma_{th} + I_r^k\right)} - \frac{\left(I_r^j\right)^2 \exp\left(-\frac{\gamma_{th}}{\xi I_r^j}\right)}{\left(\gamma_{th} + I_r^j\right)}\right] \tag{4.35}$$

Similarly for the case when $I_r^j = I_r^k$, P_{isc}^3, can be evaluated as:

$$P_{isc}^3 = 1 - \left[\frac{\left(\gamma_{th} + \xi I_r^j\right)}{\xi\left(\gamma_{th} + I_r^j\right)} + \frac{\gamma_{th} I_r^j}{\left(\gamma_{th} + I_r^j\right)^2}\right] \left(\frac{I_r^j}{I_r^j + \gamma_{th}}\right)^2 \exp\left(-\frac{\gamma_{th}}{\xi I_r^j} - \frac{2\gamma_{th}}{I_r^j \xi} - \frac{\gamma_{th}}{\xi}\right) \tag{4.36}$$

Rearranging (4.35) and (4.36), the final expression for P_{isc}^{3} can be evaluated as:

$$P_{isc}^{3}=\begin{cases} 1-\frac{1}{\left(I_r^k-I_r^j\right)}\left[\frac{I_r^j\left(I_r^k\right)^3\exp\left(-\frac{2\gamma_{th}}{\xi I_r^k}-\frac{\gamma_{th}}{\xi I_r^j}-\frac{\gamma_{th}}{\xi}\right)}{\left(\gamma_{th}+I_r^j\right)\left(\gamma_{th}+I_r^k\right)^2}-\frac{I_r^k\left(I_r^j\right)^3\exp\left(-\frac{2\gamma_{th}}{\xi I_r^j}-\frac{\gamma_{th}}{\xi I_r^k}-\frac{\gamma_{th}}{\xi}\right)}{\left(\gamma_{th}+I_r^j\right)^2\left(\gamma_{th}+I_r^k\right)}\right], \\ \qquad\qquad \forall\ I_r^j \neq I_r^k \\ 1-\frac{\left(I_r^j\right)^2}{\left(\gamma_{th}+I_r^j\right)^4}\left[\frac{\left(\gamma_{th}+\xi I_r^j\right)\left(\gamma_{th}+I_r^j\right)}{\xi}+\gamma_{th}I_r^j\right]\exp\left(-\frac{3\gamma_{th}}{\xi I_r^j}-\frac{\gamma_{th}}{\xi}\right), \\ \qquad\qquad \forall\ I_r^j = I_r^k \end{cases} \tag{4.37}$$

Scenario II

The outage probability of a desired link in the presence of an interference link was presented in [53], and is given as:

$$P_{isc}^{2}=1-\frac{I_r^j}{\left(\gamma_{th}+I_r^j\right)}\exp\left(-\frac{\gamma_{th}}{\xi I_r^j}-\frac{\gamma_{th}}{\xi}\right) \tag{4.38}$$

Scenario III

Similar to the OP method, the outage probability for Scenario III of ISC method is same as the outage probability of SNR after perfect interference cancellation, i.e, $P_{isc}^{1}=P_{pic}$.

4.5 Results and Discussion

In this section, the performance of OP method is numerically evaluated and compared with the conventional ISC method. The analysis is carried out for both single-link and multi-link D2D communication cases. The simulation tool for the analysis was developed by using MATLAB software. The simulation parameters and considered values are summarized in Table 4.1.

4.5.1 Single link D2D communication

For the single link D2D communication case, a model described in Figure 4.1 with a single BS2UE and UE2UE links was considered. Here, the UE2UE link share the resources of the BS2UE link. Comparison of the proposed method with existing interference cancellation method is required to validate the novelty of the proposed method. Performance analysis of the proposed OP method and conventional ISC method of [53] is presented considering outage probability as the performance index.

Figure. 4.5 shows the outage probabilities vs γ_{th} plot for OP and ISC methods. The outage probability without the presence of interference have been plotted. In all the three cases, the outage probability increases as γ_{th} increases. The figure also indicates that in the presence of interference, the proposed method can reduce the outage probability much better than the conventional method (i.e. ISC). At $\gamma_{th} = 0$ dB, the probability of an outage event is 0.7 for ISC method whereas the probability is only 0.3 for OP method.

Figure. 4.6 displays the outage probabilities plot for OP method, ISC method and the case without interference as a function of ξ. In a noisy environment, the probability of outage is high for all the three cases. As ξ increases, the outage

Table 4.1: Simulation Parameters for Outage Probability analysis

Parameter	**Value**
Power ratio of Interference signal to the Desired signal, $I_r = I_r^j$	0.5
I_r^k	0.65
SNR, ξ	20 dB
SINR threshold, γ_{th}	0 dB

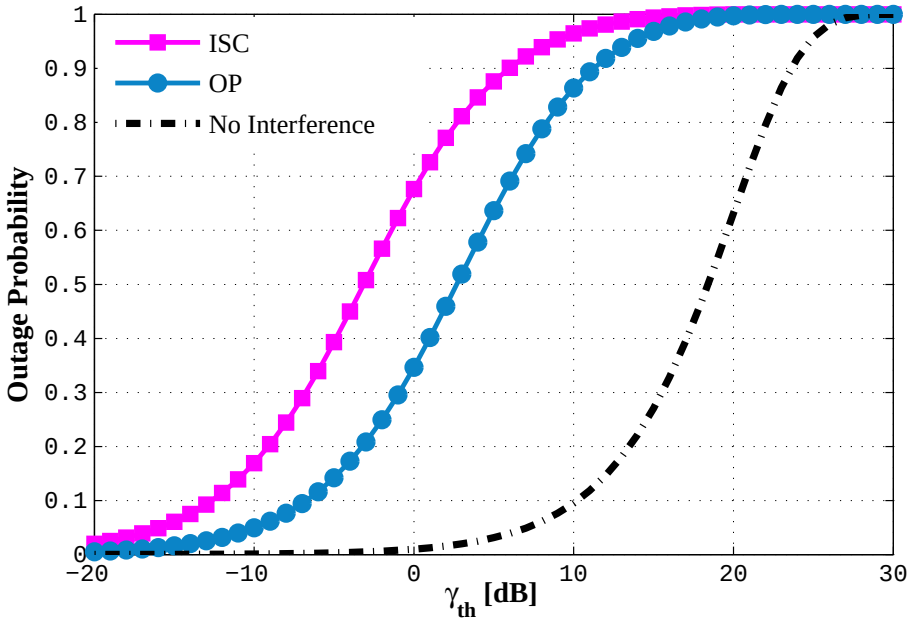

Figure 4.5: Outage Probabilities vs SINR threshold γ_{th} plot for OP method, ISC method and the case without interference

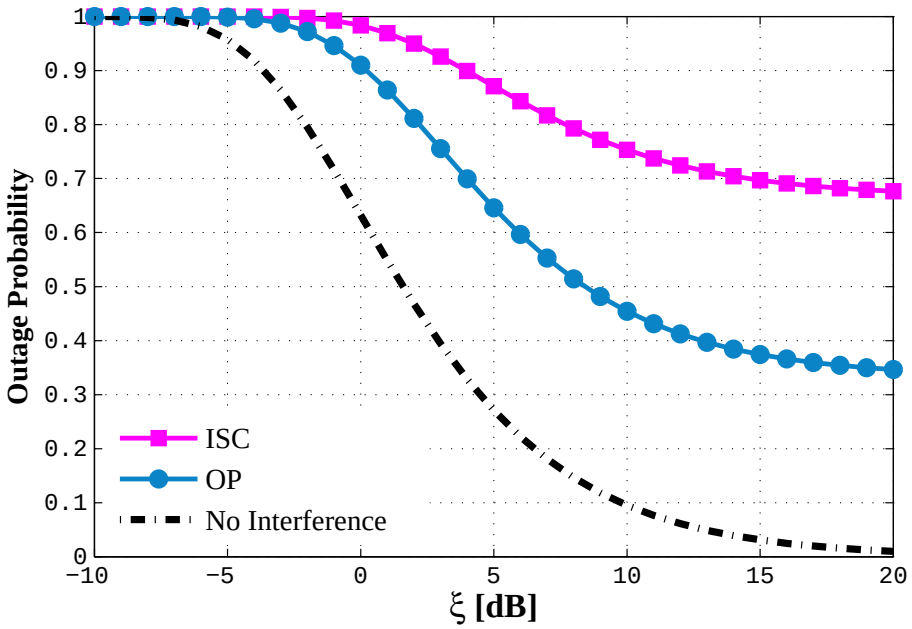

Figure 4.6: Outage Probabilities vs SNR ξ plot for OP method, ISC method and the case without interference

probability decreases. The rate of decrease in outage probability is faster with the proposed OP method than the conventional ISC method. At $\xi = 15$ dB, the probability for a link to be in outage is reduced by half with the proposed method in comparison with ISC method.

4.5.2 Multi-link D2D communication

For analysis, a mesh type cluster layout as shown in Figure 4.2, i.e., with 1 cellular and 6 D2D links, is considered. Figure. 4.7 illustrates the outage probability as a function of γ_{th} for Scenarios I, II and III with the OP and conventional ISC methods. We consider the equations (4.26) and (4.37) with the case $I_r^j \neq I_r^k$ as explained in Section 4.4 in both OP and ISC methods for Scenario I. The result shows that the probability of desired link in outage increases as the required γ_{th} at the UE receiver increases. The result also shows that the performance degrades as the number of interfering links at the UE increases. For both OP and ISC methods, the outage probability of Scenario II is better (lower outage probability) than that of Scenario I and also the outage probability of Scenario III is better than Scenario I and Scenario II. In short, for OP method, $P_{op}^1 < P_{op}^2 < P_{op}^3$ and for ISC method, $P_{isc}^1 < P_{isc}^2 < P_{isc}^3$. In comparison with ISC method, the proposed OP method provides better performance for Scenario I and Scenario II. Thus, the orthogonal precoding presents a superior approach to cancel the co-channel interference than the conventional ISC method.

Figure. 4.8 depicts the outage probabilities for the OP and ISC methods as a function of ξ for all three scenarios. Here we consider (4.26) and (4.37) with $I_r^j = I_r^k$ for both OP and ISC methods. The figure shows that the outage probability is higher for both OP and ISC methods in a noisy environment ($\xi < -5$ dB). It is understood that as ξ increases, the system performance also improves. But the improvement in performance, i.e, decline in outage probability,

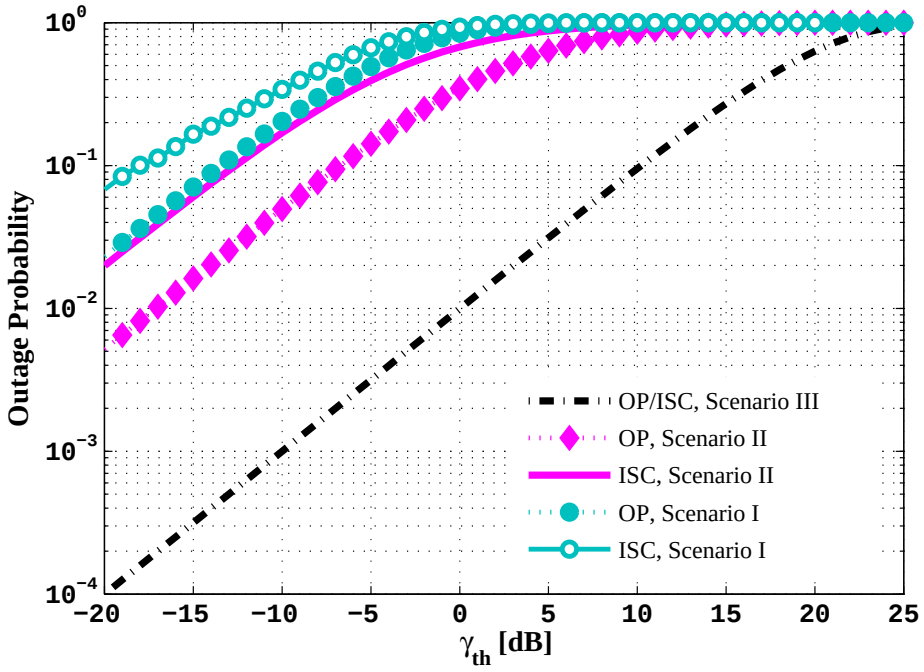

Figure 4.7: Outage Probability vs SINR threshold, γ_{th}, plot for OP and ISC methods

as ξ increases is faster for OP method than the conventional ISC method. For example, the probability for a link to be in outage is reduced by half for Scenario II and about by 20% for Scenario I when comparing the OP and ISC methods at $\xi = 15$ dB.

From Figure. 4.7 and Figure. 4.8, it is seen that assigning orthogonal precoding vectors to all links in a cluster ensures better co-channel interference reduction when compared with the ISC method. The decoding of interference signals for interference cancellation using ISC method increases the computational complexity at the receiver.

The outage probability of OP method for Scenario I with $\gamma_{th} = 0$ dB, $\gamma_{th} = 5$ dB and $\gamma_{th} = 10$ dB is presented in Figure. 4.9. For Scenario I, we have two power ratios I_r^j and I_r^k corresponding to the j^{th} and k^{th} interfering links. In this result, the power ratio varies from low interference environments, $I_r^j < 1$ and $I_r^k < 1$, to high interference environments, $I_r^j \geq 1$ and $I_r^k \geq 1$. As expected,

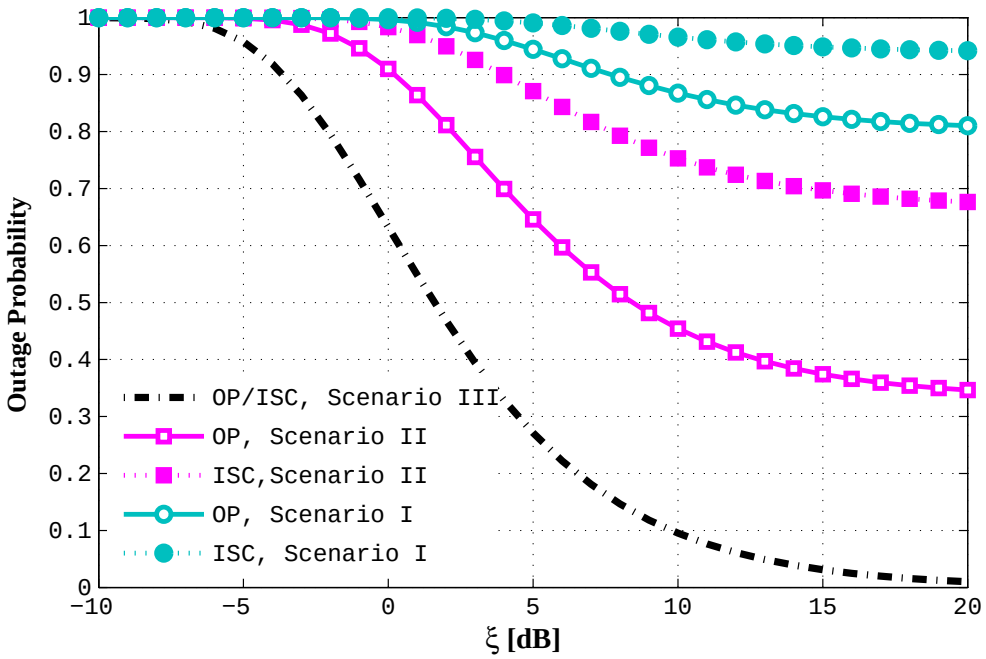

Figure 4.8: Outage Probability vs SNR, ξ, plot for OP and ISC methods

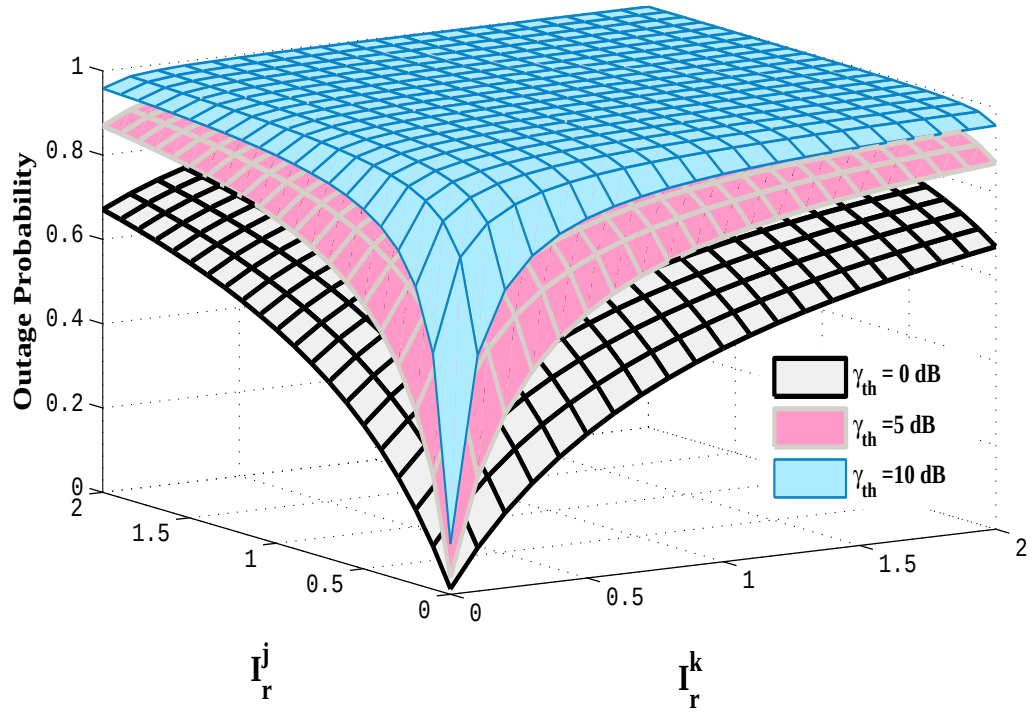

Figure 4.9: Outage Probability vs Power ratio of Interference signal to the Desired signal plot for Scenario I with OP method

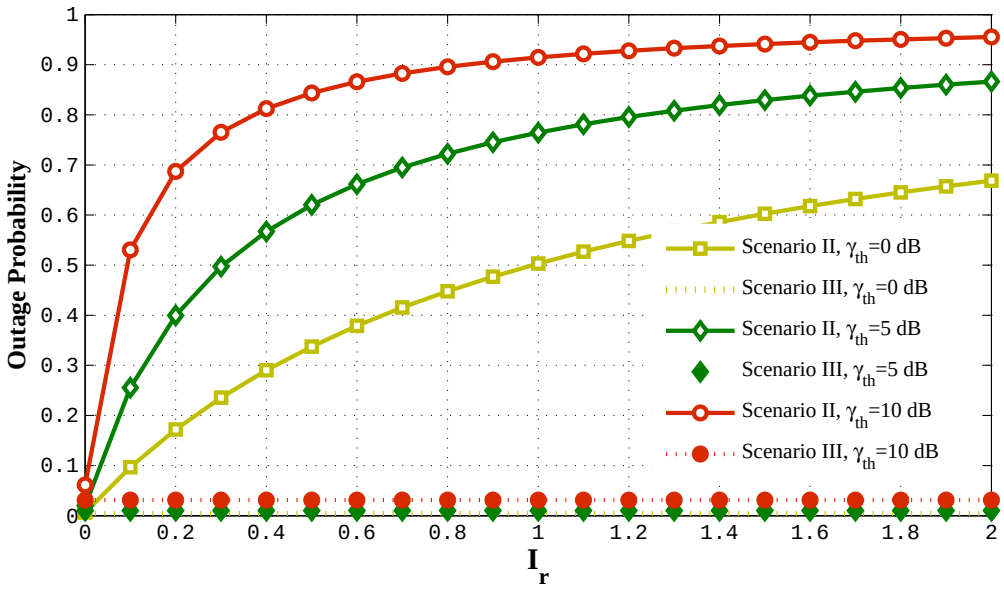

Figure 4.10: Outage Probability vs Power ratio of Interference signal to the Desired signal, I_r, plot for Scenario II and Scenario III with OP method

the probability of desired link to be in outage increases as the interference power increases. At $\gamma_{th} = 10$ dB, the outage probability is almost equal to 1 for $I_r^j \geq 1$ and $I_r^k \geq 1$ and hence have flat surface in the figure, i.e., the SINR requirement will not be satisfied in this area. The result also shows that the probability of outage event gradually increases when the γ_{th} required at the UE receiver increases. For example, the probability of outage event was only 0.5 for $\gamma_{th} = 0$ dB, whereas the outage probability increases to 0.8 and 0.96 for $\gamma_{th} = 5$ dB and $\gamma_{th} = 10$ dB respectively.

Figure. 4.10 presents the outage probability of OP method for Scenario II and Scenario III as a function of power ratio of interference signal to desired signal, I_r. Here the analysis was carried out with $\gamma_{th} = 0$ dB, $\gamma_{th} = 5$ dB and $\gamma_{th} = 10$ dB and I_r is varied from low interference to high interference environments. As observed from Figure. 4.9, the probability of desired link to be in outage increases as the interference power increases for the case of Scenario II. For Scenario III, there are no interfering links and thus P_{op}^3 is independent

of the parameter I_r. Therefore the outage probability vs I_r plot for Scenario III are all straight lines. The figure also shows that the increase in probability of outage event with increase in γ_{th} is higher for Scenario II (the scenario with an interference link) than Scenario III (the scenario without any interference links). For example, the outage probability for Scenario II changes from 0.62 to 0.85 with an increase in γ_{th} from 5 dB to 10 dB at $I_r = 0.5$, whereas the outage probability change is only from 0.01 to 0.03 for Scenario III.

4.6 Summary

The outage probability of the orthogonal precoding and the conventional interference signal cancellation methods have been derived for the case when single and multiple D2D links co-exist in the cellular radio resource. Simulation results indicate that the proposed method leads in reduction of interference and provides better outage probability when compared to the ISC method.

CHAPTER 5

Efficient Resource Allocation of Multi-link D2D Communication

Contents

For co-channel interference cancellation with OP method proposed in Chapter 3, efficient resource allocation of multi-link D2D communication is required. This chapter analyses the problem of resource allocation with efficient transmission mode selection, clustering process for grouping interconnected UEs and selection of Cluster Head in each cluster.

5.1 Introduction

The D2D communications in a cellular network possess many challenges including appropriate mode selection and resource allocation. Mode selection deals with the decision on whether a UE pair should communicate directly or via the BS whereas the resource allocation deals with appropriate selection of cellular UE resources to be shared. In addition, multiple links need to be managed in a single UE resource to improve the spectrum utilization efficiency and overall system throughput by guaranteeing QoS to both cellular and D2D UEs [64]. In comparison to previous research works, this chapter has the following major contributions:

1. Determining the mode of communication for each UEs in the cell, a mode selection algorithm is proposed. The proposition considers the quality and interference level of D2D and cellular connection to satisfy the SINR constraint of the network for mode selection.

2. Efficient utilization of cellular spectrum can be achieved by sharing cellular links with multiple D2D links. In this research work, the links that can share a common resource is determined by the process of clustering. This clustering process groups interconnected UEs to form a cluster. The advantage of the proposed clustering approach is that the multiple links established to/from a UE is served by a common resource.

3. In order to reduce the traffic load, a Cluster Head (CH) is selected for each cluster which act as a relay node to communicate with the network for every member in the cluster. In addition, all the links established in the cluster share the resource allocated to the CH. So a cluster head selection procedure is also proposed based on the maximum residual energy and minimum transmit power criteria.

4. Finally, the expression for maximum number of links that the radio resource of CH can support is analytically derived based on the quality of CH-to-BS (CH2BS) link.

Moreover, the algorithm developed has been applied to analyse in an indoor office scenario according to the WINNER II A1 office model [91]. The generalized consideration provide an appropriate scenario for D2D evaluation. These considerations provide an extensive and complete set of results on the considered problems.

5.2 System Model

This section introduces the system model for D2D underlay communication. The multiple D2D and cellular communication scenarios are firstly described and then the D2D communication issues are formulated. In this analysis, TDD mode of operation is considered.

5.2.1 Scenario Description

A model with a single BS and N_u uniformly distributed active UEs in the cell as shown in Figure.5.1 is considered. A communication link between two UEs via the BS is denoted as the cellular link and these serving UEs as the cellular UEs. Similarly, a direct link between the UEs is named as the D2D link and these

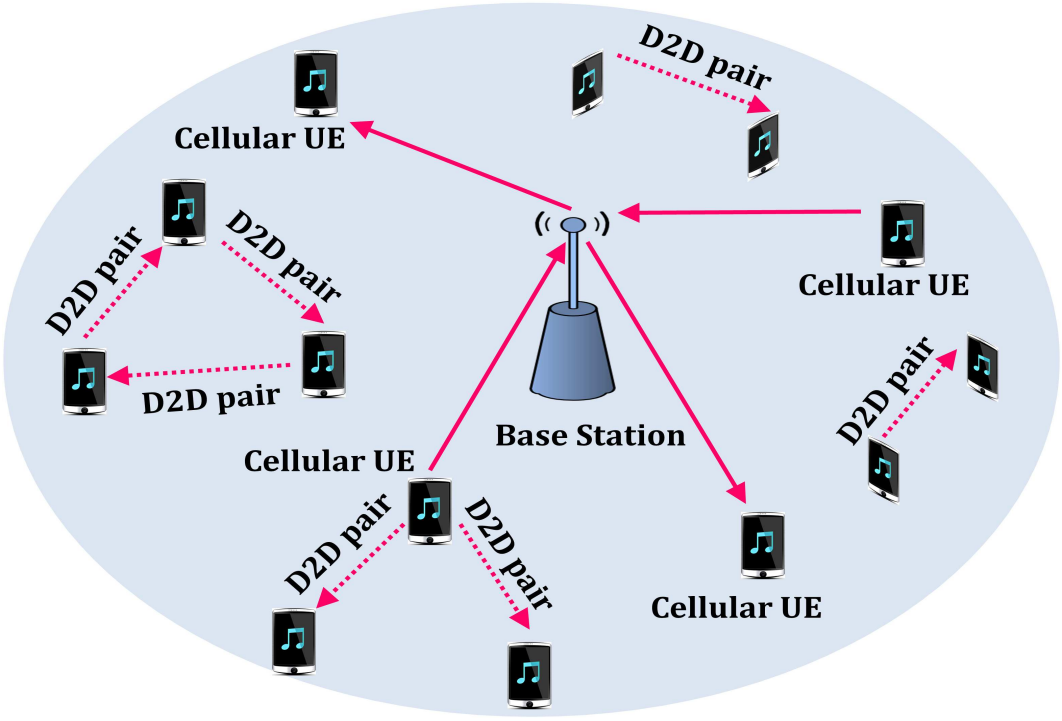

Figure 5.1: A cell with D2D and Cellular communications

serving UEs are called as the D2D UEs. It is assumed that the total available radio resources assigned for the cellular links are shared by the D2D links in the given cell.

The communication from UE_i to UE_j can be realised either through the direct D2D link or via cellular link as shown in Figure. 5.2 based on the QoS of both the links evaluated by the BS. Here SINR is considered as the indicator of QoS to maximize the network capacity.

The cellular link from UE_i (transmitter) to the UE_j (receiver) can be considered as a 2 hop relay network with the BS acting as the relay. In-order to minimize outage of cellular link, it is considered that the SINR of the whole cellular link is given by the weakest part of the link [92]

$$\gamma_{ij}^{c} = \arg\min \{\gamma_{i0}, \gamma_{0j}\} \ \forall \ i, j = \{1, 2, ..., N_u\} \tag{5.1}$$

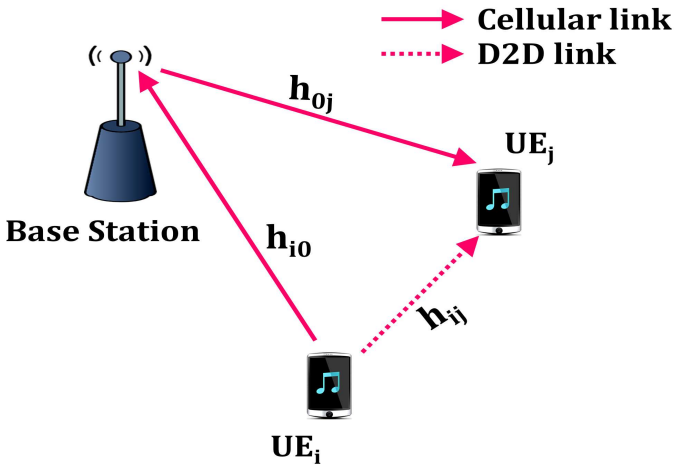

Figure 5.2: Cellular and D2D links for communication from UE_i to UE_j

where γ_{i0} and γ_{0j} denotes the SINR of link from UE_i to BS (uplink) and SINR of link from the BS to UE_j (downlink) respectively. Each transmit-receive pair is assumed to have a single antenna. Considering intra-cell interference, γ_{i0} and γ_{0j} can be calculated as [87]:

$$\gamma_{i0} = \frac{P_{i0}|h_{i0}|^2}{\sum_{k=1,k\neq i}^{N_u} P_{int,k} + N_0} \ \forall \ i \tag{5.2}$$

$$\gamma_{0j} = \frac{P_{0j}|h_{0j}|^2}{\sum_{k=1,k\neq j}^{N_u} P_{int,k} + N_0} \ \forall \ j \tag{5.3}$$

where P_{ij} and $|h_{ij}|$ denote the transmit power and channel gain of $i-j$ link respectively. $P_{int,k}$ denotes the interference power from UE_k and N_0 is the power spectral density of the Additive White Gaussian Noise (AWGN) at the receivers.

SINR of D2D link from the source UE_i to the destination UE_j is given by

$$\gamma_{ij}^{d} = \frac{P_{ij}|h_{ij}|^2}{\sum_{k=1,k\neq i}^{N_u} P_{int,k} + N_0} \ \forall \ i,j \tag{5.4}$$

5.2.2 Problem Formulation

Let the UEs in the cell be represented by a finite index set $\mathbb{U}$ of N_u elements, i.e, $\mathbb{U} = \{1, 2, ..., N_u\}$. The UE_i, $i \in \mathbb{U}$, can establish communication with UE_j, $j \in \mathbb{U}$, either through the cellular or D2D link. The end-to-end throughput of the cellular link is half of the minimum value between the uplink and the downlink throughput since the BS relays data from UE_i to UE_j and thus the same resources are used for both uplink and downlink transmissions [93].

The overall throughput optimization problem can be formulated as:

$$\max \left\{ \sum_{i,j \in \mathbb{U}} \left[\frac{1}{2} \alpha_{ij} \log_2 \left(1 + \gamma_{ij}^c\right) + (1 - \alpha_{ij}) \log_2 \left(1 + \gamma_{ij}^d\right) \right] \right\} \tag{5.5}$$

subject to

$$\gamma_{ij}^c \geqslant \gamma_{th}, \ \forall \ i, j \in \mathbb{U} \tag{5.6}$$

$$\gamma_{ij}^d \geqslant \gamma_{th}, \ \forall \ i, j \in \mathbb{U} \tag{5.7}$$

$$\sum_{i \in \mathbb{U}} \sum_{j \in \mathbb{U}} \alpha_{ij} \leqslant 1 \tag{5.8}$$

where $\alpha_{ij} \in \{0, 1\}$ is the mode indicator, $\alpha_{ij} = 1$ if $i - j$ link is a cellular link and $\alpha_{ij} = 0$ in case of D2D link. SINR threshold, γ_{th}, is the minimum SINR requirement to establish ij link for both cellular and D2D links. Constraints (5.6) and (5.7) represent the QoS requirements on cellular and D2D links. Constraint (5.8) ensures that the established ij link is either a cellular link or a D2D link.

A group of links sharing a common resource in the cell are defined as a cluster in this work. In a TDD system, the same set of resources are used for both uplink and downlink transmissions of a particular UE, in both cellular and D2D scenarios. Hence, clustering of links is done in such way that the same resource is allocated for transmissions to and from a UE. Let $\mathbb{L}$ and $\mathbb{U}_c$ denote

the index set of all links and cellular UEs in the cell. A resource reuse indicator, $\xi_{k,ij}$, is defined for each element in $\mathbb{L}$ such that $\xi_{k,ij} = 1$ if the ij link in $\mathbb{L}$ reuse the resource of UE_k in $\mathbb{U}_c$.

$$\sum_{k} \xi_{k,ij} \leqslant 1;\ \forall\ k \in \mathbb{U}_c \tag{5.9}$$

$$\sum_{m} \xi_{k,ij} = m;\ \forall\ k \in \mathbb{U}_c \tag{5.10}$$

where m is the total number of links established to and from UE_k. Constrain (5.9) ensures that ij link in $\mathbb{L}$ shares at-most one UEs resource. Constrain (5.10) ensures that the same resource is allocated for transmissions to and from a UE.

Let L be the total number of links established in a cluster which share the resources of UE_k in $\mathbb{U}_c$, where UE_k is either a member of the cluster or not. As a D2D and a cellular communications share the same resources, i.e, uplink/downlink time slots, co-channel interference arises. For simplicity other interferences are assumed to be negligible in comparison with co-channel interferences and are not taken into account in our study.

SINR of the UE_k-BS link with the co-channel interferences generated from the L allocated links for an uplink time slot can be written as:

$$\gamma^c_{k0} = \frac{P_{k0}|h_{k0}|^2}{\sum_{i=1,i\neq k}^{L} P_{ik}|h_{ik}|^2 + N_0} \tag{5.11}$$

The maximum value of allocated links, L, need to be estimated based on $\gamma^c_{k0} \geqslant \gamma_{th}$ criteria of (5.11).

5.3 Proposed Resource Allocation Scheme

A three-step scheme is proposed here to solve the problems discussed in the previous section: (A) Mode selection process, (B) Clustering process and (C) Cluster head selection process.

5.3.1 Mode Selection Process

One of the main issues in the local communication concept is the optimal selection of transmission mode, i.e, D2D or cellular communication, by satisfying the QoS requirement and maximizing the overall system throughput. A novel selection strategy for each UE based SINR is proposed here to solve the optimization of equation (5.5).

By mode selection it is meant that the network decides whether the UEs should communicate directly or via the BS. Depending on the received SINR, the BS determines whether the UEs should be interconnected either via the BS or directly. Thus each UE can operate in 2 different modes: (i) Cellular mode - a UE uses a cellular link for communication and (ii) D2D Underlay mode - a UE uses a D2D link for communication. That is UE_i, $i \in \mathbb{U}$, can establish communication with UE_j, $j \in \mathbb{U}$, either through a cellular link or D2D link. In the proposed mode selection scheme, D2D link is preferred to maximize throughput. If QoS requirement of both links are not satisfied, the UE_i remains in the idle mode meaning no communication is established.

Algorithm I summarizes the proposed procedure. Upon receiving request from UE_i to establish a communication with UE_j, the BS compares the γ_{ij}^c and γ_{ij}^d with γ_{th} (Step 4 and Step 5 in Algorithm I). Based on the comparison, UEi is assigned in $\mathbb{U}_c$ or $\mathbb{U}_d$ where $\mathbb{U}_c$ and $\mathbb{U}_d$ are defined as the set of indices of UEs in cellular mode and D2D mode respectively. If Step 4 and Step 5 are not satisfied,

then UE_i remains in the idle mode.

Algorithm I: Mode Selection Algorithm

1. Initialization: Given $\mathbb{U}$, γ_{th}
2. **for** each $i, j \in \mathbb{U}$
3. Calculate γ_{ij}^{c} and γ_{ij}^{d}
4. $\mathbb{U}_d = \left\{ i \in \mathbb{U}_d \Leftrightarrow \gamma_{ij}^{d} \geq \gamma_{th} \right\}$
5. $\mathbb{U}_c = \left\{ i \in \mathbb{U}_c \Leftrightarrow \gamma_{ij}^{d} < \gamma_{th} \text{ and } \gamma_{ij}^{c} \geq \gamma_{th} \right\}$
6. Assign the link number

   $ij \Leftrightarrow i \in \mathbb{U}_d$

   $i0 \Leftrightarrow i \in \mathbb{U}_c$
7. **end for**

Let the number of elements in the set $\mathbb{U}_c$ and $\mathbb{U}_d$ be N_c and N_d respectively where $0 \leqslant N_c(resp.N_d) \leqslant N_u$. It is considered that a UE can be associated with a cellular link, one or more D2D links or a combination of both, i.e,

$$\mathbb{U}_d \bigcap \mathbb{U}_c \neq \emptyset \tag{5.12}$$

$$N_c + N_d \geqslant N_u \tag{5.13}$$

Relationships (5.12) and (5.13) signify that UE_i can be involved in both cellular and D2D communications, i.e, it can be an element in both $\mathbb{U}_c$ and $\mathbb{U}_d$ sets.

5.3.2 Clustering Process

To increase the radio resource utilization, the resources of a cellular UE can be shared by multiple D2D links [64]. The UEs in the cell are grouped, clustered,

in such way that the links inside a particular cluster share common resources. The principle of the proposed clustering process resides in grouping UEs that are interconnected and thus solving the constrains raised in (5.9) and (5.10). The detailed procedure of the proposed clustering process is presented in Algorithm II.

	Algorithm II: Clustering Algorithm
1.	Initialization: Given $\mathbb{L}$, $k = 0$
2.	**while** $\mathbb{L} \neq \emptyset$
3.	$k \Leftarrow k + 1$
4.	$[m, n] \hookleftarrow \mathbb{L}(1)$
5.	$\mathbb{C}_k = \{m, n\} \Leftrightarrow m \neq 0, n \neq 0$ $= \{m/n\} \Leftrightarrow n = 0/m = 0$
6.	Update $\mathbb{L}$ by removing $\mathbb{L}(1)$
7.	**for** $j = 1$ to length($\mathbb{C}_k$)
8.	**for** $l = 2$ to length($\mathbb{L}$)
9.	$[x, y] \hookleftarrow \mathbb{L}(l)$
10.	**if** $\mathbb{C}_k(j) = (x/y)$ **then**
11.	$\mathbb{C}_k = \{\mathbb{C}_k\ y/x\} \Leftrightarrow y \neq 0/x \neq 0$ $= \{\mathbb{C}_k\} \Leftrightarrow y = 0/x = 0$
12.	Update $\mathbb{L}$ by removing $\mathbb{L}(l)$
13.	**end if**
14.	**end for**
16.	**end for**
17.	**end while**

Let $\mathbb{L}$ denotes the index set of all the links established in the cell using Algorithm I. In the Algorithm II, the expression $[m, n] \hookleftarrow \mathbb{L}(1)$ implies that if

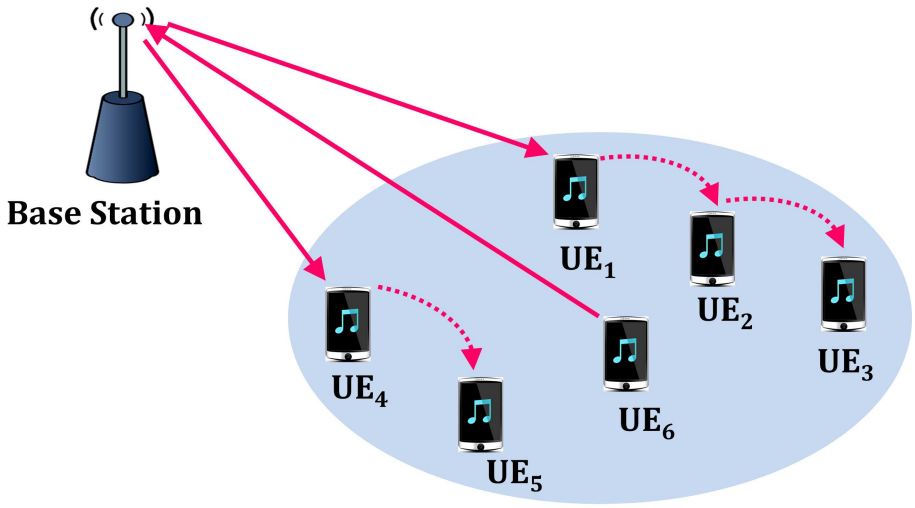

Figure 5.3: A simple scenario to illustrate the process of clustering

$\mathbb{L}(1)$=ij, then $m = i$ and $n = j$, i.e. the index of transmitter UE is saved in m and the index of receiver UE is saved in n. $\mathbb{C}_k$ denotes the set of indices of UEs in the k^{th} cluster. The index of $\mathbb{L}(1)$ forms the first elements (if D2D link) or element (if cellular link) which is specified in Step 5. Since the transmitter and receiver of $\mathbb{L}(1)$ are grouped to k^{th} cluster, $\mathbb{L}$ is updated by removing $\mathbb{L}(1)$. The first element in $\mathbb{C}_k$ is compared with the transmitter (resp. receiver) UE of the links in $\mathbb{L}$. If we find the same index of UE, $\mathbb{C}_k$ is updated by adding the index of corresponding receiver (resp. transmitter) UE. If the index correspond to a cellular link, then $\mathbb{C}_k$ is not updated whereas $\mathbb{L}$ is updated by removing the link from the set. The same procedure is repeated for the remaining elements in $\mathbb{C}_k$. Similarly, we find the elements of all clusters till $\mathbb{L}$ becomes an empty set. The clustering process is repeated when $\mathbb{L}$ is updated.

For example, an area of the cell with $N_u = 6$ and $\mathbb{L} = \{01, 23, 45, 60, 04, 13\}$ as shown in Figure 5.3 is considered. The detailed steps involved in the proposed algorithm for the considered scenario is elaborated in Table 5.1. Since $\mathbb{L} = \{01\}$, the iteration begins with $\mathbb{C}_1(1) = \{1\}$. In the first iteration, $\mathbb{C}_1(1)$, is compared with all the indices in $\mathbb{L}$ and found a matching link $\{13\}$. Hence the index $\{3\}$ is added to $\mathbb{C}_1$ and $\mathbb{L}$ is updated by removing the link index $\{13\}$. Therefore, the

Table 5.1: Clustering Procedure for Figure 5.1

	Initial $\mathbb{C}_k$	**Initial** $\mathbb{L}$	**Updated** $\mathbb{C}_k$	**Updated** $\mathbb{L}$
$\mathbb{C}_1(1) = 1$	$\{1\}$	$\{23, 45, 60, 04, 13\}$	$\{1, 3\}$	$\{23, 45, 60, 04\}$
$\mathbb{C}_1(2) = 3$	$\{1, 3\}$	$\{23, 45, 60, 04\}$	$\{1, 3, 2\}$	$\{45, 60, 04\}$
$\mathbb{C}_1(3) = 2$	$\{1, 3, 2\}$	$\{45, 60, 04\}$	$\{1, 3, 2\}$	$\{45, 60, 04\}$
$\mathbb{C}_2(1) = 4$	$\{4, 5\}$	$\{60, 04\}$	$\{4, 5\}$	$\{60\}$
$\mathbb{C}_2(2) = 5$	$\{4, 5\}$	$\{60\}$	$\{4, 5\}$	$\{60\}$
$\mathbb{C}_3(1) = 6$	$\{6\}$	$\emptyset$	$\{6\}$	$\emptyset$

updated $\mathbb{C}_1$ and $\mathbb{L}$ after the first iteration are $\mathbb{C}_1 = \{1, 3\}$ and $\mathbb{L} = \{23, 45, 60, 04\}$ which is used in next iterations. The procedure is repeated with all the elements in $\mathbb{C}_1$. The indices of UEs inside the first cluster is thus obtained. Since $\mathbb{L} \neq \emptyset$, the procedure is repeated to find the indices of UEs in the second cluster, $\mathbb{C}_2$, and similarly the case with $\mathbb{C}_3$ also.

5.3.3 Cluster Head Selection Process

A specific cellular UE is selected as CH within each cluster whose resources are shared by all D2D links in the cluster. Thus, the CH frees up resources that can be used by other cellular links to enhance the system capacity. As the control information related to D2D communication in a cluster is managed by CH, the UE behaving as a CH should be chosen to satisfy the minimum transmit power (MTP) requirement of UEs in the cluster and with the maximum residual energy (MRE).

MTP requirement optimize the battery life of all UEs in the cluster. For the sake of simplicity, consider a path-loss model, $P = P_0 \left(\frac{d}{d_0}\right)^{-\beta}$, where P_0 and P represent signal power measured at distances d_0 and d from the transmitter and β is the pathloss exponent [87]. As in [87], the received power at $d_0 = 1$ equals the transmit power which is adjusted based on γ_{th} at the receiver. A cellular UE_b is chosen as CH for $\mathbb{C}_k$ with N elements such that

$$\min_{b} \left\{ \chi_b = \sum_{a=1}^{N} \gamma_{th} N_0 d_{ab}^{\beta} \right\} \tag{5.14}$$

where d_{ab} is the distance between CH and UE_a. $b \in \{\mathbb{C}_k \bigcap \mathbb{U}_c\}$ if such cellular UEs in $\mathbb{C}_k$ exists. Otherwise b is an element of $\mathbb{U}_c$. The relationship in (5.14) guarantees that the transmit power of all UEs in the cluster is minimized.

Another requirement taken into account when selecting a CH represents residual energy of UEs. Among the cellular UEs, a UE with maximal residual energy becomes the cluster head. The probability, Pr_i, of a cellular UE_i to become a CH is a function of residual energy of the UE's battery and can be defined as [94]:

$$Pr_i = \max \left\{ \frac{E_i}{E_{total}} C, 1 \right\} \tag{5.15}$$

where E_i is the residual energy of UE_i, $E_{total} = \sum_{i=1}^{Nu} E_i$ and C is the total number of clusters in the cell. A cluster head is selected in each cluster and (5.15) is framed such that the expected number of cluster head per cell will be C [94], i.e.,

$$E[\#CH] = \sum_{i=1}^{Nu} Pr_i = \left(\frac{E_1}{E_{total}} + ... + \frac{E_{Nu}}{E_{total}} \right) C = C \tag{5.16}$$

In general, a cellular UE minimizing expression (5.14) and maximizing equation (5.15) should be chosen as the CH. Combining these two requirements, the criterion for the CH selection can be written as:

$$\min_{b} \left\{ \Upsilon_b = \frac{\sum_{a=1}^{N} \gamma_{th} N_0 d_{ab}^{\beta}}{Pr_b} \right\} \tag{5.17}$$

As explained above, the set to which the element b belongs to is determined on the basis of whether a cellular UE exists in the cluster or not. The MTP requirement in expression (5.14) can be evaluated for any other channel models in the similar way and the proposed combined criterion in (5.17) as well.

The cluster head, CH_k, selection procedure for $\mathbb{C}_k$ is illustrated in Algorithm III. We considered that the resource allocated to CH_k is shared by all links inside a cluster. In the algorithm, after assigning a UE as CH_k, the UE is removed from $\mathbb{U}_c$ as that UE resources cannot be shared by links in another cluster. This procedure is repeated whenever $\mathbb{C}_k$ is updated or until CH_k disappears from the cluster.

Algorithm III: Cluster Head Selection Algorithm

1. Initialization: Given N
2. **if** $\mathbb{C}_k \bigcap \mathbb{U}_c \neq \emptyset$ **then**
3. $\mathrm{CH}_k \Leftarrow \left\{ \mathrm{UE}_b \Leftrightarrow \min\limits_{b \in \{\mathbb{C}_k \bigcap \mathbb{U}_c\}} \left(\frac{\sum_{a=1}^{N} \gamma_{th} N_0 d_{ab}^{\beta}}{Pr_b} \right) \right\}$
4. Update $\mathbb{U}_c$ by removing b
5. **else**
6. $\mathrm{CH}_k \Leftarrow \left\{ \mathrm{UE}_b \Leftrightarrow \min\limits_{b \in \{\mathbb{U}_c\}} \left(\frac{\sum_{a=1}^{N} \gamma_{th} N_0 d_{ab}^{\beta}}{Pr_b} \right) \right\}$
7. Update $\mathbb{U}_c$ by removing b
8. **end if**

5.4 Optimum Number of Links per radio resource

The CH channel resources can be shared by more than one D2D link inorder to maximize spectral reuse efficiency. This section analytically determine the maximum number of links in the cluster that can be simultaneously shared with the CH resources. This number depends on the quality of cellular, CH2BS, link where in case of good quality of CH2BS link, it can share radio resources with more D2D links and vice versa [64]. The number of links to be shared are calculated as a function of γ_{th} and P_{out} where P_{out} defines the probability that the SINR of CH2BS link is less than the defined γ_{th}.

Let L be the total number of links established in the cluster k. Consider the fully loaded scenario where all L share the same time slot. The SINR of CH2BS link can be written as

$$\gamma = \frac{|h_0|^2}{\sum_{j=1,j\neq 0}^{L} I_j |h_j|^2 + \frac{1}{\xi}} \tag{5.18}$$

where $|h_0|^2$ and $|h_j|^2$ are the channel gains of CH2BS and j^{th} links respectively. $I_j = \frac{P_j}{P_0}$ where P_0 and P_j are the power received through channels h_0 and h_j respectively and ξ is the SNR.

The outage probability of CH2BS link can be calculated as [53]:

$$P_{out} = \int_0^{\gamma_{th}} f_\gamma(\gamma)\ d\gamma = F_\gamma(\gamma_{th}) \tag{5.19}$$

where $f_\gamma(\gamma)$ and $F_\gamma(\gamma)$ are the PDF and CDF of γ. Let $x = |h_0|^2$ and $y = \sum_{j=1,j\neq 0}^{L} I_j |h_j|^2 + \frac{1}{\xi}$. The PDFs of x and y can be expressed as [95]:

$$f_X(x) = exp(-x), \quad 0 \leq x \leq \infty \tag{5.20}$$

$$f_Y(y) = \frac{\left(y - \frac{1}{\xi}\right)^{L-1}}{I^L \Gamma(L)} exp\left(-\frac{y - \frac{1}{\xi}}{I}\right), \quad \frac{1}{\xi} \leq x \leq \infty \tag{5.21}$$

where $I = I_j$ $(j = 1, 2, ..., L)$ and $\Gamma(L)$ is a gamma function. The PDF of $z = x/y$ can be evaluated as [53, 95]

$$\begin{aligned} f_Z(z) &= \int_{\frac{1}{\xi}}^{\infty} y.f_{XY}(yz, y)\ dy \\ &= \frac{1}{I^L \Gamma(L)} \int_{\frac{1}{\xi}}^{\infty} y.exp(-yz) \left(y - \frac{1}{\xi}\right)^{L-1} exp\left(-\frac{y - \frac{1}{\xi}}{I}\right) \end{aligned} \tag{5.22}$$

Due to the complexity of the equation (5.22), we use a high SNR approxima-

tion, i.e , $\frac{1}{\xi} \approx 0$. Thus, equation (5.22) reduces to:

$$f_Z(z) = \frac{1}{I^L \Gamma(L)} \int_0^\infty y^L . exp\left(-y\left(z + \frac{1}{I}\right)\right)\ dy \tag{5.23}$$

Using equation (ETI 133(2) of [78]), equation (5.23) can be evaluated as:

$$f_Z(z) = \frac{1}{I^L \Gamma(L)} L! \left(z + \frac{1}{I}\right)^{-L-1} \tag{5.24}$$

The CDF $F_Z(z)$ can be obtained by integrating $f_Z(z)$ with limits 0 to z.

$$\begin{aligned} F_Z(z) = P_{out} &= \frac{1}{I^L \Gamma(L)} L! \int_0^z \left(z + \frac{1}{I}\right)^{-L-1}\ dz \\ &= 1 - \frac{1}{I^L \left(z + \frac{1}{I}\right)^L} \end{aligned} \tag{5.25}$$

The outage probability of CH2BS link can be written as:

$$P_{out} = f_\gamma(\gamma_{th}) = 1 - \frac{1}{I^L \left(\gamma_{th} + \frac{1}{I}\right)^L} \tag{5.26}$$

Thus, the maximum number of links that can be shared for a given SINR threshold, γ_{th}, and outage probability, P_{out}, can be presented as:

$$L = \frac{-\log(1 - P_{out})}{\log I + \log\left(\gamma_{th} + \frac{1}{I}\right)} \tag{5.27}$$

If the number of links in the cluster exceed L, then the links are scheduled in different time slots such that a maximum of L links are scheduled in one time slot.

5.5 Results and Discussion

In this section, we evaluate the performance of the proposed scheme. The proposed mode selection, clustering and cluster head selection schemes presented in Section 5.3 are applied for the WINNER II A1 indoor office channel model [91]. Next, the expressions derived in Section 5.4 are evaluated to find the optimum number of links per radio resource.

5.5.1 Simulation Parameters and Assumptions

The motivation for D2D is to enhance local cellular services. Accordingly, we consider WINNER II A1 model [91] where both the BSs and 15 active UEs are distributed inside the buildings as shown in Figure. 5.4. A line-of-sight (LOS) scenario occurs when the transmitter and the receiver are either in the same corridor or in the same room. Non-LOS (NLOS) scenario occurs in room-to-room (NLOS1) or corridor-to-room (NLOS2) communication cases. The simulation tool for the analysis was developed by using MATLAB software. The parameters considered in simulations are summarised in Table. 5.2

The end to end throughput per UE for different values of d based on the proposed mode selection method with $\gamma_{th} = 10$ dB is presented in Figure 5.5 where d is the distance between transmitter and receiver. The analysis is carried for the specified LOS, NLOS1 and NLOS2 path-loss models. The throughput per UE for the conventional cellular case with the 3 path loss models is also presented. The results show that D2D communications leads a throughput enhancement due to the single hop communication when compared to the 2 hop cellular communication. In the figure, the throughput for the proposed method converges to the conventional cellular method at d =40m and d =30m for the NLOS1 and NLOS2 cases respectively. This indicates that for NLOS1 and NLOS2 path-loss

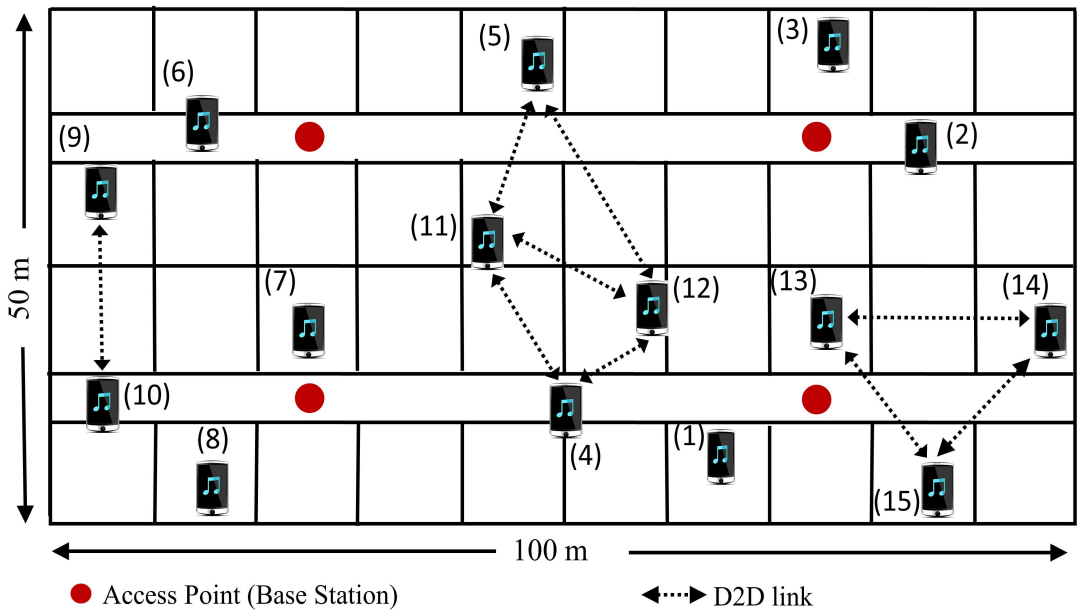

Figure 5.4: WINNER II A1 indoor office model

models, the D2D coverage is limited to 40m and 30m with a maximum transmit power of 9 dBm. Whereas for the LOS case, the D2D coverage extends to a distance greater than 100m.

5.5.2 Cluster Head Selection

The transmission mode for each UE in the building is selected based on the proposed mode selection method. Among the 15 UEs, 9 UEs establishes D2D links, $\mathbb{U}_d = \{4, 5, 9, 10, 11, 12, 13, 14, 15\}$, and the 8 UEs forms the cellular user set, $\mathbb{U}_c = \{1, 2, 3, 4, 5, 6, 7, 8\}$. Let consider 3 clusters as shown in Figure. 5.4, $\mathbb{C}_1 = \{13, 14, 15\}$, $\mathbb{C}_2 = \{12, 5, 11, 4\}$ and $\mathbb{C}_3 = \{9, 10\}$ which are formed using the proposed clustering method.

Figure. 5.6 shows the χ value for each element in $\mathbb{U}_c$ for clusters $\mathbb{C}_1$, $\mathbb{C}_2$ and $\mathbb{C}_3$ based on the MTP criterion. The result shows that the best CH candidate for $\mathbb{C}_1$ is UE_1 as it guarantees minimum transmission power to all elements in $\mathbb{C}_1$. Similarly for $\mathbb{C}_2$, the best candidate is either UE_4 or UE_7. However, as UE_4 $\in \{\mathbb{C}_2 \bigcap \mathbb{U}_c\}$, the CH for $\mathbb{C}_2$ should be UE_4. For the case of $\mathbb{C}_3$, CH is UE_7

Table 5.2: Simulation Parameters

WINNER II A1 PARAMETERS [91]	
Bandwidth, BW	10 MHz
Building Dimension	100 m × 50 m
Room Dimension	10 m × 10 m
Path-loss Models	
LOS	18.7 $\log_{10}(d)$ +46.8 +20 $\log_{10}(f_c/5)$
Room-to-room (NLOS1)	20 $\log_{10}(d)$ +46.4 +20 $\log_{10}(f_c/5)$+χ_1
Corridor-to-room (NLOS2)	36.8 $\log_{10}(d)$ +43.8 +20 $\log_{10}(f_c/5)$+χ_2
Carrier frequency, f_c	2.6 GHz
Shadow fading std [dB]	
LOS	3
NLOS1	6
NLOS2	4
Wall attenuation [dB]	
χ_1	$5n_w$
χ_2	$5(n_w$-1)
	n_w - no. of walls between transmitter and receiver
OTHER PARAMETERS [96]	
Noise Power Density, N_0	-174 dBm/Hz
SNR threshold, γ_{th}	
D2D and cellular communication	10 dB
Transmit power constraint,	$\varrho^d = 9$ dBm $\varrho^c = 23$ dBm

(minimum χ among the elements of $\mathbb{U}_c$).

Another parameter specified in Section 5.3 for the selection of CH is the battery capacity. Since the power consumption differs among different device models, we considered Samsung Galaxy Nexus Smartphone with the maximum battery capacity 6.48 Wh [97]. We consider the UEs battery capacity are randomly distributed in the range 3 Wh to 6.48 Wh. Figure. 5.7 shows the probability of an element in $\mathbb{U}_c$ to become the CH based on the MRE criterion. The result shows that UE_3, UE_5 and UE_6 have the maximum battery capacity and are more probable to become the CHs; UE_7 has the lowest battery capacity meaning

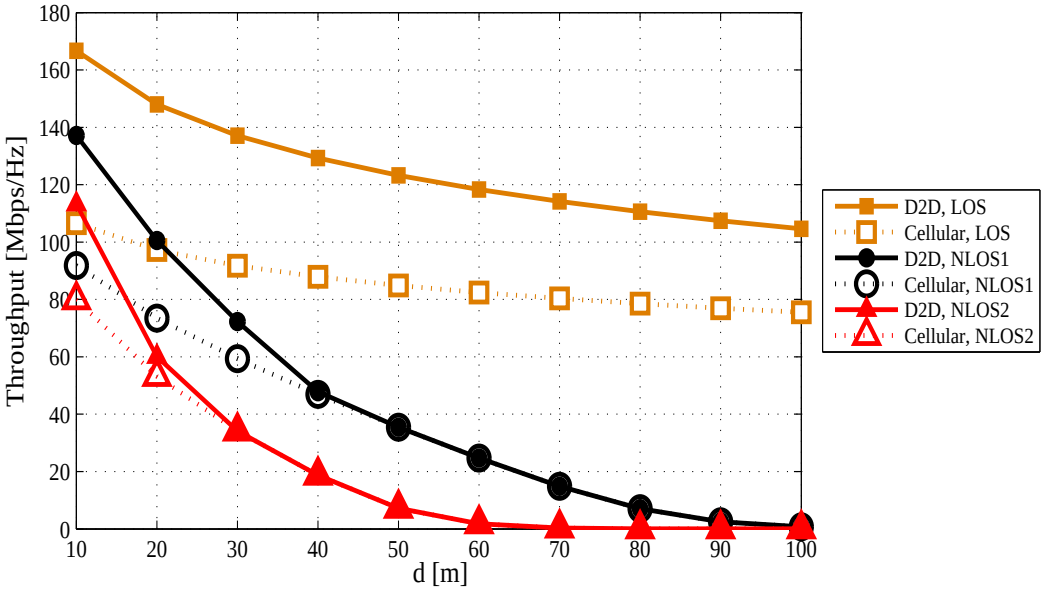

Figure 5.5: Throughput per UE for different values of d based on the proposed mode selection method with $\gamma_{th} = 10$ dB

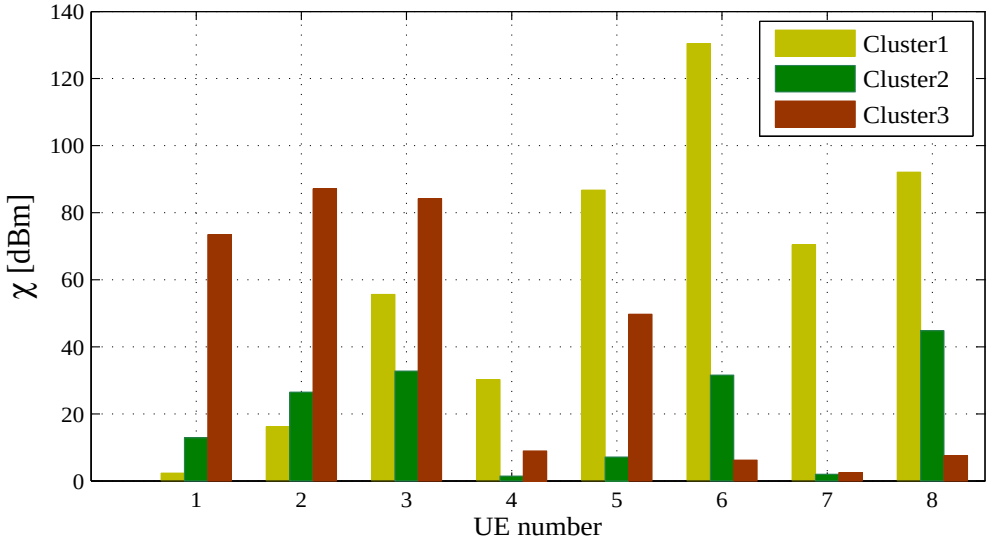

Figure 5.6: χ value for each element in $\mathbb{U}_c$ based on the MTP criterion

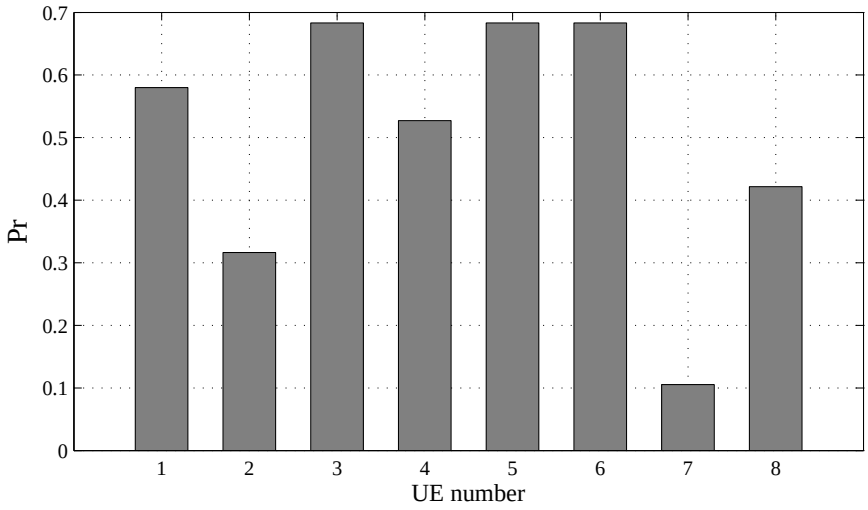

Figure 5.7: Probability of an element in $\mathbb{U}_c$ based on the MRE criterion

the chance to become CH is the lowest one. The other UEs in $\mathbb{U}_c$ have battery capacities between these two levels.

Figure. 5.8 shows the Υ value for each element in $\mathbb{U}_c$ for the selection of cluster heads for $\mathbb{C}_1$, $\mathbb{C}_2$ and $\mathbb{C}_3$ by considering both MTP and MRE requirements together. The CH selection based on the combined criteria selects UE_1 and UE_4 as the CHs for $\mathbb{C}_1$ and $\mathbb{C}_2$ which leads in the same results with the MTP criterion alone. According to the combined criteria, the UE_6 forms the CH for $\mathbb{C}_3$ since UE_7 is having low battery capacity. Thus we can take advantage of both maximum residual power requirement and the minimum transmit power requirement of UEs in the cluster for the selection of CH when using the proposed combined criterion (equation (5.17)).

5.5.3 Optimum number or links

This section numerically analyse the maximum number of links that can operate simultaneously with a CH2BS link resources based on the analytical results obtained in Section 5.4. Initially, validation of the derived result with high SNR approximation is done by comparing the performance with a reference scheme

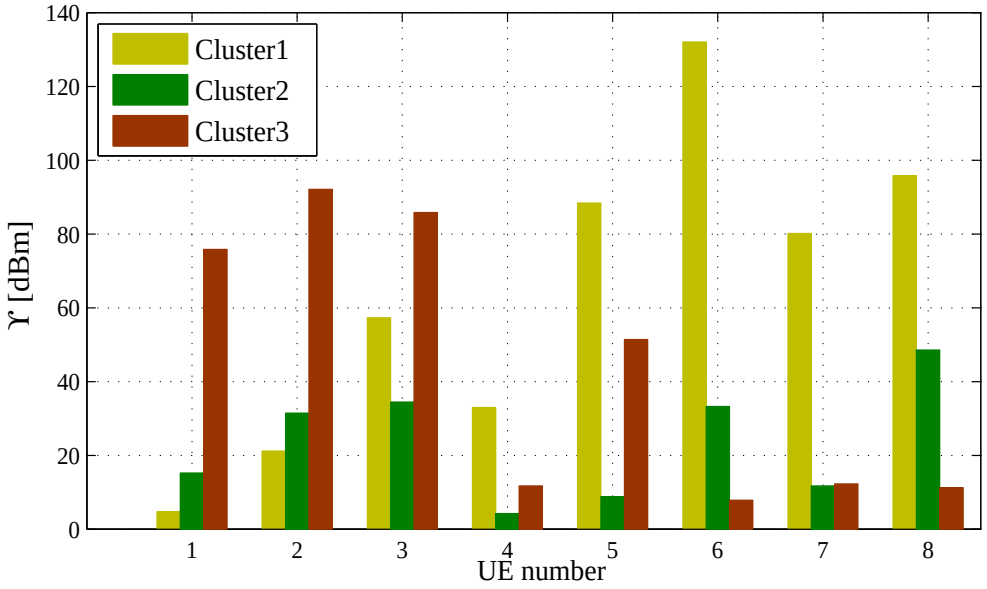

Figure 5.8: Υ value for each element in $\mathbb{U}_c$ based on the combined MTP and MRE criteria

of [53]. Then, the effect of variation of γ_{th}, I_j and P_{out} in determining the optimum number of links is analysed.

The outage probability of CH2BS link when one D2D link share the radio resource is given as (based on *Lemma 1* of [53]):

$$P_{out}^{1} = 1 - \frac{1}{1 + I_1 \gamma_{th}} exp\left(-\frac{\gamma_{th}}{\xi}\right) \tag{5.28}$$

Using (5.27), the outage probability of CH2BS link for $L = 1$ (i.e., a radio resource allocated to CH is shared by one D2D link) can be calculated as

$$P_{out}^{2} = 1 - \frac{1}{I_1\left(\gamma_{th} + \frac{1}{I_1}\right)} \tag{5.29}$$

Figure. 5.9 illustrates the outage probability vs γ_{th} for the reference scheme, (5.28), and our expression with high SNR approximation, (5.29). The analysis is carried out taking into account a high ($I_1 = 1.5$) and low ($I_1 = 0.2$) interference environments. As can be seen from the figure, the difference between curves P_{out}^{1}

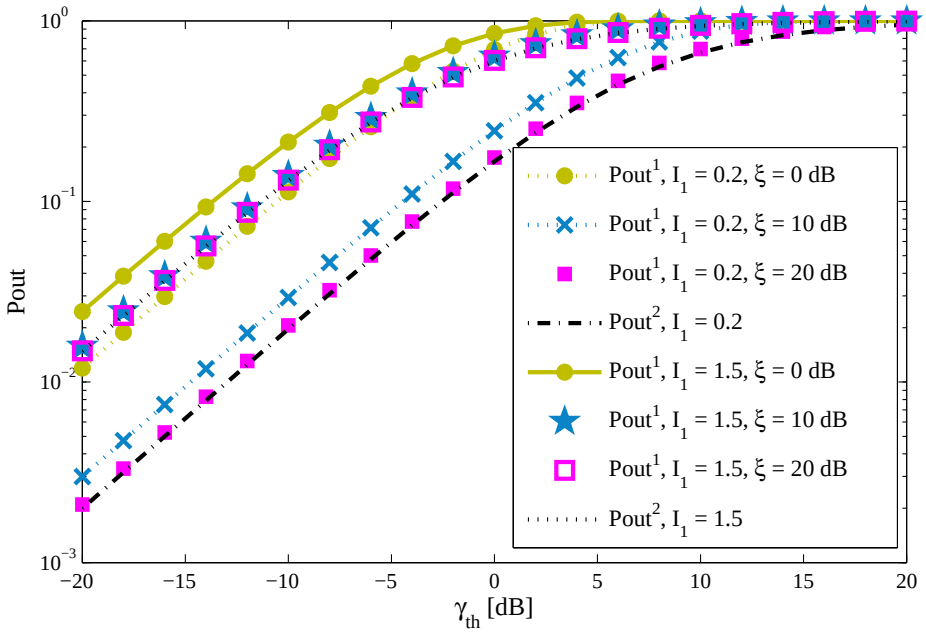

Figure 5.9: Outage probability, P_{out}, vs SINR threshold, γ_{th}, plot for high interference ($I_1 = 1.5$) and low interference ($I_1 = 0.2$) environments

for $\xi = 0$ dB and P^2_{out} is higher in case of $I_1 = 0.2$. However, the difference in performance gradually reduces as ξ increases. P^1_{out} at $\xi = 20$ dB and P^2_{out} have almost the same performance for $I_1 = 0.2$. In a strong interference environment, the difference between P^1_{out} and P^2_{out} is lower for $\xi = 0$ dB in comparison with the weak interference environment. Thus the relationship (5.27) leads in almost the same outage probability as in the case without approximation in the high SNR environment.

The effect of γ_{th} variation to estimate the optimum number of links, L, which can be shared by a CH radio resource is illustrated in Figure. 5.10. Maintaining high SINR for the CH2BS link leads to less number of D2D links that can be shared. Figure. 5.10 also shows the variation of L for different values of I. As we can observe, the high quality of CH2BS link with low value of I increases L. For example, in case of $\gamma_{th} = 0$ dB for CH2BS link, the maximum number of links that can be shared is 7 and 4 for $I = 0.1$ and $I = 0.2$ respectively. Whereas L reduces to 1 for $I = 1$.

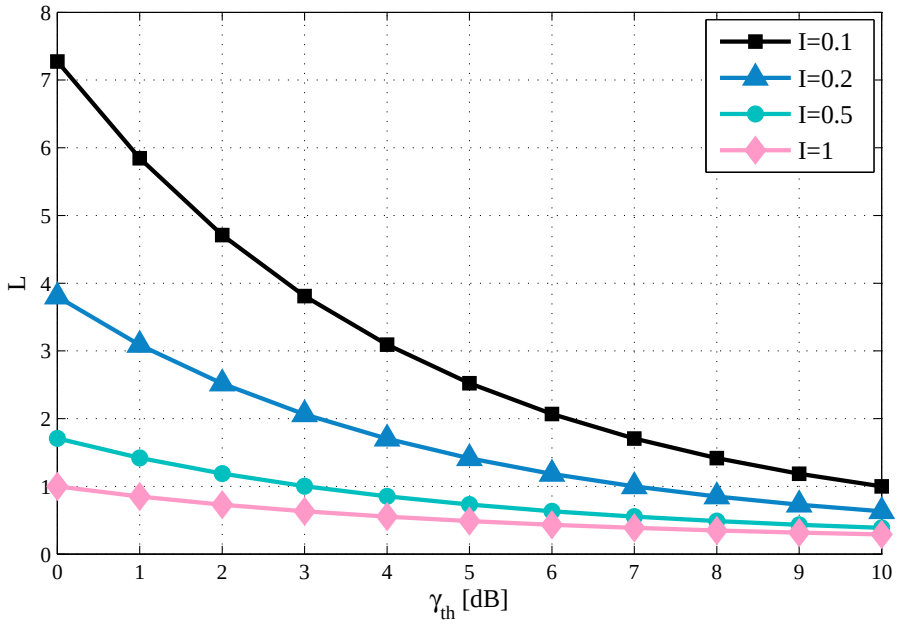

Figure 5.10: Optimum number of links, L, vs SINR threshold, γ_{th}, plot for different values of I

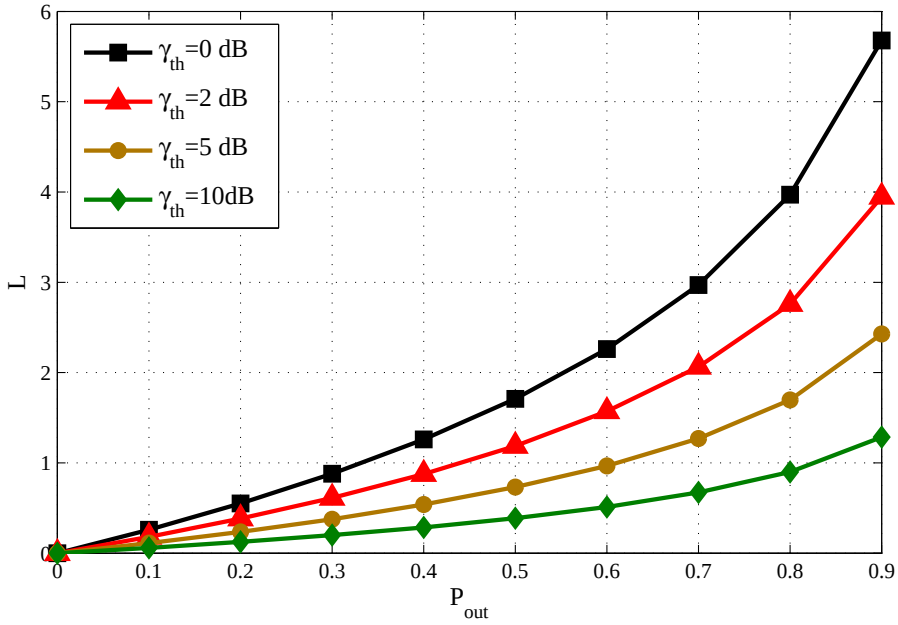

Figure 5.11: Optimum number of links, L, vs outage probability, P_{out}, plot for different values of γ_{th}

Figure. 5.11 shows L vs P_{out} for different values of γ_{th}. As explained in Figure. 5.10, L decreases as γ_{th} increases. Lower value of P_{out} means that there is less chance for CH2BS link to be in outage which inturn demands higher quality of CH2BS link and reduces number of sharing links per the resource. Similarly, CH2BS link can support more links with higher values of P_{out}.

5.6 Summary

In this chapter, a three-step scheme which includes a mode selection, clustering and cluster head selection procedures is proposed to address mode section with respect to QoS constraints, spectrum efficiency and proper resource allocation. In addition, an expression to calculate the optimal number of links that can share cellular UE resources having predefined SINR threshold and outage probability is derived. The D2D underlay system with the proposed scheme is evaluated using the WINNER II A1 indoor office model. Our proposition allows us to estimate the D2D zone in which the D2D communication can provide throughput enhancement when compared with conventional cellular communication. Clustering and resource allocation procedure based on cluster head selection algorithm improve spectral efficiency and optimize UEs energy consumption in a cluster. Validation of the derived analytical result was done in comparison to a reference scheme in [53] in terms of outage probability. The outage probability analysis shows that our derived expression leads to similar results as in the case without approximation at high SNR scenarios.

CHAPTER 6

Hungarian method based joint Mode and Relay selection

Contents

In D2D communication systems, the UEs can communicate either through cellular mode or through D2D mode. This was analysed in Chapter 5. But, long distances and poor radio conditions between potential D2D UEs limit the execution of D2D communication practically. In order to extent the coverage of D2D communication for such cases, a relay transmission mode as an additional mode of transmission can be considered along with the existing two transmission modes. A transmission mode selection method based on Hungarian algorithm is proposed in this chapter for the selection of proper transmission mode for each UE there by maximizing the overall system throughput.

6.1 Introduction

Long distances and poor radio conditions between D2D UEs limit the benefits of D2D communication practically [65]. Hence the concept of UE relaying is introduced in this chapter where the D2D UEs act as relays for data transmissions when the UEs are located at the cell edges or in a poor coverage area. This transmission relayed through a UE is referred as relay mode of transmission in this work. The relay transmission mode is considered as an additional mode of transmission along with the existing cellular and D2D transmission modes. Here, the cellular transmission mode refers to transmission between two UEs via BS whereas the D2D transmission mode refers to the direct communication between these two UEs. In this chapter, a joint transmission mode (combining cellular, D2D and relay mode) and relay selection method is proposed to maximize the overall system throughput. This is achieved by using the Hungarian algorithm [98, 99].

In this chapter, we focus on a multiple D2D relay-assisted communication scenario. The novelty of the work lies in consideration of a relay transmission mode

in addition to the existing cellular and D2D transmission modes and a transmission mode allocation method is proposed based on the Hungarian algorithm. The aim of proposed method is to solve two main problems: (i) selection of a suitable transmission mode, i.e., D2D, relay and cellular, for each scheduled transmission and (ii) selection of a suitable relay UE for in case of the relay transmission mode. Performance comparison of the proposed algorithm with conventional approaches are also presented. The simulation results show that the proposed algorithm improves the performance in terms of overall system throughput and D2D access rate in comparison with existing D2D communication scheme [59, 70] and random allocation algorithm [67, 69].

6.2 Background details

A graph $G(X, E)$ represents a graph with X and E as the vertex and edge set respectively. A graph G is bipartite if X can be divided into two disjoint subsets, U and V, such that $X = U \cup V$, $U \cap V = \emptyset$ and each edge in E has one endpoint in U and the other in V. Such a bipartite graph can be denoted as $G(U, V, E)$ [100].

In a weighted bipartite graph, $w(u, v)$ is the weight of edge (u, v) where $u \in U$ and $v \in V$. The weight matrix, $\mathbb{W}$, of the weighted bipartite graph is:

$$W = \{w\,(u_i, v_j)\}\,; \quad \begin{aligned} &1 \leq i \leq |U| \\ &1 \leq j \leq |V| \end{aligned} \tag{6.1}$$

where $|U|$ and $|V|$ denote the cardinality of set U and V respectively. A matching set, $M \subseteq E$, is a matching from U to V such that no two edges in M share a common vertex. If the sum of edge weights in the matching set M are maximum in a weighted bipartite graph, then the matching is a maximum weighted bipartite matching [100, 101].

Each node in the graph may be matched (assigned) or unmatched (unassigned). Unmatched nodes are also called exposed. Edges likewise may be matched or unmatched. An edge, E_{ij} is matched if u_i is matched to v_j and unmatched otherwise. An alternating path is a path through the graph such that each matched edge is followed by an unmatched edge and vice-versa. An augmenting path is an alternating path that begins and ends with an exposed node. All alternating paths originating from a given unmatched node form a Hungarian tree. Searching for an augmenting path in a graph involves exploring these alternating paths in a breadth-first manner, and the process can be called growing a Hungarian tree.

6.2.1 Hungarian Algorithm

The Hungarian Algorithm, also known as the Kuhn-Munkres algorithm, is used to find the maximum weighted bipartite matching. The algorithm was developed by H. Kuhn in 1955 [98] and later improved by J. Munkres in 1957 [99]. An extension of this algorithm for rectangular matrices to operate in situations where the numbers of $|U|$ and $|V|$ were unequal was introduced by Bourgeois and Lassalle in 1971 [102].

Suppose we have v resources to which u tasks need to be assigned and the weight for assigning a given resource to a given task is also known. We need to find an optimal matching on a one-to-one basis such that the sum of matching weights should be maximized. This maximum weighted matching problem can be expressed as a linear assignment problem with the objective functions:

$$\max \sum_{i=1}^{|U|} \sum_{j=1}^{|V|} w_{ij} a_{ij} \tag{6.2}$$

$$\sum_{i=1}^{|U|} a_{ij} = 1 \quad \forall j = \{1, 2, ..., |V|\} \tag{6.3}$$

$$\sum_{j=1}^{|V|} a_{ij} = 1 \quad \forall i = \{1, 2, ..., |U|\} \tag{6.4}$$

$$a_{ij} \in \{0, 1\} \qquad \forall i, j \tag{6.5}$$

where a_{ij} denotes that the edge u_i, v_j is an edge in the maximum weighted bipartite matching.

The Mathematical model

Let $w_{i,j}$ be the weight of assigning the i^{th} resource to the j^{th} task. Then the corresponding weight matrix can be written as:

$$\mathbb{W} = \begin{array}{c} \\ u_1 \\ u_2 \\ u_3 \\ \vdots \\ u_m \end{array} \begin{array}{c} \begin{array}{ccccc} v_1 & v_2 & v_3 & \cdots & v_r \end{array} \\ \begin{pmatrix} w_{1,1} & w_{1,2} & w_{1,3} & \cdots & w_{1,r} \\ w_{2,1} & w_{2,2} & w_{2,3} & \cdots & w_{2,r} \\ w_{3,1} & w_{3,2} & w_{3,3} & \cdots & w_{3,r} \\ \vdots & \vdots & \ddots & \vdots & \\ w_{m,1} & w_{m,2} & w_{m,3} & \cdots & w_{m,r} \end{pmatrix} \end{array} \tag{6.6}$$

A matching is a set of u entry positions in the weight matrix, such that no two of which lie in the same row or column. An assignment is optimal when the sum of weights of u entries is maximized.

The maximum weighted matching problem in (6.2), (6.3) and (6.4) can be solved by using the Hungarian algorithm [98, 99]. The Hungarian algorithm is a

combinatorial optimization algorithm which solves assignment problems in polynomial time [103]. A compact description of the steps of this algorithm, adapted from [104], is presented below:

Algorithm IV: Hungarian Algorithm	
Step 1:	Initialization: Find a matching M in E and generate initial labellings α_i and β_j as follows: $\forall u_i \in U, \quad \alpha_i = \max_i \{w_{ij}\}$ $\forall v_i \in V, \quad \beta_i = 0$
Step 2:	If M is a perfect matching, THEN stop and report M as a maximum weight matching. Otherwise, pick free vertex $u_i \in U$. Set $S = \{u_i\}$, $T = \emptyset$.
Step 3:	If $N_l(S) = T$, where $N_l(u) = \{v : (u, v) \in E\}$ and $N_l(S) = \cup_{u \in S} N_l(u)$, then update the labels follows. $\varepsilon = \min \{u_i + v_j - w_{ij} : u_i \in S, v_j \notin T\}$ $\alpha_i = \alpha_i - \varepsilon, \quad if u_i \in S$ $\beta_j = \beta_j + \varepsilon, \quad if v_j \in T$
Step 4:	If $N_l(S) \neq T$, pick $v \in \{N_l(S) - T\}$. • If v is an unmatched node, $u - v$ is an augmenting path. Augment M and go to **Step 2**. • If v is a matched node to z, then $S = S \cup \{z\}$, $T = T \cup \{v\}$ and go to **Step 3**

6.3 System Model

A model constituting of one BS and N_u randomly distributed active UEs in the cell is considered. A transmission from UE_m to UE_n is denoted as (m, n) where $m \in \mathbb{M} = \{1, 2, ..., m\}$ and $n \in \mathbb{N} = \{1, 2, ..., n\}$. Here the sets $\mathbb{M}$ and $\mathbb{N}$ denote the sets of transmitting and receiving UEs respectively. A Time Division Duplex (TDD) mode of operation is assumed where a UE can either receive or transmit data in each timeslot, i.e., $\mathbb{M} \cap \mathbb{N} = \emptyset$. A set $\mathbb{R} = \{1, 2, ..., r\}$ denotes the set of receivers and idle UEs in the cell such that $\mathbb{R} \cap \mathbb{M} = \emptyset$ and $\mathbb{N} \subseteq \mathbb{R}$.

As shown in Figure. 6.1, each (m, n) transmission scheduled in the cell can be realized via one of following transmission modes:

1. **Cellular transmission mode**: refers to a communication between UE_m and UE_n via the BS.

2. **D2D transmission mode**: refers to a direct communication between UE_m and UE_n.

3. **Relay transmission mode**: refers to a communication between UE_m to UE_n via UE_r that acts as the device relay. This mode includes two D2D transmissions (one between UE_m to UE_r and the other between UE_r to UE_n).

SINR is considered as the indicator of QoS to maximize the network capacity. In the cellular transmission mode, the communication between UE_m and UE_n can be seen as a 2 hop relay link with the BS serving as the relay node. To minimize outage in the cellular transmission mode, it is assumed that SINR is given by the weakest link between the 2 hop link [92]. Then SINR at UE_n for (m, n) transmission, in case of the cellular transmission mode, can be written as:

$$\gamma^c_{mn} = \min\{\gamma_{m0}, \gamma_{0n}\} \quad m \in \mathbb{M}, n \in \mathbb{N} \tag{6.7}$$

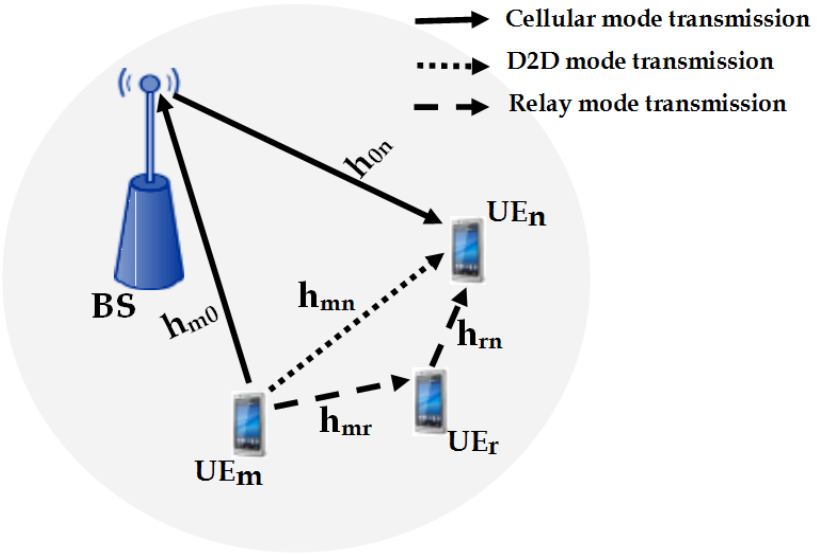

Figure 6.1: Cellular, D2D and Relay mode transmissions from UE_m to UE_n

where γ_{m0} and γ_{0n} denote the SINR of at BS for UE_m-BS link (uplink) and SINR at UE_n for BS-UE_n link (downlink) respectively. The SINRs, γ_{m0} and γ_{0n}, can be calculated as [87]:

$$\gamma_{m0} = \frac{P_{m0}|h_{m0}|^2}{\sum_{i \in M, i \neq M} P_{int,i} + N_0} \quad m \in \mathbb{M} \tag{6.8}$$

$$\gamma_{0n} = \frac{P_{0n}|h_{0n}|^2}{\sum_{i \in M, i \neq M} P_{int,i} + N_0} \quad n \in \mathbb{N} \tag{6.9}$$

where P_{mn} and $|h_{mn}|$ denote the transmit power and channel gain of link between UE_m to UE_n and $m/n = 0$ denotes the BS. $P_{int,i}$ denotes the interference power and N_0 is the power spectral density of the Additive White Gaussian Noise (AWGN) at the receiver.

Similar to the cellular transmission mode, the relay transmission mode can be also seen as a 2 hop relay with UE serving as the relay. Here UE_r act as the relay for (m, n) transmission. Then SINR at UE_n for (m, n) transmission, in case of the relay transmission mode, can be written as:

$$\gamma_{mn}^{r} = \min\{\gamma_{mr}, \gamma_{rn}\} \quad m \in \mathbb{M}, n \in \mathbb{N} \tag{6.10}$$

where γ_{mr} and γ_{rn} denote the SINR at UE_r for (m, r) transmission and SINR at UE_n for (r, n) transmission respectively.

SINR for (m, n) transmission, in case of the D2D transmission mode, can be writen as:

$$\gamma_{mn}^{d} = \frac{P_{mn}|h_{mn}|^2}{\sum_{i \in M, i \neq M} P_{int,i} + N_0} \quad m \in \mathbb{M}, n \in \mathbb{N} \tag{6.11}$$

A key mechanism to mitigate the interference among users in D2D communications is the use of power control [64]. For achieving this, the maximum allowed transmit power is limited to ϱ^c for a cellular link and ϱ^d for a D2D link [18].

6.3.1 Problem Formulation

In practice, the quality of communication channel may not be good enough for direct communication due to poor propagation medium and/or interference from other nearby UEs. Moreover, the advantages of D2D communications fail when the D2D UEs are far away from each other. These constrains considerably reduces the overall system performance. Under such unfavourable conditions, the network assisted transmission through relays can enhance the performance [65]. The aim of this work is to maximize the overall system data rate while selecting a suitable transmission mode for each scheduled transmission in the cell. The overall system data rate maximizing problem can be formulated as:

$$C = \max\left\{ \sum_{m \in M, n \in N} \alpha_{mn} \log_2\left(1 + \gamma_{mn}^{c}\right) + \beta_{mn} \log_2\left(1 + \gamma_{mn}^{r}\right) + \xi_{mn} \log_2\left(1 + \gamma_{mn}^{d}\right) \right\} \tag{6.12}$$

The formulated problem in (6.12) need to be solved subject to the following

constrains:

$$\begin{aligned} \gamma_{mn}^{c} &\geq \gamma_{th}, \quad m \in \mathbb{M}, n \in \mathbb{N} \\ \gamma_{mn}^{r} &\geq \gamma_{th}, \quad m \in \mathbb{M}, n \in \mathbb{N} \\ \gamma_{mn}^{d} &\geq \gamma_{th}, \quad m \in \mathbb{M}, n \in \mathbb{N} \end{aligned} \tag{6.13}$$

$$\begin{aligned} \sum_{n \in \mathbb{R}} \alpha_{mn} \leq 1, \quad \alpha_{mn} \in \{0,1\}, \quad m \in \mathbb{M} \\ \sum_{n \in \mathbb{R}} \beta_{mn} \leq 1, \quad \beta_{mn} \in \{0,1\}, \quad m \in \mathbb{M} \\ \sum_{n \in \mathbb{R}} \xi_{mn} \leq 1, \quad \xi_{mn} \in \{0,1\}, \quad m \in \mathbb{M} \end{aligned} \tag{6.14}$$

$$\alpha_{mn} + \beta_{mn} + \xi_{mn} = 1, \quad \forall\ m \in \mathbb{M} \tag{6.15}$$

where α_{mn}, β_{mn} and ξ_{mn} are the transmission mode indicators. $\alpha_{mn} = 1$ when the (m, n) transmission is through the cellular transmission mode, otherwise $\alpha_{mn} = 0$. Similarly β_{mn} and ξ_{mn} are mode indicators for relay and D2D transmission modes respectively. SINR threshold, γ_{th}, is the minimum SINR required to establish the (m, n) transmission.

The constrain (6.13) represents the QoS requirements for the cellular, relay and D2D transmission modes. The constrain (6.14) indicates that every element in $\mathbb{M}$ have at-most one partner in $\mathbb{R}$. Finally, the constrain (6.15) ensures that every (m, n) transmission is assigned only one of the three transmission modes.

Based on the above formulated problem, the main aim is to develop a transmission mode allocation method, i.e. a method for selecting the transmission mode of each UE in $\mathbb{M}$ such that the overall system throughput is maximized.

6.4 Proposed Transmission mode assignment algorithm

To solve the problem defined in (6.12), we propose a Transmission Mode Allocation (TMA) algorithm so as to maximize the objective function. The proposed algorithm is based on maximum weighted bipartite matching using the Hungarian algorithm. We assume that the knowledge of SINR at UEs are known at the BS and hence the method can be implemented centrally at the BS.

For assigning the transmission modes, a weighted bipartite graph, $G(U, V, E)$, as shown in Figure 6.2 is considered. Our aim here is to choose a suitable UE partner in $\mathbb{R}$ for every element in $\mathbb{M}$ such that the overall system throughput is maximized with the selected mode of transmission. Hence in the bipartite graph, U vertices are the transmitter UEs in $\mathbb{M}$ and V vertices are the remaining users in the cell, i.e, $\mathbb{R}$.

SINR is considered as the main parameter when maximizing the overall system throughput that is SINRs represent weights of the edges in Figure 6.2. For (m, n) transmission, the edge weight between a user u_i in U and user v_j in V, $w_{i,j} = \gamma_{ij}, \forall i \in \mathbb{M}$ if $n = j$. Otherwise, i.e., $n \neq j$, the SINR of the relay mode transmission, (m, j, n) is computed and assigned as weights, $w_{i,j} = \min(\gamma_{mj}, \gamma_{jn}), \forall i \in \mathbb{M}$. Accordingly the edge weight for each vertex in U for the corresponding vertex in V is calculated and the corresponding weight matrix of the graph is denoted as $\mathbb{W}$.

The Hungarian algorithm is then utilized to compute the maximum weighted bipartite matching. After matching, the corresponding transmission modes are assigned to each UEs in $\mathbb{M}$.

A detailed procedure of the proposed TMA method is presented in Algorithm V. Our proposed algorithm consists of 3 main stages including construction of weight matrix, maximum weighted matching and selection of the transmission

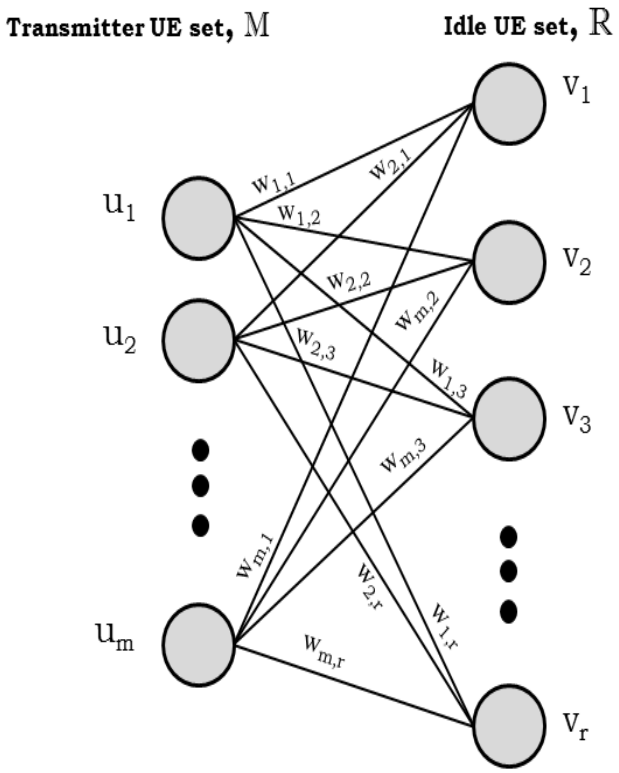

Figure 6.2: Weighted bipartite graph for the described scenario

mode based on matching. The procedure starts with initialization of the scheduled transmission and SINR threshold value. Then the corresponding weight matrix is computed in **Step 3**. **Steps 4** and **5** defines the construction of bipartite graph and maximum weighted matching based on the Hungarian algorithm. In **Step 5**, M and W denotes the matched UE set and the corresponding edge weight for each element in $\mathbb{M}$. The matches are selected such that the following objectives are satisfied:

$$\max \sum_{i=1}^{|\mathbb{M}|} \sum_{j=1}^{|M|} w_{ij} a_{ij} \tag{6.16}$$

$$\sum_{i=1}^{|\mathbb{M}|} a_{ij} = 1, \ \forall j = \{1, 2, ..., |M|\} \tag{6.17}$$

Algorithm V: TMA Algorithm

Step 1: Initialization: Given (m, n) transmissions and γ_{th}

Step 2: Form $\mathbb{M}, \mathbb{N}, \mathbb{R}$ sets

Step 3: Construct the weight matrix, $\mathbb{W}$, with weights generated as follows:

for $i = 1$ to length($\mathbb{M}$)

for $j = 1$ to length($\mathbb{R}$)

if $\mathbb{N}$(i) = $\mathbb{R}$(j) **then**

$w_{ij} = \gamma_{ij}$

else

$w_{ij} = \min(\gamma_{i,j}, \gamma_{j,n})$

end if

end for

end for

Step 4: Construct the bipartite graph, $G = (U, V; E)$, where $U = \mathbb{M}$, $V = \mathbb{R}$ and $E = \mathbb{W}$

Step 5: [M,W]= Hungarian-function ($\mathbb{W}$)

Step 6: **for** $i = 1$ to length(M)

if W(i) $< \gamma_{th}$ **then**

Assign cellular mode of transmission

else if M(i) = $\mathbb{N}$(i) **then**

Assign direct link D2D mode of transmission

else

Assign relay mode of transmission with $\text{UE}_{M(i)}$ as the relay UE

end if

end for

$$\sum_{j=1}^{|M|} a_{ij} = 1, \ \forall i = \{1, 2, ..., |\mathbb{M}|\} \tag{6.18}$$

$$a_{ij} \in \{0, 1\} \tag{6.19}$$

Relation (6.16) substantiates that our proposed algorithm solves the problem defined in (6.12). Equations (6.17) and (6.18) conveys that every element in $\mathbb{M}$ have a one-to-one matching partner in M. According to the matchings, the transmission modes are assigned based on **Step 6**. The constrains raised in (6.13), (6.14) and (6.15) can thus be solved using the proposed algorithm.

6.5 Results and Discussion

The performance of our proposed transmission mode assignment method was evaluated using computer simulations. The simulation tool for the analysis was developed by using MATLAB software. A normalized single cell system with one BS and 20 UEs was considered. The UEs are distributed randomly over the system area as shown in Figure 6.3. Among the 20 UEs, $M = \{3, 5, 7, 8, 11, 16, 17\}$ have data to communicate with their receivers, $N = \{4, 6, 14, 1, 12, 18, 20\}$ respectively. Accordingly $R = \{1, 2, 4, 6, 9, 10, 12, 13, 14, 15, 18, 19, 20\}$. Table 6.1 lists the other simulation parameters that are considered in line with [58, 96].

Two performance matrices have been used to evaluate the performance of the proposed method: (1) D2D mode access rate - defined as the ratio of number of D2D transmissions including the D2D and relay transmission modes to the total number of transmissions and (2) overall system throughput. Moreover we compare the performance of our proposed algorithm with traditional D2D communication scheme in [59, 70] and Random Allocation (RA) algorithm as

Table 6.1: Simulation Parameters for Relay-assisted D2D communication

Parameter	**Value**
Channel Bandwidth, BW	10 MHz
Noise Power Density, N_0	-174 dBm/Hz
Simulation Runs	200
SNR threshold, γ_{th} D2D and cellular mode	10 dB
Path-loss Models Cellular mode D2D mode	128.1+37.6 $\log_{10}(d[km])$ 148 + 40 $\log_{10}(d[km])$
Shadow fading standard deviation Cellular mode D2D mode	10 dB 12 dB
Maximum UE transmit power Cellular mode, ϱ^c D2D mode, ϱ^d	24 dBm 21 dBm

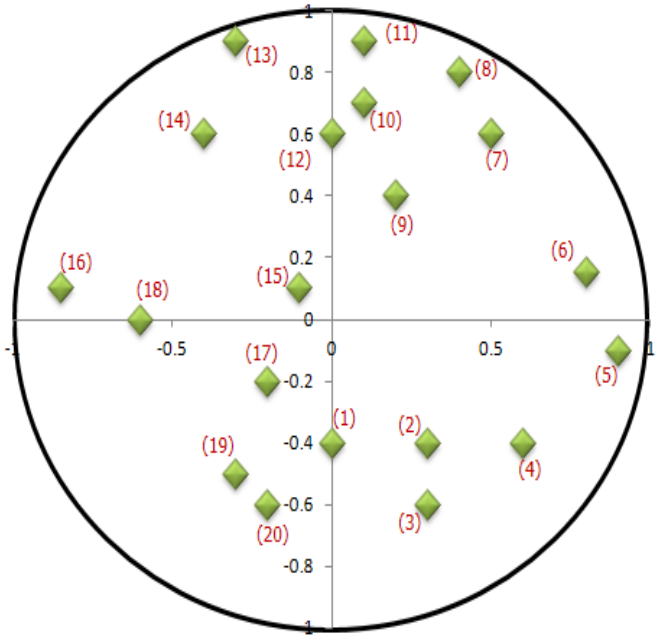

Figure 6.3: A normalized cell with different UE positions

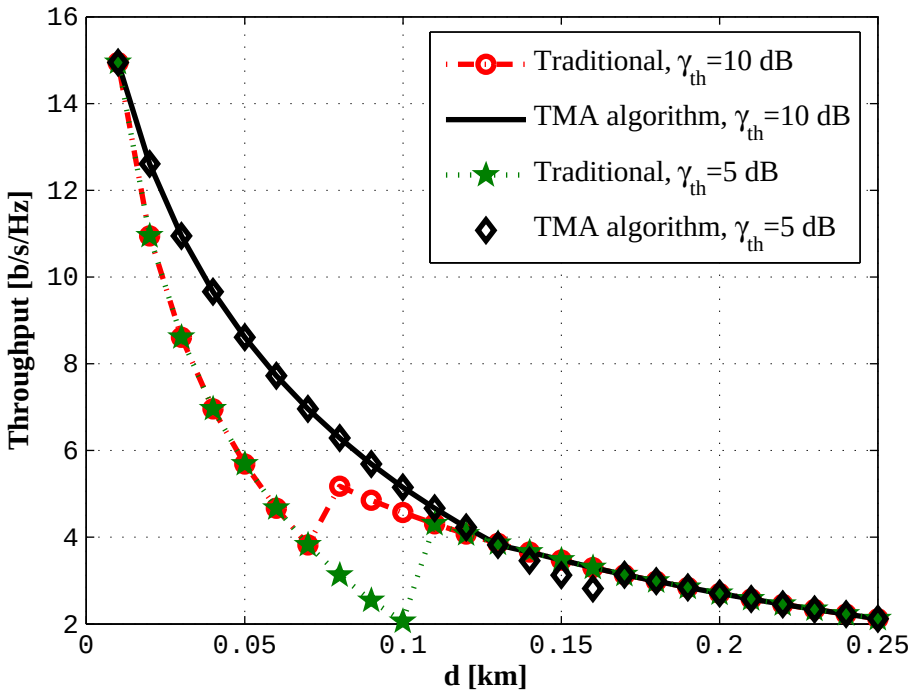

Figure 6.4: Throughput per UE vs distance, d, plot for traditional and TMA algorithms with $\gamma_{th} = 5$ dB and 10 dB

in [67, 69]. In the traditional D2D communication scheme, cellular and D2D transmission modes were only considered. There exist a SINR margin to guarantee QoS requirement and the transmission modes were decided based on the SINR margin. For RA algorithm in [67,69], a relay-assisted D2D communication was considered where the relay matching has been performed through random selection of UEs.

The end to end throughput per UE for different values of d with the proposed TMA algorithm for $\gamma_{th} = 5$ dB and 10 dB is shown in Figure 6.4, where d is the distance between the transmitter and receiver. The figure also compares the performance of the proposed scheme with the traditional D2D communication scheme. From the figure it is clear that the throughput decreases as the distance between the transmitter and receiver increases for both the schemes. For the traditional scheme [59, 70], the D2D coverage extends upto $d = 70$ m for a

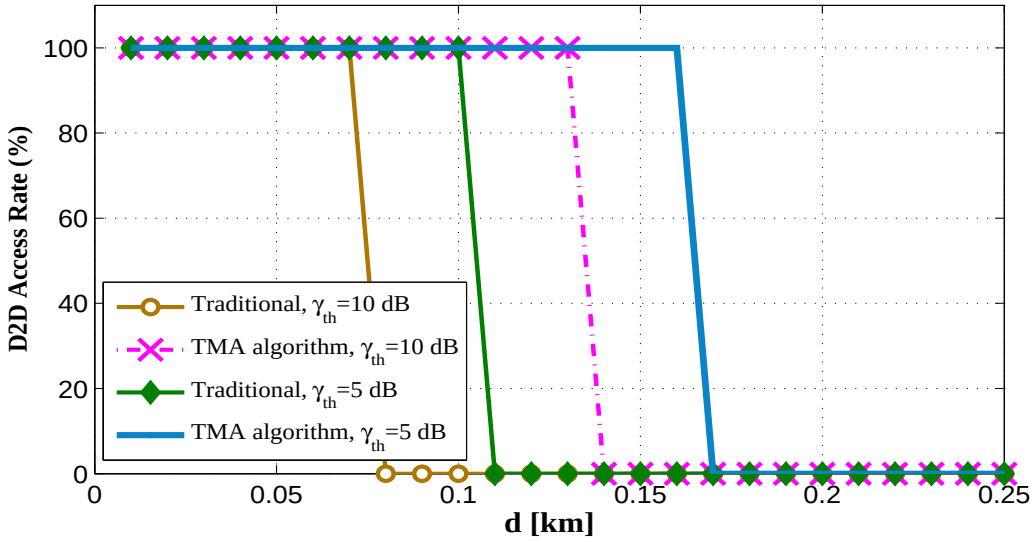

Figure 6.5: D2D access rate per UE vs distance, d, plot for traditional and TMA algorithms with $\gamma_{th} = 5$ dB and 10 dB

threshold value of $\gamma_{th} = 10$ dB and upto $d = 100\ m$ for $\gamma_{th} = 5$ dB. Beyond this range, the specified threshold value is not met and hence switches to cellular mode of transmission. This is the reason for sharp changes in the course of the graphs describing the behaviour of traditional D2D communication [59, 70]. The figure also shows that relay-assisted D2D communication with the proposed algorithm leads in throughput enhancement especially for the mode transition region of existing scheme, i.e., the region where transition from D2D to cellular mode occurs. Moreover, the proposed method provides a D2D coverage upto $d = 130\ m$ for $\gamma_{th} = 10$ dB and $d = 160\ m$ for $\gamma_{th} = 5$ dB. Figure 6.5 gives a better understanding of the improved D2D coverage by the proposed method.

Figure 6.5 shows the D2D access rate per UE for the proposed TMA algorithm and compared with traditional scheme for varying distance between transmitter and receiver. The access rate is defined as the ratio of number of D2D transmissions including the D2D and relay transmission modes to the total number of transmissions. For access rate per UE, the total number of transmissions will be 1. With D2D and relay modes of transmission, the access rate will be 100%

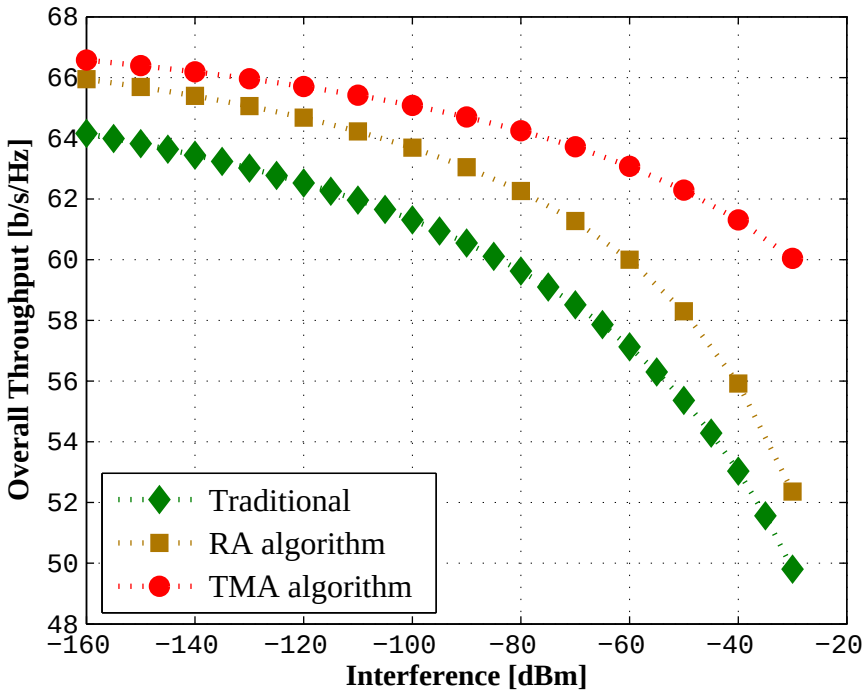

Figure 6.6: Overall throughput vs interference plot for TMA, RA and traditional algorithms

and will be 0% for cellular mode of transmission. The figure shows that the proposed TMA algorithm provides better D2D coverage by exploiting the relay transmission mode than the traditional scheme. In the figure, the D2D access rate reduces as the required γ_{th} at the receiver increases. Figure 6.4 and Figure 6.5 show that the advantages of D2D communication can be better realized through relay-assisted communication. The figures illustrate that device relaying improves the throughput performance as the distance between the transmitter and receiver increases.

Figure 6.6 compares the overall system throughput performance of the three algorithms for the scenario described in Figure 6.3. The throughput is plotted as a function of different interference power values as mentioned in [58]. As expected, the throughput gain of the traditional D2D communication scheme [59, 70] without relay mode is lower when compared to the other two algorithms.

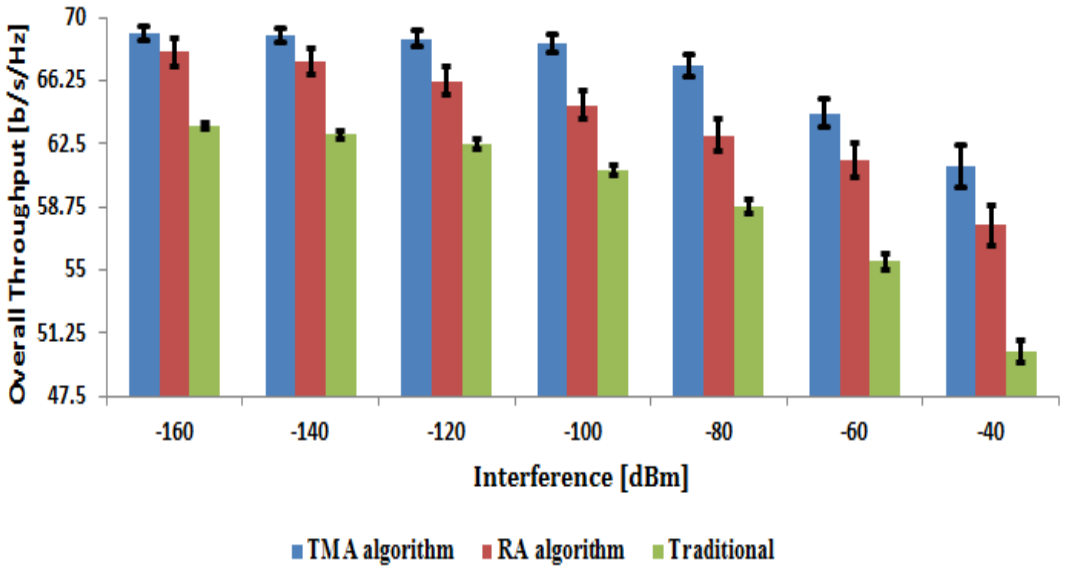

Figure 6.7: Overall throughput vs interference plot for TMA, RA and traditional algorithms with 95% confidence interval

It may be noted that the TMA algorithm provides performance improvement in comparison with RA algorithm [67,69] in case of the relay-assisted D2D communication. Comparing to TMA, the RA algorithm dose not provide correct UE relay matching for all transmissions and that is demonstrated in Figure 6.8.

The next set of analysis is concentrated on varying positions of UEs in the cell. Here, it is considered that the receiver UE positions follows uniform distribution. The simulations are conducted for 200 runs and the average value of the total achievable throughput of the TMA, RA and traditional [59, 70] algorithms are plotted in Figure. 6.7. The analysis is carried out for different interference power values. A confidence level of 95% for the total achievable throughput is also shown against each algorithm. This result also substantiates the performance improvement in terms of overall system throughput for the proposed method. The maximization problem formulated in Section 6.3.1 is thus solved using the proposed TMA algorithm.

Figure 6.8 shows the D2D access rate for the proposed TMA algorithm and is compared with RA algorithm for $\gamma_{th} = 5$ dB and 10 dB with a confidence interval

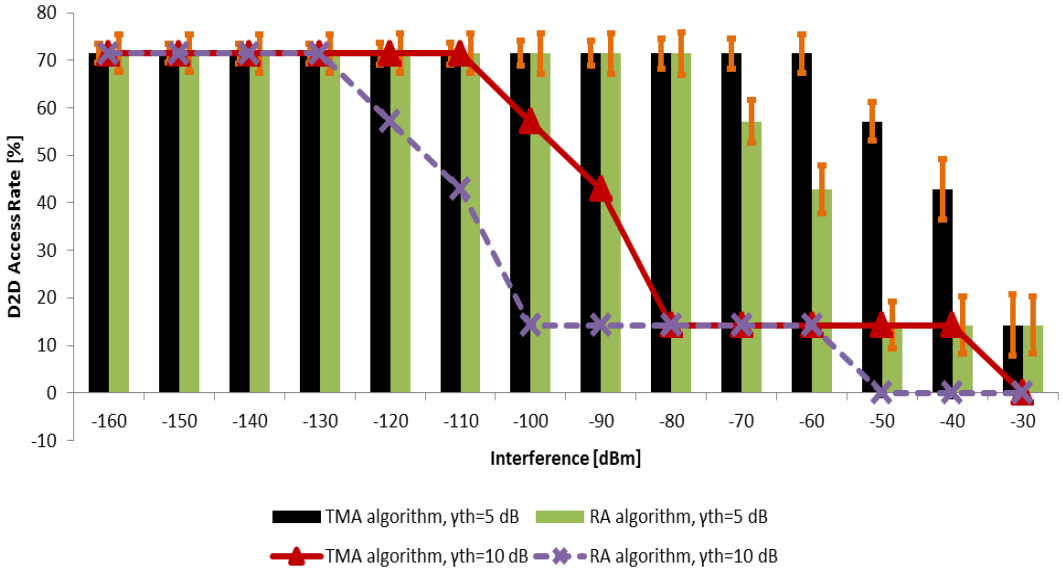

Figure 6.8: D2D access rate vs interference plot for TMA and RA algorithms with a confidence interval of 95%, $\gamma_{th} = 5$ dB and 10 dB

of 95%. The figure shows that D2D access rate is higher for TMA algorithm than RA algorithm [67,69]. For $\gamma_{th} = 10$ dB, the RA algorithm does not support D2D communication beyond an interference power of -60 dB. Whereas our proposed method support D2D communication upto an interference power of -40 dB for $\gamma_{th} = 10$ dB. This accounts for the increment in throughput performance for our proposed method in comparison to RA algorithm of Figure 6.6.

6.5.1 Complexity analysis

For the bipartite graph, $G(U, V, E)$, with $|U| = |V| = N$, the complexity of the RA algorithm is $O(N!)$ and the proposed algorithm gives a polynomial complexity of $O(N^3)$. The complexity of the RA algorithm is not practically manageable with whereas the proposed algorithm shows near optimal performance in comparison with RA algorithm.

6.6 Summary

A device relaying mode of transmission is presented in this chapter in addition to the existing cellular and D2D transmission mode to overcome the performance degradation in D2D communication in case of large distances between transmitter and receivers. A joint transmission mode and relay selection algorithm for the relay-assisted D2D communication is proposed. The proposed method, based on the Hungarian algorithm, guarantees optimal matching to maximize the overall network throughput. Simulation results demonstrate that the proposed method with the relay mode can improve the D2D coverage in comparison with existing communication modes. The proposed method also provides better performance in terms of throughput and D2D access rate in comparison with other existing schemes.

CHAPTER 7

Conclusion and Scope of Future Research work

Contents

The overall contributions of this this work are briefly summarized in this chapter. Further investigations on the research aspects of the proposed works are also outlined.

7.1 Conclusion

The concept of D2D communication as an underlay to cellular networks has emerged as a candidate technology for enhancing spectral efficiency, saving the power of UEs and offloading cellular traffics. The sharing of cellular radio resources for D2D communication results in various interference scenarios and hence interference management schemes are highly essential for the effective realization of D2D communication. In Chapter 1, an investigation on the several interference management schemes in the literature has been presented. Various usage cases of advanced topology D2D services were also investigated in Chapter 1. From the literature survey, the objectives for carrying out this research work have been framed.

An interference cancellation based on orthogonal MIMO precoding approach is proposed in this thesis. In Chapter 2, an interference cancellation approach for single link D2D communication, i.e., the cellular channel resource is being shared by a single D2D link, is proposed. The interference cancellation approach presented in Chapter 2 is extended for a cluster based multi-link scenario, i.e., the cellular channel resource is being shared by multiple D2D links, in Chapter 3. The expression for outage probability of the proposed method is derived for single link and multi-link D2D communication scenario in Chapter 4. From the analyses and discussions, the following conclusions can be made:

- The proposed orthogonal precoding approach can efficiently reduces the interferences from cellular to D2D, D2D to cellular and interference among D2D pairs for both single link and multi-link D2D communications and

thus guarantee QoS requirement for both cellular and D2D links.

- The proposed method can be applied to both uplink/downlink cellular and D2D communications. A possible allocation of different D2D communication links of a cluster in the LTE TDD frame structure was presented in Chapter 3.

- The simulation results show that the proposed method results in better interference cancellation and offers throughput enhancement compared to the conventional precoding vector selection approach. The throughput analyses also substantiate the advantage of sharing the cellular channel channel resource by multiple D2D links. The research work also highlights the importance of defining a cluster head inside the cluster in terms of energy efficiency.

- The outage probability of the proposed and a conventional interference signal cancellation methods are derived for the case when multiple D2D links co-exist in the radio resource. Simulation results indicate that the proposed method leads in reduction of interference and provides superior performance in terms of outage probability when compared with the conventional method.

A three-step resource allocation scheme was proposed in Chapter 5, to execute the proposed co-channel interference cancellation approach proposed in Chapter 3. The three-step scheme includes a mode selection, clustering and cluster head selection procedures. The following conclusions were outlined from the evaluation of the proposed scheme using the WINNER II A1 indoor office model:

- The proposed scheme allows to estimate the D2D zone in which the D2D communication can provide throughput enhancement when compared with conventional cellular communication.

- The proposed Clustering and Cluster Head selection algorithms improve spectral efficiency and optimize UEs energy consumption in a cluster.

- The expression for maximum number of links that a cellular UE resources (having predefined SINR threshold and outage probability) can share is derived. The outage probability shows that our derived expression leads to almost the same results as in the case without approximation in the high SNR scenarios.

In Chapter 6, the D2D communication is studied as an enabler of relay-assisted services. Hence a device relaying mode of transmission is presented and a joint transmission mode and relay selection algorithm is proposed. The simulation results demonstrates that the proposed method based on Hungarian algorithm provides the following advantages:

- The proposed method with the relay mode can improve the D2D coverage in comparison with existing communication modes.

- The proposed method based on the Hungarian algorithm guarantees optimal matching to maximize the overall network throughput and D2D access rate in comparison with other existing schemes.

The D2D communication can be considered as a special scenario of Machine-to-Machine (M2M) communication where the end devices are UEs and the BS plays the role of peer discovery. Thus the proposed methods can easily be extended for M2M applications as well.

7.2 Limitations and Scope of Further Research Work

The research work presented in this thesis addressed some of the challenges including interference management, resource allocation and managing advanced

topology services of D2D communication as an underlay to cellular network. The propositions presented in this thesis has the potential for wide explorations and some of the significant areas of future research works include the following:

- The proposed interference cancellation method with orthogonal precoding is limited to handle co-channel interferences in an intra-cluster communication scenario. In the future, the proposed method can be extended for handling interferences generated with inter-cluster communications.

- The proposed interference cancellation method with orthogonal precoding do not take into consideration the movement of UEs. In the future, the proposed method can be extended by considering movement of UEs.

- In this thesis, the outage probability analysis of the proposed method is limited to a cluster based D2D mesh-type topology. In our future work, we plan to derive a generalized expression for the outage probability with orthogonal precoding that is applicable to any type of cluster layout.

- The Clustering algorithm presented in Chapter 5 groups interconnected UEs to form a cluster. Efficient clustering techniques can be further investigated and optimized using different evolutionary algorithms.

- Selection of Cluster Head using multi-objective optimization technique for throughput maximization can be further investigated.

- The proposed Hungarian method based TMA algorithm assumed that the channel state information is available at the BS to calculate the edge weights in the bipartite graph. In future research, we plan to take into account also a scenario with the imperfect channel state information.

- The proposed TMA algorithm can also be extended for using more than one relays instead of just one relay.

Appendix A

Codebook for Precoding

Table 7.1 and Table 7.2 show the codebook for transmission on two antenna ports, $\mathbb{W}_{2\times2}$, and four antenna ports, $\mathbb{W}_{4\times4}$, respectively according to the 3GPP specifications [72]. The codebook contains a finite set of codewords and the codebook index of each codeword for CSI reporting is also shown in the table. In Table 7.2, $\mathbf{W}_n^{\{s\}}$ denotes the matrix defined by the columns given by the set $\{s\}$ from $\mathbf{W}_n = \mathbf{I} - \frac{2\mathbf{u}_n\mathbf{u}_n^H}{\mathbf{u}_n^H\mathbf{u}_n}$, where $\mathbf{I}$ denotes the identity matrix.

Table 7.1: Codebook for transmission on two antenna ports, $\mathbb{W}_{2\times2}$

Codebook index, n	**Number of layers** 1	2
0	$\frac{1}{\sqrt{2}}\begin{bmatrix}1\\1\end{bmatrix}$	$\frac{1}{\sqrt{2}}\begin{bmatrix}1 & 0\\0 & 1\end{bmatrix}$
1	$\frac{1}{\sqrt{2}}\begin{bmatrix}1\\-1\end{bmatrix}$	$\frac{1}{\sqrt{2}}\begin{bmatrix}1 & 1\\1 & -1\end{bmatrix}$
2	$\frac{1}{\sqrt{2}}\begin{bmatrix}1\\j\end{bmatrix}$	$\frac{1}{\sqrt{2}}\begin{bmatrix}1 & 1\\j & -1\end{bmatrix}$
3	$\frac{1}{\sqrt{2}}\begin{bmatrix}1\\-j\end{bmatrix}$	-

Table 7.2: Codebook for transmission on two antenna ports, $\mathbb{W}_{4\times4}$

n	$\mathbf{u}_n$	Number of layers			
		1	2	3	4
0	$\mathbf{u}_0 = \begin{bmatrix}1 & -1 & -1 & -1\end{bmatrix}^T$	$\mathbf{W}_0^{\{1\}}$	$\frac{\mathbf{W}_0^{\{14\}}}{\sqrt{2}}$	$\frac{\mathbf{W}_0^{\{124\}}}{\sqrt{3}}$	$\frac{\mathbf{W}_0^{\{1234\}}}{2}$
1	$\mathbf{u}_1 = \begin{bmatrix}1 & -j & 1 & j\end{bmatrix}^T$	$\mathbf{W}_1^{\{1\}}$	$\frac{\mathbf{W}_1^{\{12\}}}{\sqrt{2}}$	$\frac{\mathbf{W}_1^{\{123\}}}{\sqrt{3}}$	$\frac{\mathbf{W}_1^{\{1234\}}}{2}$
2	$\mathbf{u}_2 = \begin{bmatrix}1 & 1 & -1 & 1\end{bmatrix}^T$	$\mathbf{W}_2^{\{1\}}$	$\frac{\mathbf{W}_2^{\{12\}}}{\sqrt{2}}$	$\frac{\mathbf{W}_2^{\{123\}}}{\sqrt{3}}$	$\frac{\mathbf{W}_2^{\{3214\}}}{2}$
3	$\mathbf{u}_3 = \begin{bmatrix}1 & j & 1 & -j\end{bmatrix}^T$	$\mathbf{W}_3^{\{1\}}$	$\frac{\mathbf{W}_3^{\{12\}}}{\sqrt{2}}$	$\frac{\mathbf{W}_3^{\{123\}}}{\sqrt{3}}$	$\frac{\mathbf{W}_3^{\{3214\}}}{2}$
4	$\mathbf{u}_4 = \begin{bmatrix}1 & (-1-j)/\sqrt{2} & -j & (1-j)/\sqrt{2}\end{bmatrix}^T$	$\mathbf{W}_4^{\{1\}}$	$\frac{\mathbf{W}_4^{\{14\}}}{\sqrt{2}}$	$\frac{\mathbf{W}_4^{\{124\}}}{\sqrt{3}}$	$\frac{\mathbf{W}_0^{\{1234\}}}{2}$
5	$\mathbf{u}_5 = \begin{bmatrix}1 & (1-j)/\sqrt{2} & j & (-1-j)/\sqrt{2}\end{bmatrix}^T$	$\mathbf{W}_5^{\{1\}}$	$\frac{\mathbf{W}_5^{\{14\}}}{\sqrt{2}}$	$\frac{\mathbf{W}_5^{\{124\}}}{\sqrt{3}}$	$\frac{\mathbf{W}_5^{\{1234\}}}{2}$
6	$\mathbf{u}_6 = \begin{bmatrix}1 & (1+j)/\sqrt{2} & -j & (-1+j)/\sqrt{2}\end{bmatrix}^T$	$\mathbf{W}_6^{\{1\}}$	$\frac{\mathbf{W}_4^{\{13\}}}{\sqrt{2}}$	$\frac{\mathbf{W}_4^{\{134\}}}{\sqrt{3}}$	$\frac{\mathbf{W}_6^{\{1324\}}}{2}$
7	$\mathbf{u}_7 = \begin{bmatrix}1 & (-1+j)/\sqrt{2} & j & (1+j)/\sqrt{2}\end{bmatrix}^T$	$\mathbf{W}_7^{\{1\}}$	$\frac{\mathbf{W}_7^{\{13\}}}{\sqrt{2}}$	$\frac{\mathbf{W}_7^{\{134\}}}{\sqrt{3}}$	$\frac{\mathbf{W}_7^{\{1324\}}}{2}$
8	$\mathbf{u}_8 = \begin{bmatrix}1 & -1 & 1 & -1\end{bmatrix}^T$	$\mathbf{W}_8^{\{1\}}$	$\frac{\mathbf{W}_8^{\{12\}}}{\sqrt{2}}$	$\frac{\mathbf{W}_8^{\{124\}}}{\sqrt{3}}$	$\frac{\mathbf{W}_8^{\{1234\}}}{2}$
9	$\mathbf{u}_9 = \begin{bmatrix}1 & -j & -1 & -j\end{bmatrix}^T$	$\mathbf{W}_9^{\{1\}}$	$\frac{\mathbf{W}_9^{\{14\}}}{\sqrt{2}}$	$\frac{\mathbf{W}_9^{\{134\}}}{\sqrt{3}}$	$\frac{\mathbf{W}_0^{\{1324\}}}{2}$
10	$\mathbf{u}_{10} = \begin{bmatrix}1 & 1 & 1 & -1\end{bmatrix}^T$	$\mathbf{W}_{10}^{\{1\}}$	$\frac{\mathbf{W}_{10}^{\{13\}}}{\sqrt{2}}$	$\frac{\mathbf{W}_{10}^{\{123\}}}{\sqrt{3}}$	$\frac{\mathbf{W}_{10}^{\{1324\}}}{2}$
11	$\mathbf{u}_{11} = \begin{bmatrix}1 & j & -1 & j\end{bmatrix}^T$	$\mathbf{W}_{11}^{\{1\}}$	$\frac{\mathbf{W}_{11}^{\{13\}}}{\sqrt{2}}$	$\frac{\mathbf{W}_{11}^{\{134\}}}{\sqrt{3}}$	$\frac{\mathbf{W}_{11}^{\{1324\}}}{2}$
12	$\mathbf{u}_{12} = \begin{bmatrix}1 & -1 & -1 & 1\end{bmatrix}^T$	$\mathbf{W}_{12}^{\{1\}}$	$\frac{\mathbf{W}_{12}^{\{12\}}}{\sqrt{2}}$	$\frac{\mathbf{W}_{12}^{\{123\}}}{\sqrt{3}}$	$\frac{\mathbf{W}_{12}^{\{1234\}}}{2}$
13	$\mathbf{u}_{13} = \begin{bmatrix}1 & -1 & 1 & -1\end{bmatrix}^T$	$\mathbf{W}_{13}^{\{1\}}$	$\frac{\mathbf{W}_{13}^{\{13\}}}{\sqrt{2}}$	$\frac{\mathbf{W}_{13}^{\{123\}}}{\sqrt{3}}$	$\frac{\mathbf{W}_{13}^{\{1234\}}}{2}$
14	$\mathbf{u}_{14} = \begin{bmatrix}1 & 1 & -1 & -1\end{bmatrix}^T$	$\mathbf{W}_{14}^{\{1\}}$	$\frac{\mathbf{W}_{14}^{\{13\}}}{\sqrt{2}}$	$\frac{\mathbf{W}_{14}^{\{123\}}}{\sqrt{3}}$	$\frac{\mathbf{W}_{14}^{\{3214\}}}{2}$
15	$\mathbf{u}_{15} = \begin{bmatrix}1 & 1 & 1 & 1\end{bmatrix}^T$	$\mathbf{W}_{15}^{\{1\}}$	$\frac{\mathbf{W}_{15}^{\{12\}}}{\sqrt{2}}$	$\frac{\mathbf{W}_{15}^{\{123\}}}{\sqrt{3}}$	$\frac{\mathbf{W}_{15}^{\{1234\}}}{2}$

References

[1] H. Viswanathan and M. Weldon, "The past, present, and future of mobile communications," *Bell Labs Technical Journal*, vol. 19, pp. 8–21, 2014.

[2] W. Hequan, "Telecommunications: challenges transformation [technology leaders forum]," *IEEE Communications Magazine*, vol. 47, no. 1, pp. 10–13, January 2009.

[3] S. Yang, "Toward a Wireless World," *IEEE Technology and Society Magazine*, vol. 26, no. 2, pp. 32–42, Summer 2007.

[4] G. Lawton, "What lies ahead for cellular technology?" *Published by the IEEE Computer Society*, vol. 38, no. 6, pp. 14–17, Jun 2005.

[5] D. Raychaudhuri and N. B. Mandayam, "Frontiers of wireless and mobile communications," *Proceedings of the IEEE*, vol. 100, no. 4, pp. 824–840, April 2012.

[6] F. Hillebrand, "The creation of standards for global mobile communication: GSM and UMTS standardization from 1982 to 2000," *IEEE Wireless Communications*, vol. 20, no. 5, pp. 24–33, October 2013.

[7] J. Qiao, X. Shen, J. Mark, Q. Shen, Y. He, and L. Lei, "Enabling Device-to-Device communications in millimeter-wave 5G cellular networks," *IEEE Communications Magazine*, vol. 53, no. 1, pp. 209–215, January 2015.

[8] S. Ortiz, "4G Wireless Begins to Take Shape," *Published by the IEEE Computer Society*, vol. 40, no. 11, pp. 18–21, Nov 2007.

[9] N. Islam and R. Want, "Smartphones: Past, Present, and Future," *IEEE Pervasive Computing*, vol. 13, no. 4, pp. 89–92, Oct 2014.

[10] E. Hossain, M. Rasti, H. Tabassum, and A. Abdelnasser, "Evolution toward 5G multi-tier cellular wireless networks: An interference management perspective," *IEEE Wireless Communications*, vol. 21, no. 3, pp. 118–127, June 2014.

[11] P. Agyapong, M. Iwamura, D. Staehle, W. Kiess, and A. Benjebbour, "Design considerations for a 5G network architecture," *IEEE Communications Magazine*, vol. 52, no. 11, pp. 65–75, Nov 2014.

[12] A. Imran and A. Zoha, "Challenges in 5G: how to empower SON with big data for enabling 5G," *IEEE Network*, vol. 28, no. 6, pp. 27–33, Nov 2014.

[13] A. Osseiran and et. al, "Scenarios for 5G mobile and wireless communications: the vision of the METIS project," *IEEE Communications Magazine*, vol. 52, no. 5, pp. 26–35, May 2014.

[14] J. Monserrat, G. Mange, V. Braun, H. Tullberg, G. Zimmermann, and m. Bulakci, "METIS research advances towards the 5G mobile and wireless system definition," *EURASIP Journal on Wireless Communications and Networking*, vol. 2015, no. 1, 2015.

[15] L. Lei, Z. Zhong, C. Lin, and X. Shen, "Operator controlled Device-to-Device communications in LTE-Advanced networks," *IEEE Wireless Communications*, vol. 19, no. 3, pp. 96–104, 2012.

[16] "Technical Specification Group Radio Access Network; Study on LTE Device to Device Proximity Services; Radio Aspects," 3GPP TR 36.843, Tech. Rep. V 12.0.1, Release 12 2014-03.

[17] "Technical Specification Group Radio Access Network; LTE Device to Device (D2D) Proximity Services (ProSe); User Equipment (UE) radio transmission and reception," 3GPP TR 36.877, Tech. Rep. V 12.0.0, Release 12 2015-03.

[18] S. Mumtaz, H. Lundqvist, K. M. S. Huq, J. Rodriguez, and A. Radwan, "Smart Direct-LTE communication: An energy saving perspective," *Ad Hoc Networks*, vol. 13, Part B, no. 0, pp. 296 – 311, 2014.

[19] L. Wei, R. Hu, Y. Qian, and G. Wu, "Enable Device-to-Device communications underlaying cellular networks: challenges and research aspects," *IEEE Communications Magazine*, vol. 52, no. 6, pp. 90–96, June 2014.

[20] X. Lin, J. Andrews, A. Ghosh, and R. Ratasuk, "An overview of 3GPP device-to-device proximity services," *IEEE Communications Magazine*, vol. 52, no. 4, pp. 40–48, April 2014.

[21] D. Feng, L. Lu, Y. Yuan-Wu, G. Li, S. Li, and G. Feng, "Device-to-Device communications in cellular networks," *IEEE Communications Magazine*, vol. 52, no. 4, pp. 49–55, April 2014.

[22] S. Mumtaz, K. Saidul Huq, and J. Rodriguez, "Direct mobile-to-mobile communication: Paradigm for 5G," *IEEE Wireless Communications*, vol. 21, no. 5, pp. 14–23, October 2014.

[23] Z. Wang, H. Tian, K. Yang, and Z. Liu, "Frequency resource allocation strategy with QoS support in hybrid cellular and Device-to-Device networks," *International Journal of Communication Systems*, 2014.

[24] D. Zhu, J. Wang, A. Swindlehurst, and C. Zhao, "Downlink Resource Reuse for D2D Communications Underlaying Cellular Networks," *IEEE Signal Processing Letters*, vol. 21, no. 5, pp. 531–534, 2014.

[25] X. Lin, J. Andrews, and A. Ghosh, "Spectrum sharing for Device-to-Device communication in cellular networks," *IEEE Transactions on Wireless Communications*, vol. 13, no. 12, pp. 6727–6740, Dec 2014.

[26] N. Naderializadeh and A. Avestimehr, "Itlinq: A new approach for spectrum sharing in Device-to-Device communication systems," *IEEE Journal on Selected Areas in Communications*, vol. 32, no. 6, pp. 1139–1151, June 2014.

[27] M. Tehrani, M. Uysal, and H. Yanikomeroglu, "D2D communication in 5G cellular networks: challenges, solutions, and future directions," *IEEE Communications Magazine*, vol. 52, no. 5, pp. 86–92, May 2014.

[28] L. Song, D. Niyato, Z. Han, and E. Hossain, "Game-theoretic resource allocation methods for Device-to-Device communication," *IEEE Wireless Communications*, vol. 21, no. 3, pp. 136–144, June 2014.

[29] P. Mach, Z. Becvar, and T. Vanek, "In-Band Device-to-Device Communication in OFDMA Cellular Networks: A Survey and Challenges," *IEEE Communications Surveys Tutorials*, vol. PP, no. 99, pp. 1–1, 2015.

[30] G. Fodor, S. Parkvall, S. Sorrentino, P. Wallentin, Q. Lu, and N. Brahmi, "Device-to-Device Communications for National Security and Public Safety," *IEEE Access*, vol. 2, pp. 1510–1520, 2014.

[31] T. Koskela, S. Hakola, T. Chen, and J. Lehtomaki, "Clustering concept using Device-to-Device communication in cellular system," in *IEEE Wireless Communications and Networking Conference (WCNC)*, April 2010, pp. 1–6.

[32] B. Zhou, H. Hu, S.-Q. Huang, and H.-H. Chen, "Intracluster Device-to-Device relay algorithm with optimal resource utilization," *IEEE Transactions on Vehicular Technology*, vol. 62, no. 5, pp. 2315–2326, Jun 2013.

[33] D. Lee, S.-I. Kim, J. Lee, and J. Heo, "Performance of multihop decode-and-forward relaying assisted Device-to-Device communication underlaying cellular networks," in *International Symposium on Information Theory and its Applications (ISITA)*, Oct 2012, pp. 455–459.

[34] Y. Pei and Y.-C. Liang, "Resource allocation for Device-to-Device communications overlaying two-way cellular networks," *IEEE Transactions on Wireless Communications*, vol. 12, no. 7, pp. 3611–3621, July 2013.

[35] Y. Qin, M. Ding, M. Zhang, H. Yu, and H. Luo, "Relaying robust beamforming for Device-to-Device communication with channel uncertainty," *IEEE Communications Letters*, vol. 18, no. 10, pp. 1859–1862, Oct 2014.

[36] K. Zou, M. Wang, K. Yang, J. Zhang, W. Sheng, Q. Chen, and X. You, "Proximity discovery for Device-to-Device communications over a cellular network," *IEEE Communications Magazine*, vol. 52, no. 6, pp. 98–107, June 2014.

[37] S. Andreev, A. Pyattaev, K. Johnsson, O. Galinina, and Y. Koucheryavy, "Cellular traffic offloading onto network-assisted Device-to-Device connections," *IEEE Communications Magazine*, vol. 52, no. 4, pp. 20–31, April 2014.

[38] Y. Li, T. Wu, P. Hui, D. Jin, and S. Chen, "Social-aware D2D communications: qualitative insights and quantitative analysis," *IEEE Communications Magazine*, vol. 52, no. 6, pp. 150–158, June 2014.

[39] S. Bae, J. Gu, S. Hasan, and M. Chung, "Congestion dispersion in Device-to-Device discovery for proximity-based services," *Annals of Telecommunications*, pp. 1–13, 2014.

[40] M. J. Yang, S. Y. Lim, H. J. Park, and N. H. Park, "Solving the data overload: Device-to-Device bearer control architecture for cellular data offloading," *IEEE Vehicular Technology Magazine*, vol. 8, no. 1, pp. 31–39, March 2013.

[41] G. Fodor, E. Dahlman, G. Mildh, S. Parkvall, N. Reider, G. Miklos, and Z. Turanyi, "Design aspects of network assisted Device-to-Device communications," *IEEE Communications Magazine*, vol. 50, no. 3, pp. 170–177, 2012.

[42] C.-H. Yu, K. Doppler, C. Ribeiro, and O. Tirkkonen, "Resource sharing optimization for Device-to-Device communication underlaying cellular networks," *IEEE Transactions on Wireless Communications*, vol. 10, no. 8, pp. 2752–2763, 2011.

[43] L. Lei, Y. Kuang, X. Shen, C. Lin, and Z. Zhong, "Resource control in network assisted Device-to-Device communications: solutions and challenges," *IEEE Communications Magazine*, vol. 52, no. 6, pp. 108–117, June 2014.

[44] J. Liu, N. Kato, J. Ma, and N. Kadowaki, "Device-to-Device Communication in LTE-Advanced Networks: A Survey," *IEEE Communications Surveys Tutorials*, vol. PP, no. 99, pp. 1–1, 2014.

[45] P. Janis, V. Koivunen, C. Ribeiro, K. Doppler, and K. Hugl, "Interference-avoiding MIMO schemes for Device-to-Device radio underlaying cellular networks," in *IEEE 20th International Symposium on Personal, Indoor and Mobile Radio Communications*, 2009, pp. 2385–2389.

[46] P. Janis, V. Koivunen, C. Ribeiro, J. Korhonen, K. Doppler, and K. Hugl, "Interference-aware resource allocation for Device-to-Device radio underlaying cellular networks," in *IEEE 69th Vehicular Technology Conference, VTC Spring*, April 2009, pp. 1–5.

[47] P. Janis, C.-H. Yu, K. Doppler, C. Ribeiro, C. Wijting, K. Hugl, O. Tirkkonen, and V. Koivunen, "Device-to-Device communication underlaying cellular communications systems," *Int. J. Communications, Network and System Sciences*, vol. 9, pp. 169–247, 2009.

[48] K. Doppler, M. Rinne, C. Wijting, C. Ribeiro, and K. Hugl, "Device-to-Device communication as an underlay to LTE-advanced networks," *IEEE Communications Magazine*, vol. 47, no. 12, pp. 42–49, December 2009.

[49] C.-H. Yu, O. Tirkkonen, K. Doppler, and C. Ribeiro, "Power optimization of Device-to-Device communication underlaying cellular communication," in *IEEE International Conference on Communications, ICC*, June 2009, pp. 1–5.

[50] H. Xing and S. Hakola, "The investigation of power control schemes for a Device-to-Device communication integrated into OFDMA cellular system," in *IEEE 21st International Symposium on Personal Indoor and Mobile Radio Communications (PIMRC)*, Sept 2010, pp. 1775–1780.

[51] Y. Cheng, Y. Gu, and X. Lin, "Combined power control and link selection in Device-to-Device enabled cellular systems," *IET Communications*, vol. 7, no. 12, pp. 1221–1230, Aug 2013.

[52] X. Xu, H. Wang, H. Feng, and C. Xing, "Analysis of Device-to-Device communications with exclusion regions underlaying 5G networks," *Transactions on Emerging Telecommunications Technologies*, vol. 26, no. 1, pp. 93–101, 2015.

[53] H. Min, W. Seo, J. Lee, S. Park, and D. Hong, "Reliability improvement using receive mode selection in the Device-to-Device uplink period underlaying cellular networks," *IEEE Transactions on Wireless Communications*, vol. 10, no. 2, pp. 413–418, 2011.

[54] J. Li, M. Lei, and F. Gao, "Device-to-Device (D2D) communication in MU-MIMO cellular networks," in *IEEE Global Communications Conference (GLOBECOM)*, 2012, pp. 3583–3587.

[55] M. Hasan, E. Hossain, and D. I. Kim, "Resource Allocation Under Channel Uncertainties for Relay-Aided Device-to-Device Communication Underlaying LTE-A Cellular Networks," *IEEE Transactions on Wireless Communications*, vol. 13, no. 4, pp. 2322–2338, April 2014.

[56] H. Min, J. Lee, S. Park, and D. Hong, "Capacity enhancement using an interference limited area for Device-to-Device uplink underlaying cellular networks," *IEEE Transactions on Wireless Communications*, vol. 10, no. 12, pp. 3995–4000, December 2011.

[57] H. Wang and X. Chu, "Distance-constrained resource-sharing criteria for Device-to-Device communications underlaying cellular networks," *Electronics Letters*, vol. 48, no. 9, pp. 528–530, 2012.

[58] Y. Xu, R. Yin, T. Han, and G. Yu, "Dynamic resource allocation for Device-to-Device communication underlaying cellular networks," *International Journal of Communication Systems*, 2012.

[59] D. Feng, L. Lu, Y. Yuan-Wu, G. Li, G. Feng, and S. Li, "Device-to-Device communications underlaying cellular networks," *IEEE Transactions on Communications*, vol. 61, no. 8, pp. 3541–3551, 2013.

[60] G. Yu, L. Xu, D. Feng, R. Yin, G. Li, and Y. Jiang, "Joint mode selection and resource allocation for Device-to-Device communications," *IEEE Transactions on Communications*, vol. 62, no. 11, pp. 3814–3824, Nov 2014.

[61] J. Wang, D. Zhu, C. Zhao, J. Li, and M. Lei, "Resource sharing of underlaying Device-to-Device and uplink cellular communications," *IEEE Communications Letters*, vol. 17, no. 6, pp. 1148–1151, June 2013.

[62] M. Hajiaghayi, C. Wijting, C. Ribeiro, and M. Hajiaghayi, "Efficient and practical resource block allocation for LTE-based D2D network via graph coloring," *Wireless Networks*, vol. 20, no. 4, pp. 611–624, 2014.

[63] Q. Wang, C. Lai, Y. Dong, Y. Shu, and X. Xu, "Joint user clustering and resource allocation for device-to-device communication underlaying MU-MIMO cellular networks," *EURASIP Journal on Wireless Communications and Networking*, vol. 145, pp. 1–17, 2015.

[64] P. Phunchongharn, E. Hossain, and D. Kim, "Resource allocation for Device-to-Device communications underlaying LTE-Advanced networks," *IEEE Wireless Communications*, vol. 20, no. 4, pp. 91–100, August 2013.

[65] M. Hasan and E. Hossain, "Distributed resource allocation for relay-aided D2D communication: A message passing approach," *IEEE Transactions on Wireless Communications*, vol. 13, no. 11, pp. 6326–6341, 2014.

[66] E. Hossain, D. I. Kim, and V. K. Bhargava, Eds., *Cooperative Cellular Wireless Networks*. Cambridge University Press, March 2011.

[67] T. Han, R. Yin, Y. Xu, and G. Yu, "Uplink channel reusing selection optimization for Device-to-Device communication underlaying cellular networks," in *IEEE 23rd International Symposium on Personal Indoor and Mobile Radio Communications (PIMRC)*, Sept 2012, pp. 559–564.

[68] N. Chen, H. Tian, and Z. Wang, "Resource Allocation for Intra-Cluster D2D Communications Based on Kuhn-Munkres Algorithm," in *IEEE 80th Vehicular Technology Conference (VTC Fall)*, Sept 2014, pp. 1–5.

[69] J. Han, Q. Cui, C. Yang, and X. Tao, "Bipartite matching approach to optimal resource allocation in Device to Device underlaying cellular network," *Electronics Letters*, vol. 50, no. 3, pp. 212–214, January 2014.

[70] L. Wang and H. Wu, "Fast Pairing of Device-to-Device Link Underlay for Spectrum Sharing With Cellular Users," *IEEE Communications Letters*, vol. 18, no. 10, pp. 1803–1806, Oct 2014.

[71] T. Kim and M. Dong, "An Iterative Hungarian Method to Joint Relay Selection and Resource Allocation for D2D Communications," *IEEE Wireless Communications Letters*, vol. 3, no. 6, pp. 625–628, Dec 2014.

[72] "Technical Specification of LTE; Evolved Universal Terrestrial Radio Access (E-UTRA); Physical channels and Modulation," 3GPP TS 36.211, Tech. Rep. version 11.3.0, Release 11 2013-07.

[73] P.-J. Bouvet, M. Helard, and V. Le Nir, "Simple iterative receivers for MIMO LP-OFDM systems," *Annals of Telecommunications*, vol. 61, no. 5-6, pp. 578–601, 2006.

[74] H. Meghdadi, J.-P. Cances, and V. Meghdadi, "Simple precoding algorithms using gram-schmidt orthonormalization process for multiuser relay

communications with optimized power allocation," *Annals of Telecommunications*, vol. 68, no. 5-6, pp. 247–266, 2013.

[75] G. Ananthi and S. Thiruvengadam, "Outage probability analysis for Multiple Input-Multiple Output Ad-Hoc network with quantised beamforming," *IET Communications*, vol. 6, no. 7, pp. 708–714, May 2012.

[76] "Technical Specification of LTE; Evolved Universal Terrestrial Radio Access (E-UTRA); Physical layer procedures," 3GPP TS 36.213, Tech. Rep. version 11.3.0, Release 11 2013-07.

[77] A. Maaref and S. Aissa, "Closed-form expressions for the outage and ergodic shannon capacity of MIMO MRC systems," *IEEE Transactions on Communications*, vol. 53, no. 7, pp. 1092–1095, July 2005.

[78] A. Jeffrey and D. Zwillinger, Eds., *Table of Integrals, Series, and Products*, 7th ed. Academic Press, 2007.

[79] L. Zheng and D. Tse, "Diversity and multiplexing: a fundamental tradeoff in multiple-antenna channels," *IEEE Transactions on Information Theory*, vol. 49, no. 5, pp. 1073–1096, May 2003.

[80] E. Sengul, E. Akay, and E. Ayanoglu, "Diversity analysis of single and multiple beamforming," *IEEE Transactions on Communications*, vol. 54, no. 6, pp. 990–993, June 2006.

[81] L. Natarajan and B. Rajan, "Full-rate full-diversity finite feedback space-time schemes with minimum feedback and transmission duration," *IEEE Transactions on Wireless Communications*, vol. 12, no. 10, pp. 5022–5034, October 2013.

[82] C. Jiang, M. Wang, C. Yang, F. Shu, J. Wang, W. Sheng, and Q. Chen, "MIMO precoding using rotating codebooks," *IEEE Transactions on Vehicular Technology*, vol. 60, no. 3, pp. 1222–1227, March 2011.

[83] M. Zhang, M. Shafi, P. Smith, and P. Dmochowski, "Precoding performance with codebook feedback in a MIMO-OFDM system," in *IEEE International Conference on Communications (ICC)*, June 2011, pp. 1–6.

[84] D. Cheikh, J.-M. Kelif, M. Coupechoux, and P. Godlewski, "Multicellular Alamouti scheme performance in Rayleigh and shadow fading," *Annals of Telecommunications*, vol. 68, no. 5-6, pp. 345–358, 2013.

[85] H. Q. Ngo, H. Suraweera, M. Matthaiou, and E. Larsson, "Multipair Full-Duplex Relaying With Massive Arrays and Linear Processing," *IEEE Journal on elected Areas in Communications*, vol. 32, no. 9, pp. 1721–1737, Sept 2014.

[86] *LTE Uplink Interference Generation*, Agilent Technologies, Nomor Research GmbH, January 2011, version V2.0.

[87] C. Xu, L. Song, Z. Han, Q. Zhao, X. Wang, X. Cheng, and B. Jiao, "Efficiency resource allocation for Device-to-Device underlay communication systems: A reverse iterative combinatorial auction based approach," *IEEE Journal on Selected Areas in Communications*, vol. 31, no. 9, pp. 348–358, September 2013.

[88] H. Min, S. Lee, K. Kwak, and D. Hong, "Effect of multiple antennas at the source on outage probability for amplify-and-forward relaying systems," *IEEE Transactions on Wireless Communications*, vol. 8, no. 2, pp. 633–637, Feb 2009.

[89] A. Papoulis and S. U. Pillai, *Probability, Random Variables and Stochastic Process*, 4th edition, Ed. McGraw-Hill, 2002.

[90] P. M. H. Wilson, *Curved Spaces: From Classical Geometries to Elementary Differential Geometry*, 1st ed. Cambridge University Press, January 2008.

[91] P. Kyosti and et al., "WINNER II channel models," Tech. Rep. D1.1.2 V1.2, 2007.

[92] P. Yang, Q. Zhang, and J. Qin, "Exact outage probability of Nth-best multicast relay networks with co-channel interference," *IEEE Wireless Communications Letters*, vol. 2, no. 6, pp. 595–598, December 2013.

[93] K. Akkarajitsakul, P. Phunchongharn, E. Hossain, and V. Bhargava, "Mode selection for energy-efficient D2D communications in LTE-Advanced networks: A coalitional game approach," in *IEEE International Conference on Communication Systems (ICCS)*, Nov 2012, pp. 488–492.

[94] W. Heinzelman, A. Chandrakasan, and H. Balakrishnan, "An application-specific protocol architecture for wireless microsensor networks," *IEEE Transactions on Wireless Communications*, vol. 1, no. 4, pp. 660–670, October 2002.

[95] J. Cui and A. U. H. Sheikh, "Outage probability of cellular radio systems using maximal ratio combining in the presence of multiple interferers," *IEEE Transactions on Communications*, vol. 47, no. 8, pp. 1121–1124, Aug 1999.

[96] G. de la Roche, A. Alayon-Glazunov, and B. Allen, *LTE-Advanced and Next Generation Wireless Networks: Channel Modelling and Propagation*, 1st ed. Wiley, November 2012.

[97] S. Trifunovic, A. Picu, T. Hossmann, and K. A. Hummel, "Adaptive role switching for fair and efficient battery usage in Device-to-Device communication," *SIGMOBILE Mobile Computing and Communications Review, ACM*, vol. 18, no. 1, pp. 25–36, 2014.

[98] H. W. Kuhn, "The Hungarian method for the assignment problem," *Naval Research Logistics Quarterly*, vol. 2, no. 1-2, pp. 83–97, 1955.

[99] J. Munkres, "Algorithms for the assignment and transportation problems," *Journal of the Society for Industrial and Applied Mathematics*, vol. 5, no. 1, p. 3238, March 1957.

[100] D. B. West, *Introduction to Graph Theory*, 2nd ed. Pearson, 2000.

[101] J.-C. Fournier, *Graph Theory and Applications: With Exercises and Problems*. John Wiley & Sons, Inc., 2009.

[102] F. Bourgeois and J.-C. Lassalle, "An Extension of the Munkres Algorithm for the Assignment Problem to Rectangular Matrices," *Communications of the ACM*, vol. 14, no. 12, pp. 802–804, 1971.

[103] E. L. Lawler, *Combinatorial Optimization: Networks and Matroids*. Holt, Reinehartand Winston, NewYork, 1976.

[104] D. Dasgupta, G. Hernandez, D. Garrett, P. K. Vejandla, A. Kaushal, R. Yerneni, and J. Simien, "A Comparison of Multiobjective Evolutionary Algorithms with Informed Initialization and Kuhn-munkres Algorithm for the Sailor Assignment Problem," in *10th Annual Conference Companion on Genetic and Evolutionary Computation*. ACM, 2008, pp. 2129–2134.

Disseminations of Work

Journals

Accepted

1. **Chithra . R**, R. Bestak and S. K. Patra, "An Interference Cancellation scheme for D2D Multi-Link communication underlaying Cellular Network", Annals of Telecommunications, Springer (undergone two round of revision and got Accepted on September 2015).

2. **Chithra . R**, R. Bestak and S. K. Patra, "Efficient Resource Allocation of Network assisted Multi-link Device-to-Device Communication", International Journal of Communication Systems, Wiley (*undergone two round of revision and got Accepted on July 2016*).

Submitted

1. **Chithra . R**, R. Bestak and S. K. Patra, "Outage Probability Analysis for Multi-link D2D Communications with Orthogonal Precoding", Mobile Networks and Applications, Springer (*under review*).

Conferences

1. **Chithra. R**, R. Bestak and S. K. Patra, "Orthogonal MIMO Precoding Schemes for Device-to-Device Communication in LTE Networks", IEEE 37th International Conference on Telecommunications and Signal Processing, 1-3 Jul, 2014, Berlin, Germany.

2. **Chithra. R**, R. Bestak and S. K. Patra, "Hungarian method based joint Transmission mode and Relay selection in Device-to-Device communication", IEEE 8th IFIP Wireless and Mobile Networking Conference, 5-7 Oct, 2015, Munich, Germany.

3. **Chithra. R**, R. Bestak and S. K. Patra, "Ergodic Capacity of Device-to-Device Communication underlaying cellular network with Orthogonal Precoding", (*under preparation*)

Book chapter

1. Cloud and Fog Computing in 5G Mobile Networks: Emerging Advances and Applications, Edited by: Evangelos Markakis, George Mastorakis, Constandinos X. Mavromoustakis and Evangelos Pallis, IET, 2015
   Chapter: Devive-to-Device communication underlaying cellular networks, By: **Chithra. R**, R. Bestak and S. K. Patra (*Proposal accepted and final manuscript is under preparation*)